

Lowering the scale of Pati-Salam breaking through seesaw mixing

Matthew J. Dolan^{a,b} Tomasz P. Dutka^{a,c} Raymond R. Volkas^{a,b}

^a*ARC Centre of Excellence for Particle Physics at the Terascale, School of Physics, The University of Melbourne, Victoria 3010, Australia*

^b*ARC Centre of Excellence for Dark Matter Particle Physics, School of Physics, The University of Melbourne, Victoria 3010, Australia*

^c*Corresponding Author*

E-mail: matthew.dolan@unimelb.edu.au, tdutka@student.unimelb.edu.au, raymondv@unimelb.edu.au

ABSTRACT: We analyse the experimental limits on the breaking scale of Pati-Salam extensions of the Standard Model. These arise from the experimental limits on rare-meson decay processes mediated at tree-level by the vector leptoquark in the model. This leptoquark ordinarily couples to both left- and right-handed SM fermions and therefore the meson decays do not experience a helicity suppression. We find that the current limits vary from $\mathcal{O}(80 - 2500)$ TeV depending on the choice of matrix structure appearing in the relevant three-generational charged-current interactions. We extensively analyse scenarios where additional fermionic degrees of freedom are introduced, transforming as complete Pati-Salam multiplets. These can lower the scales of Pati-Salam breaking through mass-mixing within the charged-lepton and down-quark sectors, leading to a helicity suppression of the meson decay widths which constrain Pati-Salam breaking. We find four multiplets with varying degrees of viability for this purpose: an $SU(2)_{L/R}$ bidoublet, a pair of $SU(4)$ decuplets and either a $SU(2)_L$ or $SU(2)_R$ triplet all of which contain heavy exotic versions of the SM charged leptons. We find that the Pati-Salam limits can be as low as $\mathcal{O}(5 - 150)$ TeV with the addition of these four multiplets. We also identify an interesting possible connection between the smallness of the neutrino masses and a helicity suppression of the Pati-Salam limits for three of the four multiplets.

Contents

1	Introduction	2
2	Pati-Salam models	4
2.1	Basic Setup	4
2.2	Yukawa sector	7
2.3	Gauge Sector	8
2.4	Baryon number violation	10
3	Probing Pati-Salam models through rare meson decays	12
3.1	Neutral Pseudoscalar meson decays induced by X_μ	13
3.2	Fermion mass degeneracy	23
4	Exotic PS fermion multiplets	29
4.1	Fermion extensions	29
4.1.1	$SU(2)_{L/R}$ Triplets	31
4.1.2	$SU(2)_L/SU(2)_R$ Bi-doublet	33
4.1.3	$SU(4)_c/SU(2)_{L/R}$ Bi-fundamentals	34
4.1.4	$SU(4)_c$ Sextet	35
4.1.5	$SU(4)_c$ Decuplets	37
5	Fermion mixing	39
5.1	$e - E$ mixing	39
5.1.1	Top-right dominance: Bi-doublet fermions	45
5.1.2	Bottom-left dominance: $SU(2)_{L/R}$ Triplet fermions	51
5.2	$d - D$ mixing: Sextet fermions	55
5.3	Coupled $e - E$ and $d - D$ mixing: Decuplet fermions	57
5.4	Connection to $SO(10)$	64
6	Conclusion	65
A	Various Seesaw Properties	67
A.1	Singular Values in One Generation	67
A.2	Singular Values for Multiple Generations	69
A.3	Gap properties between the charged leptons and down quarks	71
A.4	Lepton masses with additional bi-doublets	74
A.5	Lepton masses with additional triplets	78
B	Running of Gauge and Yukawa couplings	82

1 Introduction

The quark-lepton unifying Pati-Salam (PS) gauge symmetry [1, 2] is an interesting modification of the Standard Model (SM) for a number of reasons. For example, it requires the introduction of a right-handed neutrino state and therefore can incorporate neutrino mass in a number of ways. It unifies the now six seemingly disparate multiplets in each generation of the SM into two which, in the minimal variant of PS, only leads to two Yukawa couplings. It also appears as a subgroup of a number of possible grand unified theories (GUTs). An important property of the model is that it unifies quarks and leptons of the same $SU(2)$ isospin.

Although the PS symmetry is usually considered to be broken at high scales, the theory naturally can accommodate a conserved global baryon number. Therefore, and unlike many models of gauge coupling unification, the PS breaking can occur at scales only a few orders of magnitude above the electroweak scale. Low-scale and high-scale variants of PS differ in very few ways, traditionally through a modification of the scalar sector and the inclusion of fermion singlets. However as with all models which unify the SM multiplets, the PS symmetry in its minimal form necessarily predicts two important mass equalities not observed experimentally:

$$m_\nu^{\text{Dirac}} = m_u \quad \text{and} \quad m_d = m_e. \quad (1.1)$$

The scalar content required in high-scale PS models to break the PS symmetry naturally leads to a seesaw¹ within the neutrino sector and not the up-quark sector, breaking the first mass relation; see e.g. [3]. Low-scale variants can be modified very simply in order to achieve a similar effect, although this requires extending the matter sector with, at a minimum, fermionic singlets. The second mass equality $m_d = m_e$ between the down-isospin partners also needs to be modified to produce a realistic theory

Any explanation of the broken mass degeneracy in the down-isospin sector requires a modification of the particle content of the theory. By far the most commonly considered modification is to introduce an additional scalar whose couplings to the down-quarks and charged-leptons differs by group theoretic factors; see e.g. [2]. This introduces enough free parameters such that all the masses of SM can arise without issue. An alternative idea, which we pursue further in this work, was first proposed in [4, 5] where additional fermionic states are introduced which mix with the charged-leptons inducing additional seesaw mixing. This similarly allows for a viable mass spectrum for all particles but additionally can attractively lead to phenomenologically viable PS models at much lower breaking scales than usually considered.

¹For clarity, the requirement for a seesaw in a mixing matrix is that the singular values of the blocks making up the matrix satisfy $\sigma_i(m_X) < \sigma_1(m_Y)$ for all i , where m_Y and m_X are the dominant and non-dominant block(s) respectively and we use the usual notation that $\sigma_i(\dots)$ corresponds to the singular values of given matrix sorted into ascending order.

The limits on the PS breaking scale arise from rare meson decay processes mediated by leptoquarks. In particular the theory requires the existence of a gauge-boson leptoquark, X_μ , which mediates these rare meson decays at tree level and with coupling strength similar to the strong coupling constant g_c . As X_μ couples quarks and fermions of the same isospin, the dominant decay modes that constrain PS breaking arise from the interactions of X_μ to the down-quarks and charged-leptons. Signals from up-isospin interactions result in neutrino (or missing energy) final states which are more difficult to constrain.

Interestingly, the introduction of new physics to break the down-isospin mass degeneracy can further modify the meson decay rates and hence also the limits on the PS breaking scale. Ordinarily the PS breaking limits vary between $\mathcal{O}(100 - 1000)$ TeV. However these mixing effects can reduce these limits down to $\mathcal{O}(10 - 100)$ TeV. Lower PS limits are of obvious interest as they allow for potential experimental probes of these models at scales lower than previously anticipated.

Additionally there has been a recent resurgence in interest in low-scale PS models as the leptoquarks predicted by the theory are promising candidates as explanations of anomalies in low-energy flavour-physics experiments [6–9]. The vector leptoquark X_μ itself is an attractive candidate to explain a portion of these anomalies. However, this requires a mass around $\Lambda \simeq 30$ TeV [10] which is naïvely ruled out from rare meson-decay experiments. Modifications to the PS gauge group itself have been proposed [11–13] in order to allow for lighter masses of X_μ by modifying the gauge coupling to the different generations. Alternatively the scalar leptoquark content of the theory has been considered as a candidate to explain the anomalies [10] in the standard PS scenario, by assuming some scalars develop significantly smaller masses than the PS breaking scale. This potentially leads to a hierarchy problem.

The use of charged-lepton mixing in order to both break the down-isospin mass degeneracy and reduce the allowed scale of PS breaking has already been considered in the context of the B anomalies for a specific model [14, 15]. The aim of this paper is to thoroughly analyse which PS multiplets are viable candidates in breaking the aforementioned mass degeneracy, and to evaluate the requirements on the couplings introduced in each case such that this also leads to lower experimentally allowed PS breaking scales. Therefore while we are motivated by different appealing reasons for low-scale PS, we will only focus on the requirements such that a reduction in the limits occurs.

Section 2 is an overview of the minimal PS scenario including an examination of the gauge boson and fermion masses. Section 3 evaluates the experimental limits on PS breaking as a function of the free parameters in the theory and determines the impact that fermionic mixing can have on the limits. Section 4 identifies all possible PS multiplets of low dimensionality that contain states such that mixing is induced. Finally, section 5 evaluates the requirements on the couplings involving viable multiplets which achieve both the desired suppression in the PS limits and a viable values for all relevant SM masses.

2 Pati-Salam models

2.1 Basic Setup

The Pati-Salam gauge group G_{PS} extends the SM by identifying the $SU(3)$ colour group as a subgroup of an $SU(4)$ gauge group and extending the electroweak sector to be left-right symmetric:

$$G_{\text{PS}} = SU(4)_c \otimes SU(2)_L \otimes SU(2)_R. \quad (2.1)$$

Often a discrete symmetry between the $SU(2)_L$ and $SU(2)_R$ sectors is imposed but is not necessary. Under this gauge symmetry the five SM fermion multiplets of each generation can be unified into two simple multiplets² under G_{PS}

$$f_L \sim (\mathbf{4}, \mathbf{2}, \mathbf{1}) \quad \text{and} \quad f_R \sim (\mathbf{4}, \mathbf{1}, \mathbf{2}), \quad (2.2)$$

where L/R indicates both which $SU(2)$ the fields are charged under as well as the chirality. The breaking of $SU(4)$ to the maximal subgroup $SU(3) \times U(1)_X$ is phenomenologically required and under this breaking the fundamental of $SU(4)$ decomposes as

$$\mathbf{4} \rightarrow \mathbf{1}_{-1} \oplus \mathbf{3}_{1/3} \quad (2.3)$$

indicating that the SM quarks and leptons can be unified by identifying $U(1)_X$ with a gauged $B - L$. The SM fermions are embedded into the multiplets given in eq. (2.2) as³

$$f_L = \begin{pmatrix} u_r & d_r \\ u_b & d_b \\ u_g & d_g \\ \nu_e & e \end{pmatrix}_L \quad \text{and} \quad f_R = \begin{pmatrix} u_r & d_r \\ u_b & d_b \\ u_g & d_g \\ \nu_e & e \end{pmatrix}_R, \quad (2.4)$$

with similar embeddings for the other generations. Therefore the gauge transformation rules for the fields, written as matrix multiplication, are

$$f_{L/R} \rightarrow U_4(f_{L/R}) U_{L/R}^T \quad (2.5)$$

where $U_{4,L,R}$ are special unitary matrices for the groups $SU(4)_c$, $SU(2)_L$ and $SU(2)_R$ respectively. There are multiple choices of scalars which give the correct breaking patterns. A common and near-minimal choice for electroweak symmetry breaking is a complex bidoublet

$$\phi \sim (\mathbf{1}, \mathbf{2}, \mathbf{2}) = \begin{pmatrix} \phi_1^0 & \phi_2^+ \\ \phi_1^- & \phi_2^0 \end{pmatrix}, \quad \langle \phi \rangle = \begin{pmatrix} v_1 & 0 \\ 0 & v_2 \end{pmatrix} \quad (2.6)$$

where the superscripts indicate the electric charge Q of each field and ϕ is written such that it transforms as

$$\phi \rightarrow U_L \phi U_R^\dagger. \quad (2.7)$$

²With the necessary addition of a right-handed neutrino.

³For simplicity we choose to identify the first generation of leptons with the first generation of quarks and so forth, however alternative assignments are possible [16].

Two different combinations of scalar multiplets are usually considered for the breaking of G_{PS} down to G_{SM} . Firstly, and most commonly, two scalars $\Delta_L \sim (\mathbf{10}, \mathbf{3}, \mathbf{1})$ and $\Delta_R \sim (\mathbf{10}, \mathbf{1}, \mathbf{3})$ are employed, where

$$\Delta_{L/R}^\alpha = \frac{1}{\sqrt{2}} \begin{pmatrix} \sqrt{2}\Delta_{11}^{\alpha+1/3} & \Delta_{12}^{\alpha+1/3} & \Delta_{13}^{\alpha+1/3} & \Delta_{14}^{\alpha-1/3} \\ \Delta_{12}^{\alpha+1/3} & \sqrt{2}\Delta_{22}^{\alpha+1/3} & \Delta_{23}^{\alpha+1/3} & \Delta_{24}^{\alpha-1/3} \\ \Delta_{13}^{\alpha+1/3} & \Delta_{23}^{\alpha+1/3} & \sqrt{2}\Delta_{33}^{\alpha+1/3} & \Delta_{34}^{\alpha-1/3} \\ \Delta_{14}^{\alpha-1/3} & \Delta_{24}^{\alpha-1/3} & \Delta_{34}^{\alpha-1/3} & \sqrt{2}\Delta_{44}^{\alpha-1} \end{pmatrix}_{L/R} \quad (2.8)$$

are symmetric matrices in $SU(4)$ space (written in the defining representation), $\alpha = (-1, 0, 1)$ corresponds to the non-trivial $SU(2)$ charge of the scalar (in the adjoint representation) and the superscripts on each component again corresponds to its electric charge⁴. The breaking $G_{\text{PS}} \rightarrow G_{\text{SM}}$ occurs with a non-zero vacuum expectation value (vev) in the following components

$$\left\langle \left(\Delta_{L/R}^{\alpha=1} \right)_{44} \right\rangle = v_{L/R}. \quad (2.9)$$

Alternatively, the scalars $\chi_L \sim (\mathbf{4}, \mathbf{2}, \mathbf{1})$ and $\chi_R \sim (\mathbf{4}, \mathbf{1}, \mathbf{2})$ can be used:

$$\chi_{L/R} = \begin{pmatrix} \chi_r^{2/3} & \chi_r^{-1/3} \\ \chi_b^{2/3} & \chi_b^{-1/3} \\ \chi_g^{2/3} & \chi_g^{-1/3} \\ \chi^0 & \chi^- \end{pmatrix}_{L,R}, \quad \left\langle \chi_{L/R} \right\rangle = \begin{pmatrix} 0 & 0 \\ 0 & 0 \\ 0 & 0 \\ v_{L/R} & 0 \end{pmatrix} \quad (2.10)$$

where the gauge transformation rules for these scalars are the same as $f_{L/R}$.

In both cases, Δ_R and χ_R would be sufficient without their $SU(2)_L$ counterparts as long as the bidoublet ϕ is included. Their inclusion however allows for the possibility of imposing a discrete symmetry between the left and right gauge sectors which would lead to partial unification of the gauge couplings, $g_L = g_R$, at the relevant breaking scale. An analysis of the renormalisation group running of the gauge coupling constants has shown that the inclusion of a parity symmetry requires a PS breaking scale of $\mathcal{O}(10^{12})$ GeV in order for consistency with low-energy measurements of electroweak observables [3], unless the parity breaking scale is decoupled from the scale of PS breaking [17]. In order to allow for the scale of PS breaking to be as low as possible we assume that if such a discrete symmetry exists, then its breaking occurs independently at a higher scale to the breaking of G_{PS} which allows for the scale of PS breaking to be significantly lowered. However for generality we will include the $SU(2)_L$ scalars which may be predicted by specific GUTs or lead to unique phenomenology.

⁴Unless stated otherwise superscripts on fields making up a PS multiplet will correspond to its electric charge Q under G_{SM} .

In addition to the scalars in eq. (2.10) often $\Phi \sim (\mathbf{15}, \mathbf{1}, \mathbf{1})$ is included where

$$\Phi = \frac{1}{2} \begin{pmatrix} \Phi_\pi^0 + \frac{1}{\sqrt{3}}\Phi_\eta^0 + \frac{1}{\sqrt{6}}\Phi_{15}^0 & \sqrt{2}\Phi_{12}^0 & \sqrt{2}\Phi_{13}^0 & \sqrt{2}\Phi_r^{2/3} \\ \sqrt{2}(\Phi_{12}^0)^* & -\Phi_\pi^0 + \frac{1}{\sqrt{3}}\Phi_\eta^0 + \frac{1}{\sqrt{6}}\Phi_{15}^0 & \sqrt{2}\Phi_{23}^0 & \sqrt{2}\Phi_b^{2/3} \\ \sqrt{2}(\Phi_{13}^0)^* & \sqrt{2}(\Phi_{23}^0)^* & -\frac{2}{\sqrt{3}}\Phi_\eta^0 + \frac{1}{\sqrt{6}}\Phi_{15}^0 & \sqrt{2}\Phi_g^{2/3} \\ \sqrt{2}\Phi_{\bar{r}}^{-2/3} & \sqrt{2}\Phi_{\bar{b}}^{-2/3} & \sqrt{2}\Phi_{\bar{g}}^{-2/3} & -\frac{3}{\sqrt{6}}\Phi_{15}^0 \end{pmatrix}$$

$$\langle \Phi \rangle = v_\Phi \text{diag} \left(\frac{1}{2\sqrt{6}}, \frac{1}{2\sqrt{6}}, \frac{1}{2\sqrt{6}}, -\sqrt{\frac{3}{8}} \right) \quad (2.11)$$

such that Φ transforms as

$$\Phi \rightarrow U_4 \Phi U_4^\dagger. \quad (2.12)$$

As this scalar transforms in the adjoint representation of $SU(4)_c$, a non-zero vev for Φ will break this symmetry down to one of its maximal subgroups such as $SU(3)_c \times U(1)_{B-L}$. The scalar content described above leads to the following symmetry breaking chain

$$\begin{aligned} & SU(4)_c \times SU(2)_L \times SU(2)_R \\ & \quad \downarrow \langle \Phi \rangle \\ & SU(3)_c \times SU(2)_L \times SU(2)_R \times U(1)_{B-L} \\ & \quad \downarrow \langle \chi_R / \Delta_R \rangle \\ & SU(3)_c \times SU(2)_L \times U(1)_Y \\ & \quad \downarrow \langle \phi, \chi_L / \Delta_L \rangle \\ & SU(3)_c \times U(1)_Q \end{aligned} \quad (2.13)$$

where $Y = T_{3R} + \frac{B-L}{2}$, $Q = T_{3L} + Y$ and the order of breaking is determined by the relative size of each vev. The inclusion of Φ therefore allows for all possible scales of symmetry breaking⁵ starting from G_{PS} down to the broken SM but is only necessary in scenarios where the $SU(2)_R$ gauge boson masses are desired to be smaller than the PS breaking scale.

We now turn to how the mass relations of Eq. (1.1) can be avoided. The equality between down-isospin partners will be addressed further below, however the equality between up-isospin partners allows us to restrict the scalar content of the theory. If $\Delta_{L/R}$ are present, a Majorana mass term for the neutrinos will be generated via $y_{L/R} \overline{f_{L/R}} (f_{L/R})^c \Delta_{L/R}$ and will lead to a see-saw mechanism between the neutral fermions as the hierarchy $\langle \Delta_L \rangle \ll \langle \phi \rangle \ll \langle \Delta_R \rangle$ is required due to electroweak precision tests and the Yukawa couplings are fixed by the masses of the up-type quarks. This leads to light, predominantly left-handed neutrinos, with masses given by

$$m_\nu \simeq y_L \langle \Delta_L \rangle + \frac{m_u^2}{y_R \langle \Delta_R \rangle}. \quad (2.14)$$

⁵The vevs of the scalars χ_R and Δ_R directly break $SU(4)_c \otimes SU(2)_L \otimes SU(2)_R$ down to $SU(3)_c \otimes SU(2)_L \otimes U(1)_Y$.

	Φ	ϕ	χ_L	χ_R
$SU(4)_c$	15	1	4	4
$SU(2)_L$	1	2	2	1
$SU(2)_R$	1	2	1	2

Table 1. The scalar content which we utilise and their respective dimensions under each PS gauge group.

Considering the third generation of fermions alone, $m_u = m_t \simeq 175$ GeV, requires PS breaking at large scales in order to achieve a viable low-energy neutrino mass spectrum. Setting $\langle \Delta_L \rangle = 0$ gives a rough lower-bound $\langle \Delta_R \rangle \gtrsim 10^{12}$ GeV and therefore the scalars $\Delta_{L/R}$ are not viable as models of low-scale PS.⁶

If $\chi_{L/R}$ are present, a viable neutrino mass spectrum is only possible with the inclusion of additional particles, for example a left-handed gauge-singlet fermion $S_L \sim (\mathbf{1}, \mathbf{1}, \mathbf{1})$ for each fermion generation, as otherwise $\nu_{L/R}$ are predicted to be Dirac particles with masses similar to those of the up-type quarks. Light neutrinos can arise due to the inverse and linear see-saw mechanisms [18–26] if small but non-zero lepton number violating mass terms are included. This scenario can allow for the PS breaking scale to be much lower, as we describe below, while allowing for light neutrino masses and therefore we restrict ourselves to the scalar content described in table 1.

2.2 Yukawa sector

The full Yukawa Lagrangian for the fermions f_L , f_R and S_L and the scalars ϕ , χ_L and χ_R is

$$\mathcal{L}_{\text{YUK}} = \text{Tr} \left[y_1 \bar{f}_L \phi (f_R)^T + y_2 \bar{f}_L \phi^c (f_R)^T + y_R \bar{S}_L \chi_R^\dagger f_R + y_L \bar{f}_L \chi_L (S_L)^c \right] + \frac{1}{2} \mu_S \bar{S}_L (S_L)^c + \text{H.c} \quad (2.15)$$

where generational indices are suppressed, $\phi^c = \tau_2 \phi^* \tau_2$ and $\tau_2 = \epsilon^{ab}$ is the two-dimensional Levi-Civita symbol.

After spontaneous symmetry breaking, charged-fermion masses arise from $\langle \phi \rangle$

$$\begin{aligned} m_u &= y_1 v_1 + y_2 v_2^* \\ m_d &= y_1 v_2 + y_2 v_1^* \\ m_e &= m_d, \end{aligned} \quad (2.16)$$

⁶A viable neutrino mass spectrum with $\langle \Delta_R \rangle \ll 10^{12}$ GeV may be possible with a fine-tuned cancellation between the two terms appearing in eq. (2.14) if $y_{L/R}$ have opposite sign, although we will not consider this possibility further.

whereas, within the neutrino sector, mixing between the neutral fermions leads to

$$\frac{1}{2} \begin{pmatrix} \overline{\nu_L} & \overline{\nu_R^c} & \overline{S_L} \end{pmatrix} \begin{pmatrix} 0 & m_u & y_L v_L \\ m_u & 0 & y_R v_R^* \\ y_L v_L & y_R v_R^* & \mu_S \end{pmatrix} \begin{pmatrix} \nu_L^c \\ \nu_R \\ S_L^c \end{pmatrix}. \quad (2.17)$$

Adopting the hierarchy $|\mu_S, y_L v_L| < |m_u| < |y_R v_R|$ and setting all parameters to be real for simplicity leads to

$$\begin{aligned} m_{\nu_1} &\simeq \mu_S \left(\frac{m_u}{y_R v_R} \right)^2 + 2 \frac{y_L v_L}{y_R v_R} m_u \\ m_{\nu_{2,3}} &\simeq y_R v_R \pm \mu_S \end{aligned} \quad (2.18)$$

if only one generation is considered, where the light state is predominantly made up of ν_L and the two heavy states predominantly made up of ν_R and S_L . A viable neutrino mass spectrum is possible for sufficiently small values of the lepton number violating mass terms μ_S and $y_L v_L$. These choices are technically natural and allow for the breaking scale v_R (which breaks PS) to be lowered to $\mathcal{O}(1000)$ TeV or lower.

2.3 Gauge Sector

The kinetic term for each scalar is given by

$$\mathcal{L}_{\text{KIN}}^S = (D_\mu \phi)^\dagger (D^\mu \phi) + (D_\mu \chi_R)^\dagger (D^\mu \chi_R) + (D_\mu \chi_L)^\dagger (D^\mu \chi_L) + \frac{1}{2} \text{Tr} (D_\mu \Phi) (D^\mu \Phi), \quad (2.19)$$

the covariant derivatives are given by

$$\begin{aligned} D_\mu \phi &= \partial_\mu \phi + ig_L \hat{W}_{L\mu} \phi - ig_R \phi \hat{W}_{R\mu} \\ D_\mu \chi_L &= \partial_\mu \chi_L + ig_4 \hat{G}_\mu \chi_L + ig_L \chi_L (\hat{W}_{L\mu})^T \\ D_\mu \chi_R &= \partial_\mu \chi_R + ig_4 \hat{G}_\mu \chi_R + ig_R \chi_R (\hat{W}_{R\mu})^T \\ D_\mu \Phi &= \partial_\mu \Phi + ig_4 [\hat{G}_\mu, \Phi] \end{aligned} \quad (2.20)$$

and $\hat{W}_{L[R]\mu}/\hat{G}_\mu$ are the $SU(2)_{L[R]}/SU(4)$ gauge fields respectively, written as matrices transforming in their defining representation.

After spontaneous symmetry breaking the spectrum of masses and mixings for the different gauge fields can be calculated. We find

$$m_X^2 = g_4^2 \left(\frac{1}{3} v_\Phi^2 + \frac{1}{2} v_L^2 + \frac{1}{2} v_R^2 \right) \quad (2.21)$$

where X_μ corresponds to a colour-triplet vector leptoquark with electric charge 2/3,

$$\mathcal{L}_{\text{KIN}}^S \supset \frac{1}{2} \begin{pmatrix} W_L^+ & W_R^+ \end{pmatrix}_\mu \underbrace{\begin{pmatrix} g_L^2 (v_\phi^2 + v_L^2) & -2g_L g_R v_1 v_2 \\ -2g_L g_R v_1 v_2 & g_R^2 (v_\phi^2 + v_R^2) \end{pmatrix}}_{M_{W^\pm}^2} \begin{pmatrix} W_L^- \\ W_R^- \end{pmatrix}^\mu \quad (2.22)$$

which corresponds to the mixing matrix between the two colour-neutral, electrically-charged gauge bosons with $v_\phi^2 = v_1^2 + v_2^2$ and

$$\mathcal{L}_{\text{KIN}}^{\text{S}} \supset \frac{1}{2} \begin{pmatrix} G_{15} & W_{3L} & W_{3R} \end{pmatrix}_\mu \underbrace{\begin{pmatrix} \frac{3}{2}g_4^2(v_L^2 + v_R^2) & -\sqrt{\frac{3}{2}}g_4g_Lv_L^2 & -\sqrt{\frac{3}{2}}g_4g_Rv_R^2 \\ -\sqrt{\frac{3}{2}}g_4g_Lv_L^2 & g_L^2(v_\phi^2 + v_L^2) & -g_Lg_Rv_\phi^2 \\ -\sqrt{\frac{3}{2}}g_4g_Rv_R^2 & -g_Lg_Rv_\phi^2 & g_R^2(v_\phi^2 + v_R^2) \end{pmatrix}}_{M_0^2} \begin{pmatrix} G_{15} \\ W_{3L} \\ W_{3R} \end{pmatrix}^\mu \quad (2.23)$$

which corresponds to the mixing matrix between the three colour- and electrically-neutral gauge bosons.

While the above equations can be solved numerically, simple analytic expressions can be derived in certain limits. Assuming a hierarchy in the scales of symmetry breaking, $v_{\text{EW}} = \sqrt{v_\phi^2 + v_L^2} < v_R$, leads to the following spectrum of gauge boson masses:

$$\begin{aligned} m_\gamma^2 &= 0, \quad m_Z^2 \simeq \frac{1}{2} \frac{3g_R^2g_4^2 + 3g_L^2g_4^2 + 2g_R^2g_L^2}{3g_4^2 + 2g_R^2} v_{\text{EW}}^2, \quad m_{Z'}^2 \simeq \frac{1}{2} \left(g_R^2 + \frac{3}{2}g_4^2 \right) v_R^2 \\ m_W^2 &\simeq \frac{1}{2} g_L^2 v_{\text{EW}}^2, \quad m_{W'}^2 \simeq \frac{1}{2} g_R^2 (v_R^2 + v_{\text{EW}}^2) \\ m_X^2 &= \frac{1}{2} \left(\frac{2}{3}v_\phi^2 + v_L^2 + v_R^2 \right) g_4^2. \end{aligned} \quad (2.24)$$

where the hypercharge gauge coupling is given by

$$g_Y^2 = \frac{3g_R^2g_4^2}{3g_4^2 + 2g_R^2}. \quad (2.25)$$

Note that $\langle \Phi \rangle$ only contributes to the mass of the vector leptoquark X_μ and otherwise is completely decoupled from the remaining gauge bosons and fermions.

The gauge couplings of G_{PS} (g_4 , g_L and g_R) are related to those of the SM (g_c , g_w and g_Y) at the scale of PS breaking:

$$g_4^2(\mu) = g_c^2(\mu), \quad g_L^2(\mu) = g_w^2(\mu) \quad \text{and} \quad g_R^2(\mu) = \frac{3g_Y^2(\mu)g_c^2(\mu)}{3g_c^2(\mu) - 2g_Y^2(\mu)}. \quad (2.26)$$

As the $SU(4)$ coupling constant is given by the usual colour gauge coupling, at low scales $g_c(\mu) > g_Y(\mu)$ and therefore $g_R(\mu) \simeq g_Y(\mu)$. Figure 1 plots the masses of the electroweak gauge bosons of the theory as a function of the $SU(2)_R$ breaking scale v_R . In order to decouple v_R from significantly impacting the masses of the light, SM-like gauge bosons we roughly find that $v_R > 1200$ GeV is required in order for eq. (2.24) to be a valid approximation. The heavy neutral gauge boson Z' is significantly heavier compared to the heavy charged gauge boson W' and we roughly find a ratio of $m_{Z'}/m_{W'} \simeq 3.5$ at TeV scales. Adoption of the hierarchy $v_\phi \gg v_R$ would imply that the leptoquark X is heavier than both the Z' and W' fields such that $m_{W'} < m_{Z'} \ll m_X$. However, were Φ to be absent or have $v_\phi < v_R$, the spectrum of heavy gauge bosons masses would be $m_{W'} < m_X < m_{Z'}$ with the ratio $m_{Z'}/m_X \simeq 1.3$ at TeV scales.

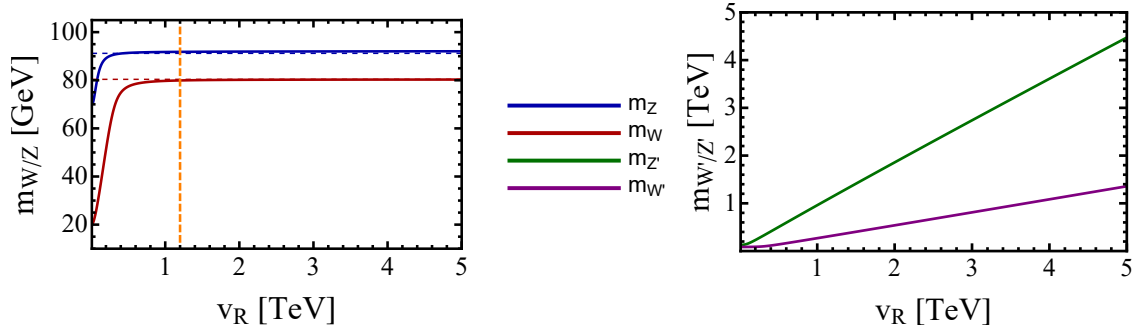


Figure 1. Plot of the masses of the SM-like gauge bosons m_Z and m_W (**left**) and the heavy gauge bosons $m_{Z'}$ and $m_{W'}$ (**right**) as a function of the $SU(2)_R$ breaking scale v_R . Here the masses were found by numerically solving eqs. (2.22) and (2.23) with gauge couplings given by eq. (2.26) assuming the normal running of the SM gauge couplings at these energy scales described in appendix B. We roughly find that $v_R > 1.2$ TeV is required for eq. (2.24) to be valid and to ensure the light gauge fields remain SM-like as indicated by the dashed vertical line, the dashed horizontal lines correspond to the measured masses of the electroweak gauge fields. We find that the Z' gauge field will be significantly heavier than the W' field and a ratio of $m_{Z'}/m_{W'} \simeq 3.5$. This is due to the additional mixing effects occurring between the neutral gauge bosons compared to the charged ones.

2.4 Baryon number violation

In order to assess the implications for baryon number violation arising from the unification of quarks and leptons within PS we consider the Yukawa and kinetic portion of the Lagrangian, and the scalar potential separately. Consider first the electroweak sector of the Yukawa Lagrangian:

$$\mathcal{L}_{\text{YUK,EW}} = \text{Tr} [y_1 \bar{f}_L \phi (f_R)^T + y_2 \bar{f}_L \phi^c (f_R)^T] + \text{H.c.} \quad (2.27)$$

This Lagrangian is invariant under a single global $U(1)_J$ transformation

$$f_L \rightarrow e^{i\theta J} f_L, \quad f_R \rightarrow e^{i\theta J} f_R \quad \text{and} \quad \phi \rightarrow \phi \quad (2.28)$$

and therefore the J charge of each field can be chosen such that

$$J(f_L) = J(f_R) = 1 \quad \text{and} \quad J(\phi) = 0. \quad (2.29)$$

As ϕ is uncharged under the $SU(4)$ of Pati-Salam and the global symmetry J , the vev $\langle \phi \rangle$ also does not break either symmetry e.g. $J(\langle \phi \rangle) = T(\langle \phi \rangle) = 0$, where T corresponds to the fifteenth generator of $SU(4)$ identified with $B - L$. Baryon and lepton number can be identified as different linear combinations of J and T

$$B = \frac{1}{4}(J + T) \quad \text{and} \quad L = \frac{1}{4}(J - 3T) \quad (2.30)$$

such that

$$B(f_L) = B(f_R) = \begin{pmatrix} 1/3 & 1/3 \\ 1/3 & 1/3 \\ 1/3 & 1/3 \\ 0 & 0 \end{pmatrix} \quad \text{and} \quad L(f_L) = L(f_R) = \begin{pmatrix} 0 & 0 \\ 0 & 0 \\ 0 & 0 \\ 1 & 1 \end{pmatrix} \quad (2.31)$$

as required for the embeddings of SM fermion in f_L and f_R defined in eq. (2.4). As the electroweak Yukawa Lagrangian is invariant under both J and T independently in both the broken and unbroken phase, it is clearly also invariant under a linear combination of the two and therefore all interactions conserve both B and L .

Turning to the remaining terms in the Yukawa Lagrangian⁷,

$$\mathcal{L}_{\text{YUK,PS}} = \text{Tr} \left[y_R \bar{S}_L \chi_R^\dagger f_R + y_L \bar{f}_L \chi_L (S_L)^c \right] + \frac{1}{2} \mu_S \bar{S}_L S_L^c + \text{H.c} \quad (2.32)$$

the global symmetry $U(1)_J$ is unbroken with the additional charge assignments

$$J(\chi_L) = J(\chi_R) = 1 \text{ and } J(S_L) = 0 \quad (2.33)$$

where the B and L numbers of each component of $\chi_{L/R}$ are identical to those of $f_{L/R}$. The scalars χ_L and χ_R are charged under both J and T , such that $\frac{1}{4}(J+T)(\langle\chi_{L/R}\rangle) = B(\langle\chi_{L/R}\rangle) = 0$, whereas $\frac{1}{4}(J-3T)(\langle\chi_{L/R}\rangle) = L(\langle\chi_{L/R}\rangle) \neq 0$. Therefore B is conserved by the Yukawa Lagrangian at all scales whereas lepton number is spontaneously broken at the scale of $SU(2)_R$ breaking. Baryon number being an accidental symmetry of the PS Yukawa Lagrangian is a feature which appears to be insensitive to the choice of scalars used to break the PS symmetry. If the scalars $\Delta_{L/R}^\alpha$ defined in eq. (2.8) were present instead of $\chi_{L/R}$ (often considered in high-scale PS models) identical conclusions are reached with baryon number remaining an accidental symmetry of the Yukawa sector while lepton number is spontaneously broken.

The kinetic portion of the Lagrangian

$$\mathcal{L}_{\text{KIN}} = i \sum_F \bar{F} \not{D} F + \sum_S (D_\mu S)^\dagger (D^\mu S), \quad (2.34)$$

where $F = (f_L, f_R, S_L)$ and $S = (\chi_L, \chi_R, \phi, \Phi)$, does not violate $B-L=T$ as it is a gauge symmetry. However it is easy to show that it also conserves a global $B+L = \frac{1}{2}(J-T)$ symmetry where

$$(B+L)(\hat{G}_\mu) = \begin{pmatrix} 0 & 0 & 0 & -2/3 \\ 0 & 0 & 0 & -2/3 \\ 0 & 0 & 0 & -2/3 \\ 2/3 & 2/3 & 2/3 & 0 \end{pmatrix} \quad (2.35)$$

as every gauge field is uncharged under $U(1)_J$ and \hat{G}_μ corresponds to the $SU(4)_c$ gauge fields. The gauge fields of $SU(2)_L$ and $SU(2)_R$ are uncharged under J and T and therefore uncharged under B and L . As the gauge interactions conserve both $B-L$ and $B+L$ simultaneously they necessarily conserve B and L separately and therefore there is no gauge-mediated baryon- or lepton-number violation predicted by PS, though these may appear if PS is embedded into some GUT at a higher scale, with the effects suppressed by the relevant unification scale (see e.g. [27]).

⁷Adopting the scalar and fermion particle content detailed in section 2.1.

A comprehensive analysis of the scalar potential including minimisation of the potential is beyond the scope of this work. Of all the possible gauge invariant terms within the scalar potential, we find only one term⁸ which will violate $U(1)_J$ for the charge assignments imposed by the Yukawa Lagrangian:

$$V(\phi, \Phi, \chi_L, \chi_R) \supset \tilde{\lambda}_{LR} (\chi_L)^{Aa} (\chi_L)^{Bb} (\chi_R)^{C\alpha} (\chi_R)^{D\beta} \epsilon_{ABCD} \epsilon_{ab} \epsilon_{\alpha\beta}, \quad (2.36)$$

where $(A, B, \dots)/(a, b, \dots)/(\alpha, \beta, \dots)$ correspond to $SU(4)/SU(2)_L/SU(2)_R$ indices respectively. As $J(\chi_{L/R}) = 1$ is required by the Yukawa sector, the existence of this term in the scalar potential violates J by four units and therefore violates B by one unit.

Therefore proton and neutron decay diagrams can exist within low-scale PS and will involve a combination of the couplings y_R, y_L and $\tilde{\lambda}_{LR}$. This requires the existence of both χ_L and χ_R . Models with only χ_R included (required for PS breaking) have exact proton stability assuming no additional particle content. Additionally, baryon number can be easily imposed when both scalars are present by setting $\tilde{\lambda}_{LR} \rightarrow 0$ which is not constrained by any other phenomenology and is technically natural and therefore insensitive to quantum corrections. Constraining the allowed size of $\tilde{\lambda}_{LR}$ from the current experimental constraints on rare proton and neutron decays is beyond the scope of this work. However, this was briefly looked at in [5] for a similar model where they found $\tilde{\lambda}_{LR} \leq 10^{-5}$ as a constraint arising from $N \rightarrow ee\nu$. PS models therefore are relatively unconstrained by baryon number violating decays compared to GUT scenarios and other experimental measurements (or lack thereof) are required in order to constrain the scale of PS breaking.

3 Probing Pati-Salam models through rare meson decays

A promising probe of the scale of Pati-Salam breaking is through the contributions of the gauge and scalar leptoquarks predicted by different realisations of the model to low-energy hadronic processes. Of particular significance is the gauge boson leptoquark X_μ which must couple universally to all three generations of fermions. This is unlike the various possible scalar leptoquarks for which the Yukawa couplings to the lighter generations could be suppressed, perhaps through a flavour symmetry. Additionally as $SU(3)_c$ is a subgroup of the $SU(4)$ appearing in G_{PS} , the coupling strength of the leptoquark X_μ to the SM quarks is related to that of g_c and cannot be treated as a free parameter. Therefore precision flavour experiments involving the lighter generations provide stringent limits⁹ on the mass

⁸Additionally there are two extra possible terms $\tilde{\lambda}_L (\chi_L)^4 = \tilde{\lambda}_L (\chi_L)^{Aa} (\chi_L)^{Bb} (\chi_L)^{C\alpha} (\chi_L)^{D\beta} \epsilon_{ABCD} \epsilon_{ab} \epsilon_{\alpha\beta}$ and $\tilde{\lambda}_R (\chi_R)^4 = \tilde{\lambda}_R (\chi_R)^{A\alpha} (\chi_R)^{B\beta} (\chi_R)^{C\gamma} (\chi_R)^{D\delta} \epsilon_{ABCD} \epsilon_{\alpha\beta} \epsilon_{\gamma\delta}$ which would also break $U(1)_J$ however we find them to be identically zero once contracted.

⁹If a scalar leptoquark is present which also mediates the same decay, destructive interference between the gauge and scalar contribution to the hadronic process can somewhat lower the limits on the mass of X by up to a factor of 2 [28] depending on the mass(es) and couplings of the relevant scalar(s). In our analysis we will focus solely on the contribution from the gauge leptoquark and neglect possible regions of destructive interference with scalar contributions by assuming the masses of the scalars to be heavier than the gauge leptoquark.

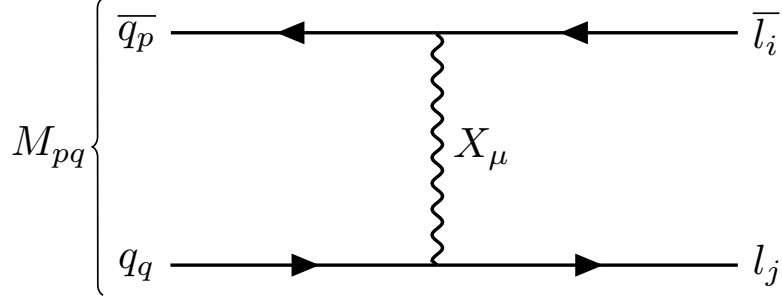


Figure 2. Tree-level Feynman diagram of the leptonic decay of a scalar meson M_{pq} , where q_p and q_q correspond to the valence quarks of the meson, to the lepton pair $l_{i,j}$ ($i, j = e, \mu, \tau$) mediated by the PS gauge leptoquark X_μ . PS unifies quarks and leptons of similar isospin, therefore the processes mediated by X_μ at tree-level are easily predicted, e.g. if q_q corresponds to an up-type quark then l_j must be a neutrino. The strongest limits on the mass of X_μ arise in the case where p and q are both down-type quarks, where $M_{pq} = (K_L^0, B_d^0, B_s^0, \dots)$, and therefore the final state comprises of charged leptons with opposite sign.

of the gauge leptoquark X_μ which directly limits the scale of PS breaking (either v_Φ or v_R) through eq. (2.24).

3.1 Neutral Pseudoscalar meson decays induced by X_μ

The most stringent constraint on the mass of X_μ arises from limits on rare leptonic decays of pseudoscalar mesons, mediated at tree level by X_μ as shown in fig. 2. As Pati-Salam unifies quarks and leptons with the same $SU(2)_{L/R}$ isospin into the same $SU(4)$ multiplet, as shown by eq. (2.4), it couples up-type quarks to neutrinos and down-type quarks to the charged leptons. Therefore the leptonic decay channels induced by X_μ at tree-level can be predicted based on the valence quark content of the relevant meson. For example, X_μ will mediate the leptonic decay $D^0 \rightarrow \bar{\nu}\nu$ as both valence quarks are up-type but not $D^0 \rightarrow \ell^+\ell^-$. Unsurprisingly the meson decay channels which lead to the most stringent limits on the mass of X_μ arise from opposite-sign charged-lepton final states where there is no missing energy, which only occurs in PS for neutral mesons with down-type valence quarks. As a result, the mass of X_μ is most constrained by measurements of the decays of K_L^0 , B_d^0 and B_s^0 mesons whose leptonic decay channels are the most well measured.

The leptoquark X_μ couples to the fermions through their kinetic terms in the Lagrangian

$$\mathcal{L}_{\text{KIN}}^{\text{F}} = i\bar{f}_L \not{D} f_L + i\bar{f}_R \not{D} f_R \quad (3.1)$$

where the covariant derivatives for $f_{L/R}$ are defined similarly to $\chi_{L/R}$ given in eq. (2.20). Expanding out eq. (3.1) explicitly with the fermion multiplets given in eq. (2.4) and leaving

only the interactions of interest gives

$$\mathcal{L}_{\text{KIN}}^{\text{F}} \supset \frac{g_4}{\sqrt{2}} (\bar{d} \not{X} P_L e + \bar{d} \not{X} P_R e) + \text{H.c.}, \quad (3.2)$$

where colour and generational indices have been suppressed. Here the fields d and e represent the gauge eigenstates. Rotating to the mass eigenstates leads to

$$\mathcal{L}_{Xde} = \frac{g_4}{\sqrt{2}} \left(\bar{d}'_i (K_L^{de})_{ij} \not{X} P_L e'_j + \bar{d}'_i (K_R^{de})_{ij} \not{X} P_R e'_j \right) + \text{H.c.} \quad (3.3)$$

where now the generational indices are explicitly shown and primed fields represent mass eigenstates¹⁰. The matrices $K_{L/R}^{de}$ are CKM-like mixing matrices between the down-type quarks and charged leptons. The existence of both left- and right-handed couplings to X_μ leads to two different mixing matrices which, without a parity symmetry, are not necessarily equal. The matrices can be expressed in terms of the unitary matrices used to diagonalise the mass matrices e.g. $(U_L^i)^\dagger M_i U_R^i = M_i^d = \text{diag}(\dots)$. For the case of G_{PS} in total there are eight different physical mixing matrices (compared to the two of the SM) given by

$$\begin{aligned} V_L^{\text{CKM}} &= (U_L^u)^\dagger U_L^d, & V_R^{\text{CKM}} &= (U_R^u)^\dagger U_R^d, & K_L^{de} &= (U_L^d)^\dagger U_L^e, & K_R^{de} &= (U_R^d)^\dagger U_R^e \\ U_L^{\text{LEPT}} &= (U_L^\nu)^\dagger U_L^e, & U_R^{\text{LEPT}} &= (U_R^\nu)^\dagger U_R^e, & K_L^{u\nu} &= (U_L^u)^\dagger U_L^\nu, & K_R^{u\nu} &= (U_R^u)^\dagger U_R^\nu \end{aligned} \quad (3.4)$$

where $U_{L/R}^\nu$ is a $3 \times (3+n)$ matrix due to the possible seesaw nature of the neutrino sector and the upper-left 3×3 block of U_L^{LEPT} is given by the PMNS matrix.

For a pseudo-scalar meson M_{pq} , where q_p and q_q correspond to the valence quarks of the meson e.g. $B_d^0 = M_{bd}$, the partial width for the two-body decay $M_{pq} \rightarrow \ell_i^+ \ell_j^-$ is given by [28, 29]

$$\Gamma_{M_{pq} \rightarrow \ell_i^+ \ell_j^-} = \frac{m_{M_{pq}}}{16\pi} \lambda(m_{M_{pq}}, m_{\ell_i}, m_{\ell_j}) \sum_h |\mathcal{M}_{pq,ij}|^2 \quad (3.5)$$

where

$$\lambda(m_{M_{pq}}, m_{\ell_i}, m_{\ell_j}) = \sqrt{\left[1 - (\mu_{\ell_i} + \mu_{\ell_j})^2\right] \left[1 - (\mu_{\ell_i} - \mu_{\ell_j})^2\right]} \quad (3.6)$$

and $\mu_X = m_X/m_{M_{pq}}$. For the decay of a scalar to two fermions the sum over helicity states is given by

$$\begin{aligned} \sum_h |\mathcal{M}_{pq,ij}|^2 &= \left(1 - \mu_{\ell_i}^2 - \mu_{\ell_j}^2\right) \left[|\mathcal{M}_{pq,ij}^L|^2 + |\mathcal{M}_{pq,ij}^R|^2 \right] \\ &\quad - 2\mu_{\ell_i}\mu_{\ell_j} \left[\mathcal{M}_{pq,ij}^L (\mathcal{M}_{pq,ij}^R)^* + \mathcal{M}_{pq,ij}^R (\mathcal{M}_{pq,ij}^L)^* \right] \end{aligned} \quad (3.7)$$

where

$$\mathcal{M}_{pq,ij} \equiv \mathcal{M}_{pq,ij}^L \bar{u}(p_{\ell_j}) P_L v(p_{\ell_i}) + \mathcal{M}_{pq,ij}^R \bar{u}(p_{\ell_j}) P_R v(p_{\ell_i}). \quad (3.8)$$

¹⁰Where there is no chance of confusion between gauge and mass eigenstates, fields will remain unprimed for both basis.

The matrix elements of the axial and pseudoscalar currents for the relevant mesons are given by [16, 28]

$$\begin{aligned}\langle 0 | \bar{d}_p \gamma^\mu \gamma^5 d_q | M_{pq} \rangle &= i f_{M_{pq}} (p_{\ell_j}^\mu + p_{\ell_i}^\mu) \\ \langle 0 | \bar{d}_p \gamma^5 d_q | M_{pq} \rangle &= -i f_{M_{pq}} \bar{m}_{pq}\end{aligned}\quad (3.9)$$

where $f_{M_{pq}}$ is the meson's decay constant and $\bar{m}_{pq} = m_{M_{pq}}^2 / (m_{q_p} + m_{q_q})$. Combining these matrix elements with fig. 2 and eq. (3.3) leads to

$$\mathcal{M}_{pq,ij}^{L/R} = f_{M_{pq}} \left[R_{pq} \bar{m}_{pq} (M_P^{L/R})_{pq,ij} - \left\{ m_{\ell_j} (M_A^{L/R})_{pq,ij} - m_{\ell_i} (M_A^{R/L})_{pq,ij} \right\} \right] \quad (3.10)$$

where

$$\begin{aligned}(M_A^{L/R})_{pq,ij} &= \mp \frac{g_4^2}{4m_V^2} (K_{L/R}^{de})_{pi} (K_{L/R}^{de})_{qj}^* \\ (M_P^{L/R})_{pq,ij} &= \mp \frac{g_4^2}{2m_V^2} (K_{L/R}^{de})_{pi} (K_{R/L}^{de})_{qj}^*\end{aligned}\quad (3.11)$$

and R_{pq} is a factor introduced to account for the running of the strong coupling from the high scale, $\mu \sim m_X$, down to the relevant hadron mass scale, $\mu \sim m_{M_{pq}}$. This leads to an enhancement in the pseudoscalar-current matrix element in eq. (3.9) [28, 30] but no enhancement for the axial current which does not run due to the Ward identity of QCD [31].

To demonstrate, for the leptonic decays of K_L^0 the correction factor is given by

$$R_{K_L^0}(m_{K_L^0}, m_X) = R(m_{K_L^0}, m_c; 3) R(m_c, m_b; 4) R(m_b, m_t; 5) R(m_t, m_X; 6) \quad (3.12)$$

where

$$R(\mu_1, \mu_2; n_f) = [g_c(\mu_1)/g_c(\mu_2)]^{8/b(n_f)}, \quad (3.13)$$

$b(n_f) = 11 - (2/3)n_f$ and n_f corresponding to the number of active quark flavours in each energy regime.

As X_μ couples to both left- and right-handed quarks and leptons, two different types of contributions can be seen in eq. (3.10). The first term does not depend on the masses of the final state leptons and corresponds to the helicity-unsuppressed contribution and only exists if both $K_{L/R}^{de}$ exist, which is only possible if X_μ couples to both fermion chiralities. The last two terms are proportional to the final state charged lepton masses. This corresponds to the helicity-suppressed contribution which arises from a mass insertion and only requires one of $K_{L/R}^{de}$ to exist. It is forbidden in the limit of massless final-state leptons, in complete analogy to weak meson decays in the SM. If the final state particle masses are ignored, the decay width is given purely by the helicity-unsuppressed contribution, and can be simplified to [28, 32, 33]

$$\Gamma_{M_{pq} \rightarrow \ell_i^+ \ell_j^-}^{\text{HU}} = \frac{m_{M_{pq}} [g_4(m_X)]^4 f_{M_{pq}}^2 \bar{m}_{pq}^2}{64 \pi m_X^4} R_{pq}^2 \left(|K_L^{de}|_{pi}^2 |K_R^{de}|_{qj}^2 + |K_R^{de}|_{pi}^2 |K_L^{de}|_{qj}^2 \right). \quad (3.14)$$

In the limit where X_μ couples to only one chirality of fermions¹¹ similar to the weak force, $M_P^{L/R} = 0$ but one of $M_A^{L/R}$ remains nonzero. This results in the total decay width depending only on the helicity-suppressed terms appearing in eq. (3.10). The usual result for helicity-suppressed meson decays is recovered

$$\Gamma_{M_{pq} \rightarrow \ell_i^+ \ell_j^-}^{\text{HS}} = \frac{m_{M_{pq}} [g_4(m_X)]^4 f_{M_{pq}}^2}{256 \pi m_X^4} \sqrt{[1 - (\mu_{\ell_i} + \mu_{\ell_j})^2] [1 - (\mu_{\ell_i} - \mu_{\ell_j})^2]} \times \left[(1 - \mu_{\ell_i}^2 - \mu_{\ell_j}^2) (m_{\ell_i}^2 + m_{\ell_j}^2) - 4\mu_{\ell_i} \mu_{\ell_j} m_{\ell_i} m_{\ell_j} \right] \quad (3.15)$$

which, in the limit $m_{\ell_j} > m_{\ell_i}$, is well approximated by

$$\Gamma_{M_{pq} \rightarrow \ell_i^+ \ell_j^-}^{\text{HS}} \simeq \frac{m_{M_{pq}} [g_4(m_X)]^4 f_{M_{pq}}^2}{256 \pi m_X^4} m_{\ell_j}^2 \left(1 - \frac{m_{\ell_j}^2}{m_{M_{pq}}^2} \right)^2 \left(|K^{de}|_{pi}^2 |K^{de}|_{qj}^2 \right), \quad (3.16)$$

where K^{de} corresponds to either K_L^{de} or K_R^{de} depending on which chirality of fermions X_μ couples to. Comparing eqs. (3.14) and (3.16) unsurprisingly suggests that generically the helicity-unsuppressed contribution is expected to dominate:

$$R_{\text{HU/HS}} = \frac{\Gamma_{\text{HU}}}{\Gamma_{\text{HS}}} \simeq \frac{4 \bar{m}_{pq}^2 R_{pq}^2}{m_{\ell_j}^2} \underbrace{\left(\frac{|K_L^{de}|_{pi}^2 |K_R^{de}|_{qj}^2 + |K_R^{de}|_{pi}^2 |K_L^{de}|_{qj}^2}{|K_L^{de}|_{pi}^2 |K_L^{de}|_{qj}^2 + |K_R^{de}|_{pi}^2 |K_R^{de}|_{qj}^2} \right)}_{\kappa}. \quad (3.17)$$

For example, for $K_L^0 \rightarrow \mu e$ we roughly find $R_{\text{HU/HS}} \simeq 10^4 \kappa$ where κ corresponds to the combination of mixing matrices involving $K_{L/R}^{de}$ above. However the helicity unsuppressed contribution can be sub-dominant if the couplings are strongly suppressed for one chirality over the other e.g. $|K_L^{de}|_{pi/qj} \neq 0$ and $|K_R^{de}|_{pi/qj} \simeq 0$. In such scenarios the limits for the vector leptoquark mass (and the therefore the PS breaking scale) will be significantly decreased due to a reduction in the decay rate with $R_{\text{HU/HS}} < 1$. However this would require the hierarchy

$$\frac{4 \bar{m}_{pq}^2 R_{pq}^2}{m_{\ell_j}^2} < \frac{1}{\kappa} \quad (3.18)$$

implying a difference in the couplings of X_μ to f_L and f_R of several order of magnitude at least.

The contribution to the decay widths from the PS gauge leptoquark in eq. (3.5) depends on both the mass of the leptoquark m_X as well as to the different elements of $K_{L/R}^{de}$. These physical mixing matrices are currently unconstrained and different textures within each matrix can significantly change the relative strength of specific lepton flavour decay channels over others for a given meson. As limits and measurements of different

¹¹This is a special case of the general case which occurs for example by setting $K_R^{de} = 0_{3 \times 3}$ but K_L^{de} remains unitary.

processes differ in sensitivity, the limits on the leptoquark mass (and therefore the scale of PS breaking) can vary significantly for different choices of the mixing matrices $K_{L/R}^{de}$.

To demonstrate this, we define general unitary matrices for $K_{L/R}^{de}$,

$$K_{L/R}^{de} = K_{23}(\theta_{23}^{L/R}, \delta^{L/R}) K_{13}(\theta_{13}^{L/R}) K_{12}(\theta_{12}^{L/R})$$

$$= \begin{pmatrix} c_{12} c_{13} & c_{13} s_{12} & s_{13} \\ -c_{23} s_{12} - e^{i\delta} c_{12} s_{13} s_{23} & c_{12} c_{23} - e^{i\delta} s_{12} s_{13} s_{23} & e^{i\delta} c_{13} s_{23} \\ -c_{12} c_{23} s_{13} + e^{-i\delta} s_{12} s_{23} & -c_{23} s_{12} s_{13} - e^{-i\delta} c_{12} s_{23} & c_{13} c_{23} \end{pmatrix}^{L/R} \quad (3.19)$$

where $c_x := \cos(x)$ and $s_x := \sin(x)$ as usual. In principle the matrix K_L^{de} should contain all six possible phases as by convention rephasing of quark and lepton fields fixes the phases appearing in V_L^{CKM} and U_L^{LEPT} and therefore no rephasing¹² can occur for K_L^{de} or $K_L^{u\nu}$. However only one complex phase is important for the discussion below and therefore we ignore all other possible complex phases which can appear in $K_{L/R}^{de}$.

Table 2 lists the meson decay channels of interest¹³ alongside either their measured branching fractions or the current experimental upper limit. Additionally we indicate which two matrix elements of $K_{L/R}^{de}$ are required to be non-zero in order for X_μ to mediate this process through fig. 2. Note that for lepton-flavour violating decays there are two possible combinations of non-zero matrix elements which mediate a decay which is taken into account in our calculations. It is clear from table 2 that the decays of K_L^0 are currently the most experimentally probed channels, with the lepton-flavour violating decay $K_L^0 \rightarrow \mu e$ having the most sensitive upper limit of any process.

In contrast the current experimental precision for the decays of $B_{d/s}^0$ is, for most channels, significantly weaker and will lead to weaker limits. Therefore the lower mass bound on X_μ will vary most depending on whether the structure of $K_{L/R}^{de}$ leads to decays of K_L^0 or not. A thorough analysis for general unitary matrices similar to eq. (3.19) for the PS gauge leptoquark has been performed [33] to find what conditions are required on $K_{L/R}^{de}$ in order to suppress the decays of K_L^0 , either preventing them completely or significantly reducing the predicted decay width by removing the helicity-unsuppressed contribution. Two possible scenarios were found. Firstly if

$$\theta_{23}^L = \theta_{23}^R = \frac{\pi}{2}, \quad \theta_{13}^L = \theta_{13}^R = \theta, \quad \delta^L = \delta \quad \text{and} \quad \delta^R = \pi - \delta \quad (3.20)$$

¹²In contrast K_R^{de} could be chosen to contain one complex phase if the other right-handed physical mixing matrices are left as general unitary matrices. However a more natural choice of basis would be to rephase the fields appearing in V_R^{CKM} and U_R^{LEPT} in analogy with the left-handed mixing matrices.

¹³All neutral-pseudoscalar mesons will receive a similar contribution however in the cases of other mesons not listed (such as the π^0 , η , η' , Υ etc) we find the limits on m_X are subdominant compared to the mesons listed in table 2 when comparing the predicted branching fraction induced by X_μ compared to the experimental sensitivity.

Hadronic Process	Measured value or upper limit	$(p, i)(q, j)$
$\mathcal{B}(K_L^0 \rightarrow ee)$	$9.0_{-4.0}^{+6.0} \times 10^{-12}$	(1,1)(2,1)
$\mathcal{B}(K_L^0 \rightarrow \mu\mu)$	$6.84_{-0.11}^{+0.11} \times 10^{-12}$	(1,2)(2,2)
$\mathcal{B}(K_L^0 \rightarrow \mu e)$	$< 4.7 \times 10^{-12}$	(1,2)(2,1)/(1,1)(2,2)
$\mathcal{B}(B_d^0 \rightarrow ee)$	$< 8.3 \times 10^{-8}$	(1,1)(3,1)
$\mathcal{B}(B_d^0 \rightarrow \mu\mu)$	$< 3.6 \times 10^{-10}$	(1,2)(3,2)
$\mathcal{B}(B_d^0 \rightarrow \tau\tau)$	$< 2.1 \times 10^{-3}$	(1,3)(3,3)
$\mathcal{B}(B_d^0 \rightarrow \mu e)$	$< 1.0 \times 10^{-9}$	(1,2)(3,1)/(1,1)(3,2)
$\mathcal{B}(B_d^0 \rightarrow \tau e)$	$< 2.8 \times 10^{-5}$	(1,3)(3,1)/(1,1)(3,3)
$\mathcal{B}(B_d^0 \rightarrow \tau\mu)$	$< 2.2 \times 10^{-5}$	(1,3)(3,2)/(1,2)(3,3)
$\mathcal{B}(B_s^0 \rightarrow ee)$	$< 2.8 \times 10^{-7}$	(2,1)(3,1)
$\mathcal{B}(B_s^0 \rightarrow \mu\mu)$	$3.0_{-0.4}^{+0.4} \times 10^{-9}$	(2,2)(3,2)
$\mathcal{B}(B_s^0 \rightarrow \tau\tau)$	$< 6.8 \times 10^{-3}$	(2,3)(3,3)
$\mathcal{B}(B_s^0 \rightarrow \mu e)$	$< 5.4 \times 10^{-9}$	(2,2)(3,1)/(2,1)(3,2)
$\mathcal{B}(B_s^0 \rightarrow \tau e)$	—	(2,3)(3,1)/(2,1)(3,3)
$\mathcal{B}(B_s^0 \rightarrow \tau\mu)$	—	(2,2)(3,3)/(3,2)(2,3)

Table 2. Experimental measurements and upper limits on rare leptonic decays of various pseudo-scalar mesons which form the dominant constraint on the scale of Pati-Salam breaking. The third column represents which entries of the matrices $(K_{L/R}^{de})_{pi}$ and $(K_{L/R}^{de})_{qj}$ need to be non-zero for the given decay channel to occur via X_μ where p, q correspond to the valence down-type quarks, $(d, s, b) = (1, 2, 3)$ and i, j to the final state charged leptons $(e, \mu, \tau) = (1, 2, 3)$ for the diagram in fig. 2. Lepton-flavour violating decay modes can occur via two different possible diagrams. For example the process $B_d^0 \rightarrow \mu e$ can arise from the (3, 1) and (1, 2) entries which corresponds to the couplings $\bar{b}\not{X}e$ and $\bar{d}\not{X}\mu$ leading to $B_d^0 \rightarrow \mu^- e^+$, but can also have a contribution from (3, 2) and (1, 1) which corresponds to $\bar{b}\not{X}\mu$ and $\bar{d}\not{X}e$ and leads to $B_d^0 \rightarrow e^- \mu^+$.

is satisfied by eq. (3.19), this leads to

$$K_L^{de} = \begin{pmatrix} c_{12}^L c_\theta & s_{12}^L c_\theta & s_\theta \\ -e^{i\delta} c_{12}^L s_\theta & -e^{i\delta} s_{12}^L s_\theta & e^{i\delta} c_\theta \\ e^{-i\delta} s_{12}^L & -e^{-i\delta} c_{12}^L & 0 \end{pmatrix} \quad \text{and} \quad K_R^{de} = \begin{pmatrix} c_{12}^R c_\theta & s_{12}^R c_\theta & s_\theta \\ e^{-i\delta} c_{12}^R s_\theta & e^{-i\delta} s_{12}^R s_\theta & -e^{-i\delta} c_\theta \\ -e^{i\delta} s_{12}^R & e^{i\delta} c_{12}^R & 0 \end{pmatrix}. \quad (3.21)$$

These matrix structures will not completely prevent the decays of K_L^0 . However, they will prevent the helicity-unsuppressed terms from contributing and therefore will be suppressed by the final-state lepton masses similar to weak decays in the SM. Note that all the entries of the upper-left 2×2 block of $K_{L/R}^{de}$ are non-zero, but an important cancellation in the amplitude arises as $\delta^{L/R}$ are exactly out of phase. Note that the (3, 3) entry of both matrices is zero and therefore for this scenario the decays $B_d^0 \rightarrow \tau\tau$ and $B_s^0 \rightarrow \tau\tau$ cannot occur. It

is interesting to note that if δ is maximally CP violating then the helicity unsuppressed contribution completely disappears and therefore there is no contribution to the decay of K_L^0 , whereas the helicity-suppressed contribution to this decay is maximised if δ is CP conserving.

Alternatively the desired decays can be completely prevented with the simple condition

$$\theta_{13}^L = \theta_{13}^R = \frac{\pi}{2} \quad (3.22)$$

which leads to

$$K_{L/R}^{de} = \begin{pmatrix} 0 & 0 & 1 \\ -c_{23} s_{12} - e^{i\delta} c_{12} s_{23} & c_{12} c_{23} - e^{i\delta} s_{12} s_{23} & 0 \\ -c_{12} c_{23} + e^{-i\delta} s_{12} s_{23} & -c_{23} s_{12} - e^{-i\delta} c_{12} s_{23} & 0 \end{pmatrix}^{L/R}. \quad (3.23)$$

Here the decays of K_L^0 trivially do not occur as both the $(1, 1)$ and $(1, 2)$ entries of $K_{L/R}^{de}$ are exactly zero and as can be seen in table 2, X_μ will not mediate the relevant decays. Similar to the previous scenario the decays $B_d^0 \rightarrow \tau\tau$ and $B_s^0 \rightarrow \tau\tau$ do not occur. Additionally, the processes $B_d^0 \rightarrow (ee, \mu\mu, \tau e)$ and $B_s^0 \rightarrow (\tau e, \tau\mu)$ will not occur as the $(2, 3)$ entry is also zero. Therefore, for low-scale PS, the suppressed decay channels for $B_{d/s}^0 \rightarrow \tau\tau$ are directly correlated with suppressed decays of K_L^0 . Increasing the experimental sensitivity of these channels could therefore provide a powerful test of PS, especially if a non-SM signal was detected in these channels as no such signal has been seen in the decays of K_L^0 .

In both scenarios above which lead to the lowest possible limits on the PS gauge leptoquark, the matrices K_L^{de} and K_R^{de} are required to have a similar structure to each other. The first scenario allows for only four free parameters between the two matrices whereas in the second scenario six free parameters exist. In order for both these matrices (which are naïvely unrelated) to have the same structure suggests that a parity symmetry must be enforced at some scale. The two matrices do not have to be exactly equal to each other, although this is also possible. However in both scenarios at least one angle has to be identical for both matrices. As discussed previously it has been found that enforcing a parity symmetry alongside the PS gauge groups requires parity to be broken at $\mathcal{O}(10^{12})$ GeV or higher [3, 17]. As we are interested in minimising the scale of PS breaking it would seem quite coincidental for both K_L^{de} and K_R^{de} to be so similar at low scales (and rather unlikely for them to be exactly equal) with such a high scale of parity breaking. However, this requires a full analysis of the running of the relevant mixing angles which we will not explore further. It may be possible that at some high scale $K_{L/R}^{de}$ are equal to each other and after parity breaking some (all) angles are insensitive to running effects whereas others (none) run significantly, leading to the desired form for the mixing matrices.

In addition to the two scenarios above which completely prevent X_μ from inducing decays of K_L^0 we identify two additional scenarios which would prevent the LFV decay $K_L^0 \rightarrow \mu e$ but not necessarily the decays $K_L^0 \rightarrow ee$ or $K_L^0 \rightarrow \mu\mu$. For example if the

conditions

$$\theta_{12}^L = \theta_{12}^R = 0 \quad \text{and} \quad \theta_{23}^L = \theta_{23}^R = \frac{\pi}{2} \quad (3.24)$$

are satisfied, this leads to

$$K_{L/R}^{de} = \begin{pmatrix} c_{13} & 0 & s_{13} \\ -e^{i\delta} s_{13} & 0 & e^{i\delta} c_{13} \\ 0 & -e^{-i\delta} & 0 \end{pmatrix}^{L/R}, \quad (3.25)$$

and the decays $K_L^0 \rightarrow \mu e$ and $K_L^0 \rightarrow \mu\mu$ do not occur via X_μ . However the decay $K_L^0 \rightarrow ee$ does occur as suggested by table 2. Similarly if

$$\theta_{12}^L = \theta_{12}^R = \frac{\pi}{2} \quad \text{and} \quad \theta_{23}^L = \theta_{23}^R = \frac{\pi}{2} \quad (3.26)$$

is satisfied, this leads to

$$K_{L/R}^{de} = \begin{pmatrix} 0 & c_{13} & s_{13} \\ 0 & -e^{i\delta} s_{13} & e^{i\delta} c_{13} \\ e^{-i\delta} & 0 & 0 \end{pmatrix}^{L/R}. \quad (3.27)$$

The decays $K_L^0 \rightarrow \mu e$ and $K_L^0 \rightarrow ee$ will not occur, but $K_L^0 \rightarrow \mu\mu$ will, forming a strong constraint on the mass of X_μ .

Finally as the decay channel $K_L^0 \rightarrow \mu e$ is currently the most precisely constrained of all relevant meson decay channels the *largest* lower bound on the mass of X_μ will occur for $K_{L/R}^{de}$ which have a form that maximises this particular decay channel. Table 2, which indicates which entries of $K_{L/R}^{de}$ mediate this decay, suggests that if for example the mixing matrices were given by

$$K_{L/R}^{de} = \begin{pmatrix} 1 & 0 & 0 \\ 0 & 1 & 0 \\ 0 & 0 & 1 \end{pmatrix} \quad (3.28)$$

then the contribution to the decay channel would be maximised. Therefore the current mass limits on the PS gauge leptoquark (and the breaking scale) can fluctuate between the mass limits obtained if the mixing matrices are given by eqs. (3.21) and (3.23) up to the limits obtained if the matrices are given by eq. (3.28).

In order to numerically find the lower-bound mass range for X_μ we fix the values of the total decay width of each relevant meson to the experimentally observed central values

$$\Gamma_{K_L^0}^{\text{TOT}} = 1.29 \times 10^{-17} \text{ GeV}, \quad \Gamma_{B_d^0}^{\text{TOT}} = 4.33 \times 10^{-13} \text{ GeV} \quad \text{and} \quad \Gamma_{B_s^0}^{\text{TOT}} = 4.36 \times 10^{-13} \text{ GeV}, \quad (3.29)$$

which we take from the PDG [34]. The parameter R_{pq} which appears in the helicity-unsuppressed contribution to a given decay and is defined in eq. (3.12) requires running

from the scale $\mu = m_X$ down to $\mu = m_{M_{pq}}$ and the gauge coupling constant g_4 is related to the strong coupling constant at the scale of PS breaking:

$$\begin{aligned}
g_4(m_X) &= g_c(m_X) = 2\sqrt{\pi} \left(\frac{17}{2} + \frac{7}{2\pi} \log \left[\frac{m_X}{90} \right] \right)^{-1/2} \\
R_{K_L^0} &\simeq 0.51 \left(\frac{17}{2} + \frac{7}{2\pi} \log \left[\frac{m_X}{90} \right] \right)^{4/7} \\
R_{B_s^0} &\simeq R_{B_d^0} \simeq 0.37 \left(\frac{17}{2} + \frac{7}{2\pi} \log \left[\frac{m_X}{90} \right] \right)^{4/7}
\end{aligned} \tag{3.30}$$

where m_X is in units of GeV and for simplicity we assume the one-loop SM running of the gauge coupling constant g_c which can be found in appendix B. We calculate lower bound limits on the leptoquark mass by numerically solving eqs. (3.5) and (3.30) as a function of the leptoquark mass and comparing to the experimental limits listed in table 2.

Table 3 shows the calculated lower bound on the gauge leptoquark masses for the relevant decay channel with different choices of $K_{L/R}^{de}$ corresponding to the five scenarios above. Maximising the leptoquark's contribution to $K_L^0 \rightarrow \mu e$ as in eq. (3.28) leads to limits on the gauge leptoquark mass of roughly 2500 TeV, similar to previous studies [16, 30, 32]. The other non-zero decays in this case indicate which other channels will occur in this scenario: $B_d^0 \rightarrow \tau e$ and $B_s^0 \rightarrow \tau \mu$. More realistically we would expect the matrices $K_{L/R}^{de}$ to be approximately diagonal rather than exactly, and therefore other processes would also be mediated by X_μ , but the three listed would have the strongest signals.

If $K_{L/R}^{de}$ is of the form described in eq. (3.21), decays of K_L^0 still occur but are helicity suppressed. This reduces the limits obtained from 2500 TeV down to $\mathcal{O}(100)$ TeV (with some sensitivity to the free mixing angles) where notably the channel $K_L^0 \rightarrow ee$ leads to limits on the gauge leptoquark mass of $\mathcal{O}(10)$ TeV. This significant reduction compared to other channels of K_L^0 is due to the helicity-suppression of electron final states being significantly larger than for muon final states. For this scenario neglecting the electron and muon mass, as was done in [33], would suggest that X_μ does not mediate K_L^0 decays. However, we find when included they lead to comparable limits for m_X to the helicity-unsuppressed B_d^0 and B_s^0 decays. This is due to the larger experimental precision obtained for K_L^0 decays and therefore we find that the muon mass cannot be ignored. As mentioned previously, if δ is maximally violating the helicity-unsuppressed decays of K_L^0 are forbidden and in this limit the results of [33] remain valid.

If the mixing matrices are given by eq. (3.23), decays of K_L^0 do not occur via X_μ either helicity-suppressed or -unsuppressed. Only five decay channels are non-zero in this scenario and the dominant mass limit will arise from decays of B_s^0 and are of similar order to the previous scenario: $m_X \sim \mathcal{O}(100)$ TeV. The final two scenarios described by eqs. (3.25) and (3.27) completely suppress the channel $K_L^0 \rightarrow \mu e$ but does not suppress the lepton-flavour conserving channels of K_L^0 . Here the resulting mass limits are $\mathcal{O}(1900)$ TeV unless the mixing angles in κ were significantly tuned (e.g. $\theta_{12}^L \simeq -\theta_{12}^R$) in order to suppress

	$K_L^{de} = K_R^{de} = \mathbb{1}_{3 \times 3}$	SCENARIO 1	SCENARIO 2	SCENARIO 3	SCENARIO 4
$\mathcal{B}(K_L^0 \rightarrow ee)$	0	$13 \kappa_1^{K^{ee}} \text{ TeV}$	0	$1817 \kappa_3^{K^{ee}} \text{ TeV}$	0
$\mathcal{B}(K_L^0 \rightarrow \mu\mu)$	0	$177 \kappa_1^{K^{\mu\mu}} \text{ TeV}$	0	0	$1900 \kappa_4^{K^{\mu\mu}} \text{ TeV}$
$\mathcal{B}(K_L^0 \rightarrow \mu e)$	2467 TeV	$230 \kappa_1^{K^{\mu e}} \text{ TeV}$	0	0	0
$\mathcal{B}(B_d^0 \rightarrow ee)$	0	$39.7 \kappa_1^{B^{ee}} \text{ TeV}$	0	0	0
$\mathcal{B}(B_d^0 \rightarrow \mu\mu)$	0	$151 \kappa_1^{B^{\mu\mu}} \text{ TeV}$	0	0	0
$\mathcal{B}(B_d^0 \rightarrow \tau\tau)$	0	0	0	0	0
$\mathcal{B}(B_d^0 \rightarrow \mu e)$	0	$140 \kappa_1^{B^{\mu e}} \text{ TeV}$	0	$140 \kappa_3^{B^{\mu e}} \text{ TeV}$	$140 \kappa_4^{B^{\mu e}} \text{ TeV}$
$\mathcal{B}(B_d^0 \rightarrow \tau e)$	12.1 TeV	$10.6 \kappa_1^{B^{\tau e}} \text{ TeV}$	$10.6 \kappa_2^{B^{\tau e}} \text{ TeV}$	0	$10.6 \kappa_4^{B^{\tau e}} \text{ TeV}$
$\mathcal{B}(B_d^0 \rightarrow \tau\mu)$	0	$11.3 \kappa_1^{B^{\tau\mu}} \text{ TeV}$	$11.3 \kappa_2^{B^{\tau\mu}} \text{ TeV}$	$11.3 \kappa_3^{B^{\tau\mu}} \text{ TeV}$	0
$\mathcal{B}(B_s^0 \rightarrow ee)$	0	$29.5 \kappa_1^{B_s^{ee}} \text{ TeV}$	$29.5 \kappa_2^{B_s^{ee}} \text{ TeV}$	0	0
$\mathcal{B}(B_s^0 \rightarrow \mu\mu)$	0	$90.0 \kappa_1^{B_s^{\mu\mu}} \text{ TeV}$	$90.0 \kappa_2^{B_s^{\mu\mu}} \text{ TeV}$	0	
$\mathcal{B}(B_s^0 \rightarrow \tau\tau)$	0	0	0	0	0
$\mathcal{B}(B_s^0 \rightarrow \mu e)$	0	$92.3 \kappa_1^{B_s^{\mu e}} \text{ TeV}$	$92.3 \kappa_2^{B_s^{\mu e}} \text{ TeV}$	$92.3 \kappa_3^{B_s^{\mu e}} \text{ TeV}$	$92.3 \kappa_4^{B_s^{\mu e}} \text{ TeV}$
$\mathcal{B}(B_s^0 \rightarrow \tau e)$	0	—	0	0	—
$\mathcal{B}(B_s^0 \rightarrow \tau\mu)$	—	—	0	—	0

Table 3. Limits on the gauge leptoquark mass m_X compared to current measurements (or upper limits) for the mesons K_L^0 , B_d^0 and B_s^0 . Each column represents different choices for the matrices $K_{L/R}^{de}$ where scenarios 1-4 are given by eqs. (3.21), (3.23), (3.25) and (3.27) respectively. Each scenario corresponds to possible structures of the mixing matrices which would in some way suppress the decays of K_L^0 . In scenario 1 the decays to K_L^0 are non-zero albeit helicity-suppressed, leading to mass limits similar to what is obtained from decays of B_d^0 and B_s^0 . Scenario 2 completely suppresses the decays of K_L^0 and the most significant mass limits now come from the decays of B_s^0 . Scenario 3 and 4 correspond to examples of mixing matrices which would suppress the decay channel $K_L^0 \rightarrow \mu e$ but not $K_L^0 \rightarrow ee$ or $K_L^0 \rightarrow \mu\mu$ which would form the dominant limit. The first column represents a scenario which maximises the rate of $K_L^0 \rightarrow \mu e$ decays leading to the largest mass limit on X_μ . In all the scenarios above the parameter κ_α^X corresponds to the combination of mixing angles relevant to that decay chain. We find the lower bound on the PS breaking scale to be no smaller than $\mathcal{O}(100)$ TeV. For the final two channels $B_s^0 \rightarrow \tau e/\tau\mu$ there are currently no measured upper bounds, however non-zero contributions to these channels are indicated by ‘—’ and their future measurement will form a constraint for a given choice of $K_{L/R}^{de}$.

these channels. In all cases the last two channels $B_s^0 \rightarrow \tau e$ and $B_s^0 \rightarrow \tau \mu$ are currently unconstrained by measurement and therefore do not lead to limits on m_X . In cases where a scenario predicts a contribution to these channels, future measurement will be a relevant constraint which we indicate in table 3 by ‘–’.

For simplicity, the interference between the SM and PS contributions to the decay channels with lepton-flavour conserving final states has not been calculated. As the PS contribution to the decay rate is inversely proportional to the fourth power of m_X , the decay rate will decrease by orders of magnitude for small increases in m_X . The derived lower bound on m_X from such channels should be understood as a conservative lower bound and will slightly change by order one factors once the SM contribution is incorporated. Obviously when the dominant limit arises from a LFV decay channel no such interference occurs and the derived limit can be considered even more robust.

In all cases, non-zero decay channels listed in table 3 come with factors of κ corresponding to the combination of mixing angles arising from $K_{L/R}^{de}$. These expressions, particularly in the cases of scenario 1 and 2, are quite complicated due to the large number of free parameters allowed. Therefore minimising the decay widths as a function of the free mixing angles is difficult. Instead, we perform a numerical scan of the free parameters in order to estimate the maximum and minimum lower bound on the mass of X_μ for a given scenario.

Tables 4 and 5 explicitly calculate the leptoquark mass limits for different choices of the mixing angles appearing in scenario 1 and 2 ordered from largest to smallest limits. The limit on the leptoquark mass varies for different choices but not significantly. The decay channel which forms the dominant constraint also varies for different choices of angles, which we indicate. A numerical scan over the parameter space shows that for scenario 1 the mass limits on X_μ vary from 81 – 177 TeV for different values of the mixing angles. The fourth entry of table 4 is a benchmark taken from [33] who found in their case a lower bound mass limit of 86 TeV compared to the 117 TeV we find. In their analysis they neglected the final-state muon mass and therefore assumed no induced decays of K_L^0 from X_μ , whereas we find, when included, it forms the dominant constraint. When neglected we find a limit of 84 TeV from the process $B_{d/s}^0 \rightarrow \mu\mu$ in full agreement with [33]. For table 4 we find that, though helicity-suppressed, decays of K_L^0 are important to consider for PS breaking limits. For the case of scenario 2 we conducted a similar scan of parameters and found the mass limits on X_μ varies roughly from 84 – 102 TeV as indicated by table 5.

3.2 Fermion mass degeneracy

Although the dominant constraint on the PS breaking scale arises from pseudoscalar meson decays, a secondary requirement for a viable Pati-Salam model is to address the lack of mass degeneracy between fermion pairs with the same $SU(2)_{L/R}$ isospin. As indicated

SCENARIO 1	Limit on m_X	Dominant channel
$\theta_{12}^L = \frac{3\pi}{2}, \theta_{12}^R = 2\pi, \theta = \frac{7\pi}{4}, \delta = \pi$	177 TeV	$K_L^0 \rightarrow \mu\mu$
$\theta_{12}^L = \frac{\pi}{4}, \theta_{12}^R = \frac{\pi}{4}, \theta = \frac{\pi}{4}, \delta = 0$	164 TeV	$K_L^0 \rightarrow \mu e$
$\theta_{12}^L = \frac{\pi}{2}, \theta_{12}^R = \frac{\pi}{8}, \theta = 0, \delta = \frac{\pi}{2}$	145 TeV	$B_d^0 \rightarrow \mu\mu$
$\theta_{12}^L = 0, \theta_{12}^R = 0.81, \theta = 1.183, \delta = 0$	117 TeV	$K_L^0 \rightarrow \mu e$
$\theta_{12}^L = \frac{\pi}{4}, \theta_{12}^R = \frac{\pi}{4}, \theta = \frac{\pi}{4}, \delta = \frac{\pi}{2}$	107 TeV	$B_d^0 \rightarrow \mu\mu$
$\theta_{12}^L = 2.06, \theta_{12}^R = 2.4, \theta = 5.11, \delta = 4.58$	81 TeV	$B_s^0 \rightarrow \mu e$

Table 4. Limits obtained for the gauge leptoquark mass X_μ for different choices of the mixing angles appearing in eq. (3.21) ordered from largest to smallest. The decay process from which the dominant limit arises is also listed. In some cases, even though it is helicity-suppressed, the dominant limit will still arise from K_L^0 decays. The angles in the fourth row were first used in [33] from which they obtained a limit of 86 TeV from $B_{d/s}^0 \rightarrow \mu\mu$ when the muon and electron mass were neglected. We find similar limits however we highlight the importance of including the muon mass as the channel $K_L^0 \rightarrow \mu e$ still forms the dominant limit for this scenario. A numerical scan finds the limits in this scenario can vary from 81 – 177 TeV.

SCENARIO 2	Limit on m_X	Dominant channel
$\theta_{12}^L = 2.4, \theta_{12}^R = 2.3, \theta_{23}^L = \frac{\pi}{2}, \theta_{23}^R = 0, \delta^L = 2\pi, \delta^R = 2.77$	102 TeV	$B_s^0 \rightarrow \mu e$
$\theta_{12}^L = \frac{\pi}{9}, \theta_{12}^R = \frac{\pi}{2}, \theta_{23}^L = 1, \theta_{23}^R = 0, \delta^{L/R} = 0$	100 TeV	$B_s^0 \rightarrow \mu e$
$\theta_{12}^L = \frac{\pi}{3}, \theta_{12}^R = \frac{\pi}{6}, \theta_{23}^L = \frac{\pi}{2}, \theta_{23}^R = 1, \delta^{L/R} = 0$	92 TeV	$B_s^0 \rightarrow \mu\mu$
$\theta_{12}^L = \frac{\pi}{3}, \theta_{12}^R = \frac{\pi}{6}, \theta_{23}^L = \frac{\pi}{2}, \theta_{23}^R = 1, \delta^{L/R} = \frac{\pi}{2}$	86 TeV	$B_s^0 \rightarrow \mu\mu$
$\theta_{12}^L = \frac{\pi}{4}, \theta_{12}^R = \frac{\pi}{8}, \theta_{23}^L = 0, \theta_{23}^R = 0, \delta^{L/R} = 0$	85 TeV	$B_s^0 \rightarrow \mu e$
$\theta_{12}^L = 0.72, \theta_{12}^R = 3.05, \theta_{23}^L = 4.02, \theta_{23}^R = 2\pi, \delta^L = 0, \delta^R = \frac{3\pi}{2}$	84 TeV	$B_s^0 \rightarrow \mu e$

Table 5. Limits obtained for the gauge leptoquark mass X_μ for some different choices of mixing angles appearing in eq. (3.23) ordered from largest to smallest. The decay process from which the dominant limit arises is also listed. Here the decays of K_L^0 are completely forbidden and the dominant limit will always arise either from $B_s^0 \rightarrow \mu\mu$ or $B_s^0 \rightarrow \mu e$. Through a numerical scan we find the mass of the PS leptoquark varies between roughly 84 – 102 TeV depending on different choices of mixing angles, a much closer range compared to the results of Scenario 2.

by eq. (2.16) the simplest PS models lead to the fermion mass relations

$$m_d = m_e \quad \text{and} \quad m_u = m_\nu^{\text{Dirac}} \quad (3.31)$$

for all three generations of SM fermions.

	$\mu = m_Z$	$\mu = 1 \text{ TeV}$	$\mu = 10 \text{ TeV}$	$\mu = 100 \text{ TeV}$	$\mu = 1000 \text{ TeV}$
m_e/m_d	0.177	0.205	0.230	0.251	0.271
m_μ/m_s	1.891	2.195	2.454	2.688	2.902
m_τ/m_b	0.612	0.724	0.823	0.913	0.997

Table 6. Measured mass ratios m_e/m_d for each generation at fixed energy scales μ at one-loop and assuming SM running of the Yukawas. Additional details of the running calculations performed can be found in appendix B.

Comparing this prediction to the measured masses of the down-isospin fermions shown in table 6 for the different generations at different energy scales demonstrates that this tree-level relation must be broken. As discussed previously, the mass relation between the up-isospin components can be easily broken due to seesaw mixing in the neutral fermion sector as demonstrated in section 2.2. In the case of the down-isospin components, with no additional particle content, the mass relation is unbroken at tree level and holds at the scale of PS breaking. In scenarios where PS is broken at high scales, this relation could potentially be viable as threshold effects as well as renormalisation group running can potentially be sufficient to explain the observed mass differences of the different generations. PS breaking scales as low as $\mathcal{O}(1000)$ TeV can explain the bottom and tau lepton mass differences [35] as the two Yukawa couplings unify at around this scale. It therefore could be possible for high-scale PS models to explain the mass differences between all three generations in the same way. Table 6 shows that for PS breaking scales below 1000 TeV the different generations of down-quark and charged-lepton Yukawa couplings cannot be equal at the PS breaking scale and therefore there should be some tree-level explanation for their difference.

The mass relations can be broken at tree level by the existence of additional particle content, either scalar or fermion, necessarily transforming as complete PS multiplets above the scale of PS breaking. For example, the inclusion of a scalar $(\mathbf{15}, \mathbf{2}, \mathbf{2})$ Higgs particle, sometimes referred to as the Minimal Quark-Lepton Symmetric Model (MQLS), which has a non-zero vev will induce a Georgi-Jarlskog like texture [36] lifting the degeneracy between the down quark and charged lepton masses [1, 2]. The additional Yukawa couplings results in enough freedom such that the mass ratios measured and shown in table 6 can arise.

We explore an alternative possibility first noted in [4, 5] where additional anomaly-free fermion multiplets transforming under the PS gauge group are introduced. If the additional multiplets contain components with the same quantum numbers as the down quarks or charged leptons, mixing effects could induce a see-saw which can decouple the down-quark and charged-lepton Yukawas, breaking the tree-level mass relations obtained without their inclusion. In this scenario, both the up- and down-isospin components have their PS mass relations broken due to see-saw effects, so the breaking of the mass relations

between all SM fermions is explained by a similar mechanism.

An additional consequence of introducing extra fermionic states is that they can cause the gauge boson leptoquark X_μ to couple in a chiral-like way to the light SM-like fermions. As an example, consider the introduction of fermion multiplets $F_{L/R}$ that contain components $E_{L/R}^-$ that have the same quantum numbers as the SM charged leptons:

$$f_{L/R} = \begin{pmatrix} u_r & d_r \\ u_b & d_b \\ u_g & d_g \\ \nu_e & e \end{pmatrix}_{L/R} \oplus F_{L/R} = \begin{pmatrix} \cdots & & & \\ \vdots & \ddots & & \\ & & E_{L/R}^- & \\ & & & \ddots \end{pmatrix}. \quad (3.32)$$

Here both E_L^- and E_R^- are required phenomenologically such that no massless charged fermion states appear and the exotic multiplets F_L and F_R need not transform in the same way. However, the combination must be anomaly free.

If Yukawa interactions connecting the multiplets $F_{L/R}$ and $f_{L/R}$ exist, mass mixing will be induced as per

$$\mathcal{L}_{eE} = \begin{pmatrix} \overline{e_L} & \overline{E_L} \end{pmatrix} \begin{pmatrix} m_{ee} & m_{eE} \\ m_{Ee} & m_{EE} \end{pmatrix} \begin{pmatrix} e_R \\ E_R \end{pmatrix} + \text{H.c.} \quad (3.33)$$

Diagonalising into the mass basis for the charged fermions leads to

$$(e'_{L/R})_\ell = c_{\theta_{L/R}} e_{L/R} + s_{\theta_{L/R}} E_{L/R} \quad (E'_{L/R})_{\mathfrak{h}} = -s_{\theta_{L/R}} e_{L/R} + c_{\theta_{L/R}} E_{L/R} \quad (3.34)$$

where the subscripts ℓ and \mathfrak{h} indicate the light and heavy eigenstates respectively. The pseudoscalar meson decays discussed above are induced by the gauge leptoquark interactions between the colour triplet d and charged lepton e from the multiplet $f_{L/R}$.

Expanding eq. (3.2) with eq. (3.34) leads to

$$\mathcal{L}_{Xde} = \frac{g_4}{\sqrt{2}} \left(\overline{d'} K_L^{de} \not{X} P_L (c_{\theta_L} e' - s_{\theta_L} E') \right) + \overline{d'} K_R^{de} \not{X} P_R (c_{\theta_R} e' - s_{\theta_R} E') + \text{H.c} \quad (3.35)$$

for the gauge interactions in the mass basis where generational indices have been suppressed for simplicity. Because of phenomenological constraints, any fermions with SM quantum numbers must be significantly heavier than the pseudoscalar mesons whose decays supply the dominant constraint on PS breaking; therefore, processes such as $K_L^0 \rightarrow EE$ or $K_L^0 \rightarrow eE$ are kinematically forbidden. The decay $K_L^0 \rightarrow ee$ will exist as before, but now suppressed by the relevant mass mixing angles. Therefore the only relevant interactions in eq. (3.35) for meson decay are

$$\mathcal{L}_{Xde} \supset \frac{g_4}{\sqrt{2}} \left(\overline{d'} (c_{\theta_L} K_L^{de}) \not{X} P_L e' + \overline{d'} (c_{\theta_R} K_R^{de}) \not{X} P_R e' \right) + \text{H.c} \quad (3.36)$$

which will lead to a decay rate given by eqs. (3.14) and (3.16) with the replacement $K_{L/R}^{de} \rightarrow \mathcal{K}_{L/R}^{de} = c_{\theta_{L/R}} K_{L/R}^{de}$. As the mixing angles θ_L and θ_R can significantly differ,

this can effectively lead to a chiral coupling between X_μ and the fermions d and e causing a suppression in the helicity-unsuppressed contribution of the total meson decay rates in eq. (3.5). This therefore allows for an overall weaker lower bound on the leptoquark mass compared to those in table 3 and therefore the scale of PS breaking. As noted previously, however, in order to significantly helicity-suppress the decays mediated by X_μ , one of the angles $\theta_{L/R}$ is required to be very small e.g. $\theta_R \lesssim 10^{-4}$ in the case of $K_L^0 \rightarrow \mu e$ decays.

Table 7 demonstrates the impact this can have on the mass limits in the extreme case of an exactly chiral theory ($m_E \rightarrow \infty$) where for example $c_{\theta_L} = 1$ and $c_{\theta_R} = 0$ for all three generations¹⁴, assuming the same matrix textures for $K_{L/R}^{de}$ as in table 3. The leptoquark mass limits are significantly lowered compared to table 3 as the helicity unsuppressed contribution from eq. (3.14) no longer contributes and therefore the decay rate is suppressed by the charged lepton masses. Scenario 1, which already had helicity-suppressed K_L^0 decays, will have its limits largely unchanged except for when the dominant channel arises from $B_{d/s}^0$. If there are no contributions to the decays of K_L^0 , as in scenario 2, then the helicity suppression on the other decay channels allows for PS breaking scales as low as $\mathcal{O}(10)$ TeV. Interestingly, in these scenarios with a chiral-like coupled X_μ , if there is a significant contribution to $K_L^0 \rightarrow ee$, then the limits are significantly smaller compared to $K_L^0 \rightarrow \mu\mu[\mu e]$ due to the large helicity-suppression present for the electron. Therefore with the presence of exotic fermion multiplets, a significant contribution to K_L^0 decays can be possible with small leptoquark masses provided it only couples K_L^0 to electrons. This is unlike the case without mass mixing where any induced decay for K_L^0 by X_μ causes mass limits larger than 1000 TeV irrespective of the final decay product. In such a chiral scenario only one of K_L^{de} and K_R^{de} is required to have a matrix structure given by each indicated scenario as the other is significantly suppressed through seesaw effects. Therefore for scenarios involving charged-lepton or down-quark seesaws, $K_{L/R}^{de}$ do not need to be related and therefore no parity symmetry needs to be imposed at a high scale.

In tables 8 and 9 the limits on m_X are re-evaluated for the same benchmark scenarios in tables 4 and 5 now assuming an exact helicity suppression. In both scenarios a significant reduction in the mass limits can occur. This reduction occurs for any choice of mixing angles in scenario 2, whereas in scenario 1, a significant reduction occurs only when the dominant decay channel comes from either B_d^0 or B_s^0 . In general a reduction in the limits on m_X by a factor of 0.05 – 0.07 naturally occurs compared to the scenario without additional mass mixing. We find that the limits on m_X can be as low as 5 TeV potentially allowing for discovery signals of different PS particles comfortably within reach of current and possible future hadron colliders.

Exotic fermion multiplets are therefore an attractive feature for low scale Pati Salam models. It is curious that they allow for significantly lighter PS breaking scales whilst also

¹⁴These limits are also valid for scenarios where quark-lepton unification occurs for only one chirality of fermions, e.g. a gauge group given by $SU(4)_L \times SU(3)_R \times SU(2)_L \times SU(2)_R \rightarrow SU(3)_c \times SU(2)_L \times SU(2)_R$ where the vector leptoquark X couples to only one chirality of fermions.

	$K_L^{de} = \mathbb{1}_{3 \times 3}$	SCENARIO 1	SCENARIO 2	SCENARIO 3	SCENARIO 4
$\mathcal{B}(K_L^0 \rightarrow ee)$	0	$13 \kappa_1^{K^{ee}}$ TeV	0	$13 \kappa_3^{K^{ee}}$ TeV	0
$\mathcal{B}(K_L^0 \rightarrow \mu\mu)$	0	$177 \kappa_1^{K^{\mu\mu}}$ TeV	0	0	$177 \kappa_4^{K^{\mu\mu}}$ TeV
$\mathcal{B}(K_L^0 \rightarrow \mu e)$	194 TeV	$230 \kappa_1^{K^{\mu e}}$ TeV	0	0	0
$\mathcal{B}(B_d^0 \rightarrow ee)$	0	$0.2 \kappa_1^{B^{ee}}$ TeV	0	0	0
$\mathcal{B}(B_d^0 \rightarrow \mu\mu)$	0	$10.8 \kappa_1^{B^{\mu\mu}}$ TeV	0	0	0
$\mathcal{B}(B_d^0 \rightarrow \tau\tau)$	0	0	0	0	0
$\mathcal{B}(B_d^0 \rightarrow \mu e)$	0	$10.0 \kappa_1^{B^{\mu e}}$ TeV	0	$10.0 \kappa_3^{B^{\mu e}}$ TeV	$10.0 \kappa_4^{B^{\mu e}}$ TeV
$\mathcal{B}(B_d^0 \rightarrow \tau e)$	2.7 TeV	$3.2 \kappa_1^{B^{\tau e}}$ TeV	$3.2 \kappa_2^{B^{\tau e}}$ TeV	0	$3.2 \kappa_4^{B^{\tau e}}$ TeV
$\mathcal{B}(B_d^0 \rightarrow \tau\mu)$	0	$3.2 \kappa_1^{B^{\tau\mu}}$ TeV	$3.2 \kappa_2^{B^{\tau\mu}}$ TeV	$3.2 \kappa_3^{B^{\tau\mu}}$ TeV	0
$\mathcal{B}(B_s^0 \rightarrow ee)$	0	$0.2 \kappa_1^{B_s^{ee}}$ TeV	$0.2 \kappa_2^{B_s^{ee}}$ TeV	0	0
$\mathcal{B}(B_s^0 \rightarrow \mu\mu)$	0	$6.5 \kappa_1^{B_s^{\mu\mu}}$ TeV	$6.5 \kappa_2^{B_s^{\mu\mu}}$ TeV	0	0
$\mathcal{B}(B_s^0 \rightarrow \tau\tau)$	0	0	0	0	0
$\mathcal{B}(B_s^0 \rightarrow \mu e)$	0	$6.7 \kappa_1^{B_s^{\mu e}}$ TeV	$6.7 \kappa_2^{B_s^{\mu e}}$ TeV	$6.7 \kappa_3^{B_s^{\mu e}}$ TeV	$6.7 \kappa_4^{B_s^{\mu e}}$ TeV
$\mathcal{B}(B_s^0 \rightarrow \tau e)$	0	–	0	0	–
$\mathcal{B}(B_s^0 \rightarrow \tau\mu)$	–	–	0	–	0

Table 7. Limits on the gauge leptoquark mass m_X compared to current measurements (or upper limits) for the mesons K_L^0 , B_d^0 and B_s^0 in the chiral limit (e.g. $c_{\theta_R} = 0$) where all decays are now helicity suppressed. Each scenario is given by eqs. (3.21), (3.23), (3.25) and (3.27) respectively. As *all* decays are now helicity-suppressed, the dominant decay channel in scenario 1 will arise from $K_L^0 \rightarrow \mu e$ unless forbidden by a specific choice of κ . As Scenario 2 completely suppresses the decays of K_L^0 and now the decays of $B_{d/s}^0$ are helicity-suppressed, the limits on the leptoquark mass quite substantially decrease, similarly the limits from scenarios 3 and are significantly reduced. In particular scenario 3 allows for incredibly low mass scales due to the large helicity-suppression present for electron final-states. The first column represents a scenario which maximises the rate of $K_L^0 \rightarrow \mu e$ decays leading to the largest mass limit on X_μ which in this case is roughly 200 TeV. In all the scenarios above the parameter κ_α^X corresponds to the combination of mixing angles relevant to that decay chain. We find the lower bound on the PS breaking scale to be no smaller than $\mathcal{O}(10)$ TeV. For the final two channels $B_s^0 \rightarrow \tau e/\tau\mu$ there are currently no measured upper bounds, however non-zero contributions to these channels are indicated by ‘–’ and their future measurement will form a constraint for a given choice of $K_{L/R}^{de}$.

potentially breaking the mass degeneracy amongst the down-isospin fermions. This effect is possible not only for mixing between the charged leptons as discussed above, but also if heavy versions of the down quarks, D , were to be included which mix with the light d quarks. This would lead to a similar reduction in the mass limits on X_μ as above for the same reasons.

4 Exotic PS fermion multiplets

As discussed above, exotic PS fermion multiplets which contain states with the correct quantum numbers to mix with the charged leptons or down quarks can simultaneously explain the experimentally observed mass non-degeneracy between these two types of fermions as well as lower the phenomenologically-allowed scale of PS breaking. A number of different viable PS multiplets are possible; for consistency we require that the multiplets added do not introduce anomalies and that they allow for a phenomenologically valid mass spectrum. For simplicity we focus on small multiplets which transform with no more than two indices total under all three gauge groups when written in their defining representations. All possible combinations satisfying this requirement are listed in table 10. We take the scalar content of the theory to remain unchanged but will note where additional exotic scalars may be required for a viable model in some cases. Although the PS gauge group is an attractive subgroup of some GUTs e.g. $SO(10)$ or E_6 , we will not require successful gauge-coupling unification or partial unification. We will not consider the location of Landau poles¹⁵ or require that the extra exotic fermions fit into complete GUT multiplets. We simply focus on the specific particle content required at low scales sufficient to lift the mass degeneracy between ℓ and d and simultaneously lower the scale of PS breaking.

4.1 Fermion extensions

Considering the relevant exotic multiplets indicated in table 10, below we study basic phenomenological implications of introducing each given multiplet. We indicate heavy, exotic versions of down quarks, charged leptons and neutrinos by D , E and N respectively. We will also briefly comment on the implications for baryon number violation in each case. As we are only introducing exotic fermions, the Yukawa sector of the Lagrangian is the only possible area where additional violation could arise.

¹⁵These would further motivate considering multiplets of small dimensionality as large multiplets will have a much more significant impact on RGE evolution relevant for viable GUT theories.

SCENARIO 1	Limit on m_X	Reduction	Dominant channel
$\theta_{12}^L = \frac{3\pi}{2}, \theta = \frac{7\pi}{4}, \delta = \pi$	177 TeV	1	$K_L^0 \rightarrow \mu\mu$
$\theta_{12}^L = \frac{\pi}{4}, \theta = \frac{\pi}{4}, \delta = 0$	139 TeV	0.85	$K_L^0 \rightarrow \mu e$
$\theta_{12}^L = 2.06, \theta = 5.11, \delta = 4.58$	51 TeV	0.63	$K_L^0 \rightarrow \mu\mu$
$\theta_{12}^L = 0, \theta = 1.183, \delta = 0$	11 TeV	0.09	$K_L^0 \rightarrow ee$
$\theta_{12}^L = \frac{\pi}{2}, \theta = 0, \delta = \frac{\pi}{2}$	8.5 TeV	0.06	$B_d^0 \rightarrow \mu e$
$\theta_{12}^L = \frac{\pi}{4}, \theta = \frac{\pi}{4}, \delta = \frac{\pi}{2}$	7.8 TeV	0.07	$B_d^0 \rightarrow \mu\mu$

Table 8. Limits obtained for the gauge leptoquark mass X_μ for different choices of the mixing angles appearing in eq. (3.21) with an exact helicity suppression where we have chosen $K_R^{de} = 0_{3 \times 3}$. The decay process from which the dominant limit arises is also listed as well as the percentage reduction from the non-helicity suppressed scenario given in table 4. In some cases only a small reduction in the mass limits occurs, this is a result of the Kaon decay channels being helicity suppressed as a result of the structure of the mixing matrices instead of due to a chiral coupling of X_μ . Only the benchmark scenarios which initially had dominant decay channels arising from B_d or B_s experience a significant reduction in their limits as they were initially not helicity suppressed.

SCENARIO 2	Limit on m_X	Reduction	Dominant channel
$\theta_{12}^L = 2.4, \theta_{23}^L = \frac{\pi}{2}, \delta^L = 2\pi$	6.2 TeV	0.06	$B_s^0 \rightarrow \mu e$
$\theta_{12}^L = \frac{\pi}{9}, \theta_{23}^L = 1, \delta^L = 0$	6.0 TeV	0.06	$B_s^0 \rightarrow \mu e$
$\theta_{12}^L = \frac{\pi}{4}, \theta_{23}^L = 0, \delta^L = 0$	6.0 TeV	0.07	$B_s^0 \rightarrow \mu e$
$\theta_{12}^L = 0.72, \theta_{23}^L = 4.02, \delta^L = 0$	5.9 TeV	0.07	$B_s^0 \rightarrow \mu e$
$\theta_{12}^L = \frac{\pi}{3}, \theta_{23}^L = \frac{\pi}{2}, \delta^L = 0$	5.6 TeV	0.06	$B_s^0 \rightarrow \mu\mu$
$\theta_{12}^L = \frac{\pi}{3}, \theta_{23}^L = \frac{\pi}{2}, \delta^L = \frac{\pi}{2}$	5.6 TeV	0.065	$B_s^0 \rightarrow \mu\mu$

Table 9. Limits obtained for the gauge leptoquark mass X_μ for some different choices of mixing angles appearing in eq. (3.23) with an exact helicity suppression where we have chosen $K_R^{de} = 0_{3 \times 3}$. The decay process from which the dominant limit arises is also listed as well as the percentage reduction from the non helicity-suppressed scenarios in table 5. Each benchmark experiences a significant reduction in their mass limits of over an order of magnitude allowing for extremely light masses of X_μ and significantly lower scales of PS breaking.

	PS multiplet	$A(R)$	$SU(3) \otimes U(1)_Q$ decomposition	Candidate
f^a	$(\mathbf{1}, \mathbf{2}, \mathbf{1})$	0	$\mathbf{1}_{-1/2} \oplus \mathbf{1}_{+1/2}$	✗
f^α	$(\mathbf{1}, \mathbf{1}, \mathbf{2})$	0	$\mathbf{1}_{-1/2} \oplus \mathbf{1}_{+1/2}$	✗
f^A	$(\mathbf{4}, \mathbf{1}, \mathbf{1})$	± 1	$\mathbf{1}_{-1/2} \oplus \mathbf{3}_{+1/6}$	✗
f_b^a	$(\mathbf{1}, \mathbf{3}, \mathbf{1})$	0	$\mathbf{1}_{-1} \oplus \mathbf{1}_0 \oplus \mathbf{1}_{+1}$	✓
f_β^α	$(\mathbf{1}, \mathbf{1}, \mathbf{3})$	0	$\mathbf{1}_{-1} \oplus \mathbf{1}_0 \oplus \mathbf{1}_{+1}$	✓
f^{AB}	$(\mathbf{6}, \mathbf{1}, \mathbf{1})$	0	$\mathbf{3}_{-1/3} \oplus \bar{\mathbf{3}}_{+1/3}$	✓
f^{AB}	$(\mathbf{10}, \mathbf{1}, \mathbf{1})$	± 8	$\mathbf{1}_{-1} \oplus \mathbf{3}_{-1/3} \oplus \mathbf{6}_{+1/3}$	✓
f_B^A	$(\mathbf{15}, \mathbf{1}, \mathbf{1})$	0	$\bar{\mathbf{3}}_{-2/3} \oplus \mathbf{1}_0 \oplus \mathbf{8}_0 \oplus \mathbf{3}_{+2/3}$	✗
$f^{a\alpha}$	$(\mathbf{1}, \mathbf{2}, \mathbf{2})$	0	$\mathbf{1}_{-1} \oplus \mathbf{1}_0 \oplus \mathbf{1}_0 \oplus \mathbf{1}_{+1}$	✓
f^{Aa}	$(\mathbf{4}, \mathbf{2}, \mathbf{1})$	± 2	$\mathbf{1}_{-1} \oplus \mathbf{3}_{-1/3} \oplus \mathbf{1}_0 \oplus \mathbf{3}_{+2/3}$	✓
$f^{A\alpha}$	$(\mathbf{4}, \mathbf{1}, \mathbf{2})$	± 2	$\mathbf{1}_{-1} \oplus \mathbf{3}_{-1/3} \oplus \mathbf{1}_0 \oplus \mathbf{3}_{+2/3}$	✓

Table 10. Different dimensional representations of fermions f (with indices in their defining representation) under PS where a , α and A correspond to $SU(2)_L$, $SU(2)_R$ and $SU(4)_c$ indices respectively. Multiplets are considered good candidates if they contain states with the same quantum numbers as either the down quarks or charged leptons, which will mix with its SM counterpart, when broken to $SU(3)_c \otimes U(1)_Q$. Additionally the $SU(4)$ anomaly coefficient $A(R)$ for each fermion is indicated where the sign depends on whether the fermion is left- or right-handed.

4.1.1 $SU(2)_{L/R}$ Triplets

If a triplet fermion is added, for example $\Psi_3^R \sim (\mathbf{1}, \mathbf{1}, \mathbf{3})$, the extra terms appearing in the Yukawa Lagrangian are

$$\mathcal{L}_{\text{YUK}} \supset \text{Tr} \left[\sqrt{2} y_{\Psi_3} \overline{(\Psi_3^R)^c} \chi_R^\dagger f_R + \frac{1}{2} \mu_{\Psi_3} \overline{(\Psi_3^R)^c} (\Psi_3^R)^T \right] + \text{H.c.} \quad (4.1)$$

As Ψ_3^R is uncharged under the colour group $SU(4)_c$, it contains no quark states. However, it contains components which can mix with both the charged and neutral SM leptons

$$f_{L/R} = \begin{pmatrix} \cdot & \cdot \\ \cdot & \cdot \\ \cdot & \cdot \\ \nu & e \end{pmatrix}_{L/R}, \quad \Psi_3^R = \frac{1}{\sqrt{2}} \begin{pmatrix} N_R & \sqrt{2} (E_L^-)^c \\ \sqrt{2} E_R^- & -N_R \end{pmatrix} \quad (4.2)$$

where the dotted components of $f_{L/R}$ do not mix with Ψ_3^R but the undotted do and $\Psi_3^R \rightarrow U_R \Psi_3^R U_R^\dagger$. Here we have assigned Ψ_3^R to be a right-handed fermion without loss of generality. Expanding out eqs. (2.15) and (4.1) with the parameterisation given in eq. (4.2)

leads to a mixing matrix given by

$$\mathcal{L}_{eE} = \begin{pmatrix} \overline{e_L} & \overline{E_L} \end{pmatrix} \begin{pmatrix} m_e & 0 \\ \sqrt{2} y_{\Psi_3}^R v_R^* & \mu_{\Psi_3^R} \end{pmatrix} \begin{pmatrix} e_R \\ E_R \end{pmatrix} \quad (4.3)$$

for the charged lepton states and

$$\mathcal{L}_{\nu N} = \frac{1}{2} \begin{pmatrix} \overline{\nu_L} & \overline{\nu_R^c} & \overline{N_R^c} \end{pmatrix} \begin{pmatrix} 0 & m_u & 0 \\ m_u & 0 & y_{\Psi_3}^R v_R^* \\ 0 & y_{\Psi_3}^R v_R^* & \mu_{\Psi_3^R} \end{pmatrix} \begin{pmatrix} \nu_L^c \\ \nu_R \\ N_R \end{pmatrix} \quad (4.4)$$

for the neutral states. If f_L , f_R and Ψ are the only fermions introduced, the PS symmetry enforces that the singular values of m_d and m_u are given by the down and up quark masses respectively. Equation (4.4) assumes that the fermion singlets S_L discussed in section 2, appearing in the usual low-scale PS scenario, are not included. As can be seen from the neutrino mass mixing matrix, S_L may no longer be necessary for light neutrino masses as an inverse seesaw arises naturally with the triplet. We therefore neglect S_L , and if it were to be included eq. (4.4) would be trivially extended by the last row and column of eq. (2.17).

The terms introduced in eq. (4.1) do not violate the global $U(1)_J$ symmetry which eq. (2.15) obeys and is the only global accidental symmetry of this Yukawa Lagrangian. These terms unsurprisingly enforce the assignment

$$J(\Psi_3^R) = 0 \quad (4.5)$$

as Ψ_3^R transforms as a real representation. Therefore baryon number remains an unbroken global symmetry of the Yukawa sector similar to the vanilla scenario described in section 2.4. Interestingly if the singlet S_L is not included, the scalar χ_L no longer Yukawa couples to any of the fermions and the relevant term of the scalar potential given in eq. (2.36) no longer violates the $U(1)_J$ global symmetry as we are free to choose $J(\chi_L) = -1$. The proton would therefore remain absolutely stable (assuming no additional particle content) after breaking of the PS symmetry, whereas lepton number would be broken.

If instead an $SU(2)_L$ triplet fermion Ψ_3^L was introduced, similar conclusions are reached related to the leptonic mass mixing matrices and baryon number violation¹⁶. The Yukawa Lagrangian in this case is similar to the one appearing in eq. (4.1) with the replacements $\Psi_3^R \rightarrow (\Psi_3^L)^c$, $\chi_R \rightarrow (\chi_L)^*$ and $f_R \rightarrow (f_L)^c$ leading to the mixing matrix

$$\mathcal{L}_{eE} = \begin{pmatrix} \overline{e_L} & \overline{E_L} \end{pmatrix} \begin{pmatrix} m_e & \sqrt{2} y_{\Psi_3}^L v_L \\ 0 & \mu_{\Psi_3^L} \end{pmatrix} \begin{pmatrix} e_R \\ E_R \end{pmatrix} \quad (4.6)$$

¹⁶However if both Ψ_3^L and Ψ_3^R are included simultaneously, the Yukawa Lagrangian enforces $J(\chi_L) = J(\chi_R) = 1$ and the relevant quartic term of the scalar potential would once again violate $U(1)_J$ and therefore B regardless of the existence of S_L .

for the charged lepton states and

$$\mathcal{L}_{\nu N} = \frac{1}{2} \begin{pmatrix} \bar{\nu}_L & \bar{\nu}_R^c & \bar{N}_L \end{pmatrix} \begin{pmatrix} 0 & m_u & y_{\Psi_3}^L v_L \\ m_u & 0 & 0 \\ y_{\Psi_3}^L v_L & 0 & \mu_{\Psi_3^L} \end{pmatrix} \begin{pmatrix} \nu_L^c \\ \nu_R \\ N_L^c \end{pmatrix} \quad (4.7)$$

for the neutral states.

If both Ψ_3^L and Ψ_3^R are included simultaneously the mass mixing matrices for the charged and neutral sectors are simply a combination of eqs. (4.3), (4.4), (4.6) and (4.7). Explicitly writing out the mass mixing matrices gives

$$\mathcal{L}_{eE\mathcal{E}} = \begin{pmatrix} \bar{e}_L & \bar{E}_L & \bar{\mathcal{E}}_L \end{pmatrix} \begin{pmatrix} m_e & 0 & \sqrt{2} y_{\Psi_3}^L v_L \\ \sqrt{2} y_{\Psi_3}^R v_R & \mu_{\Psi_3^R} & 0 \\ 0 & 0 & \mu_{\Psi_3^L} \end{pmatrix} \begin{pmatrix} e_R \\ E_R \\ \mathcal{E}_R \end{pmatrix} \quad (4.8)$$

for the charged leptons, where $E_{L/R}$ and $\mathcal{E}_{L/R}$ correspond to the charged lepton states appearing in Ψ_3^R and Ψ_3^L respectively, and

$$\mathcal{L}_{\nu N} = \frac{1}{2} \begin{pmatrix} \bar{\nu}_L & \bar{\nu}_R^c & \bar{N}_L & \bar{N}_R^c \end{pmatrix} \begin{pmatrix} 0 & m_u & y_{\Psi_3}^L v_L & 0 \\ m_u & 0 & 0 & y_{\Psi_3}^R v_R^* \\ y_{\Psi_3}^L v_L & 0 & \mu_{\Psi_3^L} & 0 \\ 0 & y_{\Psi_3}^R v_R^* & 0 & \mu_{\Psi_3^R} \end{pmatrix} \begin{pmatrix} \nu_L^c \\ \nu_R \\ N_L^c \\ N_R \end{pmatrix} \quad (4.9)$$

for the neutral states.

4.1.2 $SU(2)_L/SU(2)_R$ Bi-doublet

If a fermion transforming as a bi-doublet under the two $SU(2)$ gauge groups of PS $\Psi_{22} \sim (\mathbf{1}, \mathbf{2}, \mathbf{2})$ is added, the Yukawa Lagrangian is extended by

$$\mathcal{L}_{\text{YUK}} \supset \text{Tr} \left[y_{\Psi_{22}}^R \bar{f}_L \chi_R (\Psi_{22}^T)^c (i\tau_2) + y_{\Psi_{22}}^L \bar{\Psi}_{22} (i\tau_2) \chi_L^\dagger f_R + \mu_{\Psi_{22}} \bar{\Psi}_{22} (i\tau_2) (\Psi_{22})^c (i\tau_2) \right] + \text{H.c.} \quad (4.10)$$

As before, Ψ_{22} is uncharged under the $SU(4)_c$ colour group and therefore only contains uncoloured states which can mix with the SM leptons:

$$f_{L/R} = \begin{pmatrix} \cdot & \cdot \\ \cdot & \cdot \\ \cdot & \cdot \\ \nu & e \end{pmatrix}_{L/R}, \quad \Psi_{22} = \begin{pmatrix} -(E_R^-)^c & N_L^0 \\ (N_R^0)^c & E_L^- \end{pmatrix} \quad (4.11)$$

where Ψ_{22} is written with two raised indices and therefore transforms as $\Psi_{22} \rightarrow U_L \Psi_{22} U_R^T$. Expanding out eqs. (2.15) and (4.10) with eq. (4.11) leads to

$$\mathcal{L}_{eE} = \begin{pmatrix} \bar{e}_L & \bar{E}_L \end{pmatrix} \begin{pmatrix} m_e & y_{\Psi_{22}}^R v_R \\ y_{\Psi_{22}}^L v_L^* & \mu_{\Psi_{22}} \end{pmatrix} \begin{pmatrix} e_R \\ E_R \end{pmatrix} \quad (4.12)$$

for the charged lepton mass mixing matrix and

$$\mathcal{L}_{\nu N} = \frac{1}{2} \begin{pmatrix} \overline{\nu_L} & \overline{\nu_R^c} & \overline{N_L} & \overline{N_R^c} \end{pmatrix} \begin{pmatrix} 0 & m_u & 0 & y_{\Psi 22}^R v_R \\ m_u & 0 & 0 & y_{\Psi 22}^L v_L^* \\ 0 & 0 & 0 & \mu_{\Psi 22} \\ y_{\Psi 22}^R v_R & y_{\Psi 22}^L v_L^* & \mu_{\Psi 22} & 0 \end{pmatrix} \begin{pmatrix} \nu_L^c \\ \nu_R \\ N_L^c \\ N_R \end{pmatrix} \quad (4.13)$$

for the neutral mass mixing.

Similar to the case of the triplet, eq. (4.10) does not violate the global $U(1)_J$ symmetry (which, recall, is the only accidental symmetry in this Yukawa Lagrangian) and implies

$$J(\Psi_{22}) = 0. \quad (4.14)$$

Therefore $U(1)_J$ is not violated in the Yukawa Lagrangian and baryon number violation proceeds through the scalar sector as before. Unlike the scenarios involving only one triplet, in the absence of the fermion S_L , eq. (4.10) still enforces the choice $J(\chi_L) = J(\chi_R) = 1$ and therefore baryon number will remain violated if both scalars are included and will proceed via similar diagrams to those presented in section 2.4.

4.1.3 $SU(4)_c/SU(2)_{L/R}$ Bi-fundamentals

In the case where additional copies of the usual PS fermions exist, there are a number of different possible scenarios depending on the chirality of the fermions introduced. An even number of fermion bi-fundamentals needs to be introduced, as can be seen in table 10, for anomaly cancellation and therefore we focus on the minimal scenario where a pair of bi-fundamentals is added. If two exact copies of f_L and f_R are added, that is a left-handed fermion transforming as $(F_L)_\alpha \sim (\mathbf{4}, \mathbf{2}, \mathbf{1})$ under PS and a right-handed fermion transforming as $(F_R)_{\dot{\alpha}} \sim (\mathbf{4}, \mathbf{1}, \mathbf{2})$ where we explicitly show the dotted and undotted Lorentz indices for clarity, then the Yukawa Lagrangian is extended by the terms

$$\begin{aligned} \mathcal{L}_{\text{YUK}} = \text{Tr} \Big[& \left\{ y_{f_L f_R} \overline{f_L} \phi (f_R)^T + \widetilde{y}_{f_L f_R} \overline{f_L} \phi^c (f_R)^T + y_{f_R} \overline{S_L} \chi_R^\dagger f_R + y_{f_L} \overline{f_L} \chi_L (S_L)^c \right. \\ & \left. + (f_L \rightarrow F_L) + (f_R \rightarrow F_R) \right\} \Big] + \frac{1}{2} \mu_S \overline{S_L} S_L^c + \text{H.c} \end{aligned} \quad (4.15)$$

with the additional fermion multiplets

$$f_{L/R} = \begin{pmatrix} u_r & d_r \\ u_b & d_b \\ u_g & d_g \\ \nu & e \end{pmatrix}_{L/R}, \quad F_{L/R} = \begin{pmatrix} U_r & D_r \\ U_b & D_b \\ U_g & D_g \\ N^0 & E^- \end{pmatrix}_{L/R} \quad (4.16)$$

where U_i and D_i ($i = r, b, g$) have electric charge $+2/3$ and $-1/3$ respectively. Note that no bare mass terms are present in eq. (4.15) and therefore the expansion will be similar to that of eq. (2.15) in the vanilla PS scenario. In particular all mass terms between the

SM and exotic charged fermions will be related to the electroweak vevs v_1 and v_2 implying that the heavy exotic charged fermions E , D and U would be expected to appear near the electroweak scale which is ruled out phenomenologically.

Alternatively two fermions with the same PS representations but *opposite* chirality to the bi-fundamentals already included in PS could be added, that is a right-handed fermion transforming as $(F_L)_{\dot{\alpha}} \sim (\mathbf{4}, \mathbf{2}, \mathbf{1})$ under PS and a left-handed fermion transforming as $(F_R)_{\alpha} \sim (\mathbf{4}, \mathbf{1}, \mathbf{2})$. In this case the Yukawa Lagrangian will be similar, albeit with additional bare mass terms:

$$\begin{aligned} \mathcal{L}_{\text{YUK}} = \text{Tr} \Big[& \left\{ y_{f_L f_R} \overline{f_L} \phi (f_R)^T + \widetilde{y}_{f_L f_R} \overline{f_L} \phi^c (f_R)^T + y_{f_R} \overline{S_L} \chi_R^{\dagger} f_R + y_{f_L} \overline{f_L} \chi_L (S_L)^c \right. \\ & \left. + (f_L \rightarrow F_R \text{ \& } f_R \rightarrow F_L) \right\} + \mu_L \overline{f_L} F_L + \mu_R \overline{F_R} f_R \Big] + \frac{1}{2} \mu_S \overline{S_L} S_L^c + \text{H.c.} \end{aligned} \quad (4.17)$$

Now the exotic charged fermions can have their masses decoupled from the electroweak scale for large bare mass terms. However as the exotic fermion multiplets transform in the exact same way as the multiplets containing the SM fields, there is no mechanism to decouple the masses of the down-quark and charged lepton states, implying their mass mixing matrices satisfy $M_{eE} = M_{dD}$ and therefore have the same singular values. Therefore both the SM down-quarks and charged leptons would have the same mass at the scale of PS breaking as well as the exotic, heavy down-quark and charged lepton states. Similar results occur for pairs of opposite chirality but same PS representation fermions, e.g. two fermions transforming as $(F_L^1)_{\alpha} \sim (\mathbf{4}, \mathbf{1}, \mathbf{2})$ and $(F_L^2)_{\dot{\alpha}} \sim (\mathbf{4}, \mathbf{1}, \mathbf{2})$. While they may still be acceptable candidates in leading to a chiral-like coupling of X_{μ} to the SM states, these fermion extensions are not viable at low scales for lifting the mass degeneracy between the d and ℓ states and we therefore do not pursue this possibility further.

It is easy and unsurprising to see that for both eqs. (4.15) and (4.17) the accidental global symmetry $U(1)_J$ is unbroken and therefore for these scenarios all baryon number violating interactions will proceed similarly to section 2.4.

4.1.4 $SU(4)_c$ Sextet

Adding a fermion which transforms as an $SU(4)$ sextet $\Psi_6 \sim (\mathbf{6}, \mathbf{1}, \mathbf{1})$, extends the Yukawa Lagrangian by

$$\mathcal{L}_{\text{YUK}} \supset \text{Tr} \left[y_{\Psi}^L \overline{f_L} (i\tau_2) \chi_L^{\dagger} \Psi_6 + y_{\Psi}^R \overline{(\Psi_6)^c} \chi_R (i\tau_2) (f_R)^T + \frac{1}{2} \mu_{\Psi_6} \overline{(\Psi_6)^c} \Psi_6 \right] + \text{H.c} \quad (4.18)$$

where $(\Psi_6)_{mn} = (\Psi_6)^{ij} \epsilon_{ijmn}$. As this multiplet is uncharged under $SU(2)_{L/R}$, the electric charge of each component is given by the generator of $SU(4)$ identified with $B - L$. The branching rule for this multiplet is

$$(\mathbf{6}, \mathbf{1}, \mathbf{1}) \rightarrow \overline{\mathbf{3}}_{+1/3} \oplus \mathbf{3}_{-1/3} \quad (4.19)$$

when broken to $SU(3)_c \times U(1)_Q$ of the SM. This irreducible representation therefore contains the correct states to mix with the down quarks of the standard model:

$$f_{L/R} = \begin{pmatrix} \cdot & d_r \\ \cdot & d_b \\ \cdot & d_g \\ \cdot & \cdot \end{pmatrix}_{L/R}, \quad \Psi_6 = \begin{pmatrix} 0 & (D_{L,g})^c & -(D_{L,b})^c & D_{R,r} \\ -(D_{L,g})^c & 0 & (D_{L,r})^c & D_{R,b} \\ (D_{L,b})^c & -(D_{L,r})^c & 0 & D_{R,g} \\ -D_{R,r} & -D_{R,b} & -D_{R,g} & 0 \end{pmatrix} \quad (4.20)$$

where the components $D_{(L/R),i}$ ($i = r, g, b$) have electric charge $-1/3$ and $\Psi_6 \rightarrow U_4 \Psi_6 U_4^T$.

The resulting mixing matrix for the down quark and its partners can be found by expanding eqs. (2.15) and (4.18) with eq. (4.20), giving

$$\mathcal{L}_{dD} = \begin{pmatrix} \overline{d}_L & \overline{D}_L \end{pmatrix} \begin{pmatrix} m_d & y_{\Psi_6}^L v_L^* \\ y_{\Psi_6}^R v_R & \mu_{\Psi_6} \end{pmatrix} \begin{pmatrix} d_R \\ D_R \end{pmatrix}, \quad (4.21)$$

and, in the absence of additional fermionic states which mix with ℓ , the singular values of m_d are given by the charged-lepton masses.

The additional Yukawa interactions involving Ψ_6 lead to explicit violation of the global symmetry $U(1)_J$: the bare mass term requires $J(\Psi_6) = 0$, while the two Yukawa terms of eq. (4.18) imply $J(\Psi_6) = 2$ and $J(\Psi_6) = -2$ respectively, assuming the singlet S_L is included for neutrino mass and therefore $J(\chi_{L/R}) = J(f_{L/R}) = 1$ is enforced. Therefore any two of the three terms in eq. (4.18) in combination with the Yukawa couplings of $f_{L/R}$ to S_L in eq. (2.15) leads to baryon number violating interactions. Interestingly for a more minimal PS model where the only scalars¹⁷ present are χ_R and ϕ , a global baryon number is restored in the limit $\mu_{\psi_6} \rightarrow 0$ which therefore could be argued to be small from technical naturalness.

Evaluating the full implications of baryon number violation with a realistic mass spectrum for the SM particles is quite complicated for the sextet and beyond the scope of this work. However, an example diagram for $p \rightarrow \pi^0 e^+$ is shown in fig. 3 in the case where χ_L is removed. The diagram involves the couplings

$$\mathcal{L} \supset y_R \overline{S}_L (\chi_R^{+2/3})^*_i (u_R)^i + y_{\Psi}^R ((\overline{D}_L)_k e_R + \epsilon_{ijk} (\overline{D}_R^c)^i (d_R)^j) (\chi_R^{+2/3})^k + \mu_{\Psi_6} (\overline{D}_L)_i (D_R)^i + \text{H.c.} \quad (4.22)$$

where $SU(3)$ indices are explicitly shown and the above couplings are found by expanding out eqs. (2.15) and (4.18). This decay diagram leads to an effective four-fermion interaction very similar to the coloured Higgsino mediated $p \rightarrow K^+ \bar{\nu}$ in minimal SUSY $SU(5)$, see e.g. [37]. As this usually requires very large Higgsino masses (at or larger than the GUT scale) and the SM quantum numbers of D_L and D_R are the same as the coloured Higgsino,

¹⁷Therefore the Yukawa terms $y_{\Psi}^L f_L \chi_L^\dagger \Psi_6$ and $y_L \overline{f_L} \chi_L (S_L)^c$ will not be present.

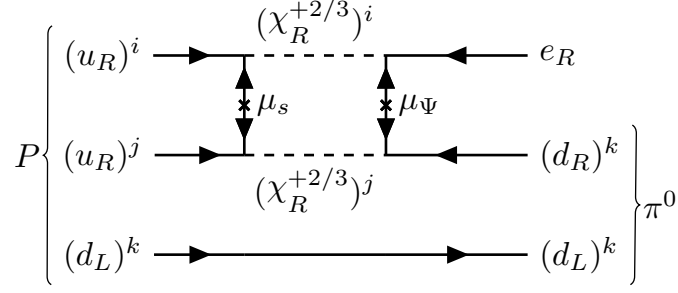


Figure 3. An example box diagram of proton decay implied by a PS model extended by a fermionic $SU(4)$ sextet fermion. The $p \rightarrow \pi^0 e^+$ diagram above is similar to the coloured Higgsino mediated proton decay, $p \rightarrow K^+ \bar{\nu}$, predicted by the minimal SUSY $SU(5)$ GUT model which typically requires GUT scale masses for the Higgsinos, see e.g. [37].

we expect that in scenarios where baryon number is not imposed (by setting μ_Ψ to be small), this diagram alone would likely lead to significant limits on the masses of the particles running in the loop which would translate into large limits on the PS breaking scale. An additional suppression factor of μ_S appears in fig. 3 which is required to be small for neutrino mass generation which may interestingly connect the large proton lifetime to the smallness of neutrino mass in this suggested minimal model.

4.1.5 $SU(4)_c$ Decuplets

Finally we consider the possibility that two fermions of opposite handedness¹⁸ transforming as $\Psi_{L/R}^{10} \sim (\mathbf{10}, \mathbf{1}, \mathbf{1})$ are added. The relevant, non-zero terms added to the Yukawa Lagrangian are

$$\begin{aligned} \mathcal{L}_{\text{YUK}} \supset \text{Tr} \Big[& \sqrt{2} y_{\Psi_{10}}^R \overline{\Psi}_L^{10} \chi_R (i\tau_2) (f_R)^T - \sqrt{2} y_{\Psi_{10}}^L (\overline{f}_L)^T (i\tau_2) \chi_L^\dagger \Psi_R^{10} \\ & + \mu_{\Psi_{10}} \overline{\Psi}_L^{10} \Psi_R^{10} + \sqrt{6} y_\Phi \overline{\Psi}_L^{10} \Phi \Psi_R^{10} \Big] + \text{H.c.} \end{aligned} \quad (4.23)$$

Similar to the case of the sextet above, these multiplets are uncharged under $SU(2)_{L/R}$ and therefore the branching rule for their breaking to $SU(3)_c \otimes U(1)_Q$ is simply given by

$$(\mathbf{10}, \mathbf{1}, \mathbf{1}) \rightarrow \mathbf{6}_{1/3} \oplus \mathbf{3}_{-1/3} \oplus \mathbf{1}_{-1}. \quad (4.24)$$

¹⁸Both are required for anomaly cancellation.

These multiplets therefore contain the necessary states to mix with *both* the down quarks and the charged leptons:

$$f_{L/R} = \begin{pmatrix} \cdot & d_r \\ \cdot & d_b \\ \cdot & d_g \\ \cdot & e \end{pmatrix}_{L/R}, \quad \Psi_{L/R}^{10} = \frac{1}{\sqrt{2}} \begin{pmatrix} \cdot & \cdot & \cdot & D_r \\ \cdot & \cdot & \cdot & D_b \\ \cdot & \cdot & \cdot & D_g \\ D_r & D_b & D_g & \sqrt{2} E^- \end{pmatrix}_{L/R} \quad (4.25)$$

where the components $D_{(L/R),i}$ ($i = r, b, g$) have electric charge $-1/3$. Contained in $\Psi_{L/R}^{10}$ is an exotic colour sextet Dirac fermion, which is embedded in the upper-left 3×3 block of the second multiplet in eq. (4.25). If such a sextet was discovered alongside heavy copies of the charged leptons and down quarks it would suggest the existence of these exotic fermion multiplets within a PS symmetry.

In this scenario, the mixing matrices for the charged leptons and down quarks are related to each other as they exist in the same multiplet. The charged lepton mixing matrix is given by

$$M_{eE} = \begin{pmatrix} \overline{e_L} & \overline{E_L} \end{pmatrix} \begin{pmatrix} m_F & \sqrt{2} y_{\Psi_{10}}^L v_L^* \\ \sqrt{2} y_{\Psi_{10}}^R v_R & \mu_{\Psi_{10}} \end{pmatrix} \begin{pmatrix} e_R \\ E_R \end{pmatrix} \quad (4.26)$$

and the down quark mixing matrix is of a similar form and only differs by some group theoretic factors

$$M_{dD} = \begin{pmatrix} \overline{d_L} & \overline{D_L} \end{pmatrix} \begin{pmatrix} m_F & y_{\Psi_{10}}^L v_L^* \\ y_{\Psi_{10}}^R v_R & \mu_{\Psi_{10}} \end{pmatrix} \begin{pmatrix} d_R \\ D_R \end{pmatrix} \quad (4.27)$$

where m_F is enforced by the PS symmetry to appear in both mass matrices and its singular values are no longer given by the charged-lepton or down-quark masses individually. The colour sextet fermion ψ develops a mass given by $m_\psi = \mu_{\Psi_{10}}$ and therefore the mass spectrum of the exotic states depends on the relative sizes of the dimensionful parameters $y_{\Psi_{10}}^R v_R$, $\mu_{\Psi_{10}}$ and $y_\Phi v_\Phi$ ¹⁹. For example assuming $\mu_{\Psi_{10}} > y_\Phi v_\Phi \gg y_{\Psi_{10}}^R v_R$ leads to a mass spectrum where the colour sextet would be the heaviest of the three exotics and the heavy, charged leptons would be the lightest.

The global symmetry $U(1)_J$ remains unbroken in the Yukawa sector and enforces the charge assignment

$$J(\Psi_L^{10}) = J(\Psi_R^{10}) = 2 \quad (4.28)$$

regardless of whether S_L is included or not and therefore baryon number remains an accidental symmetry of the Yukawa sector. The additional multiplets $\Psi_{L/R}^{10}$ do not contain any neutral states under $U(1)_Q$ and there are no lepton number violating terms present

¹⁹For phenomenological reasons the parameters m_e and $y_{\Psi_{10}}^L v_L^*$ are required to be smaller in size than these parameters.

in eq. (4.23). This is easy to see as in the absence of S_L the Yukawa Lagrangian obeys a secondary global symmetry

$$J'(\phi, \Phi) = 0, \quad J'(f_L, f_R) = 1, \quad J'(\chi_L, \chi_R) = -3 \quad \text{and} \quad J'(\Psi_L^{10}, \Psi_R^{10}) = -2. \quad (4.29)$$

Lepton number can be identified as $L = \frac{1}{4}(J' - 3T)$ such that

$$L(f_{L/R}) = \begin{pmatrix} 0 & 0 \\ 0 & 0 \\ 0 & 0 \\ 1 & 1 \end{pmatrix} \quad \text{and} \quad L(\Psi_{L/R}^{10}) = \begin{pmatrix} -1 & -1 & -1 & 0 \\ -1 & -1 & -1 & 0 \\ -1 & -1 & -1 & 0 \\ 0 & 0 & 0 & 1 \end{pmatrix} \quad (4.30)$$

which is unbroken by $\langle \chi_L, \chi_R \rangle$ and therefore ν_L and ν_R develop a Dirac mass of order m_u . Therefore, for a realistic model, S_L or some other lepton number violating physics needs to be included in order to break $L = \frac{1}{4}(J' - 3T)$ and allow for small neutrino masses. If S_L is included the neutrino mass matrix is given by eq. (2.18) as before. Baryon number violation will therefore proceed similarly to section 2.4 and therefore will lead to the same order of magnitude limits on the relevant quartic coupling of the scalar potential.

5 Fermion mixing

From the results of section 4.1 only a few PS multiplets lead to mass mixing in the charged-lepton and/or down-quark sectors in the desired way. Table 11 summarises viable multiplets from the ones considered and indicates in which sector mixing will occur. Charged-lepton mixing exclusively will occur with the addition of $SU(2)_{L/R}$ triplets or bidoublets, in the down-sector exclusively with the addition of $SU(4)$ sextets²⁰ and will occur in both sectors either through a combination of the aforementioned multiplets or with the addition of $SU(4)$ decouplets.

We analyse, where possible, the conditions necessary on the parameters of the Lagrangian which lead to the desired effects of decreasing the experimentally allowed PS breaking scale through helicity suppression and generating a viable fermion mass spectrum through mixing for all SM-like particles. We will separately consider the validity of charged-lepton mixing and down-quark mixing and finally comment on the more general scenarios where mixing occurs for both fermion types.

5.1 $e - E$ mixing

Mixing with heavy exotics within the charged-lepton sector will arise if at least one $SU(2)_{L/R}$ triplet or $SU(2)_{L/R}$ bi-doublet is included. As the minimal low-scale PS model already requires an additional singlet S_L for viable neutrino mass, it would be attractive if these

²⁰With the caveat that the additional baryon number violating Yukawa interactions do not lead to proton and neutron decay rates larger than the experimental bounds.

PS multiplet	$e - E$ mixing	$d - D$ mixing
$(\mathbf{1}, \mathbf{1}, \mathbf{3})$	✓	✗
$(\mathbf{1}, \mathbf{3}, \mathbf{1})$	✓	✗
$(\mathbf{1}, \mathbf{2}, \mathbf{2})$	✓	✗
$(\mathbf{6}, \mathbf{1}, \mathbf{1})$	✗	✓
$(\mathbf{10}, \mathbf{1}, \mathbf{1})$	✓	✓

Table 11. Summary of the results of section 4.1 which indicates which viable fermion extensions lead to a seesaw with the charged leptons by adding heavy states E or with the down quarks by adding heavy states D , required to explain the lack of mass-degeneracy predicted by PS. Including an $SU(2)_{L/R}$ triplet or bi-doublet will induce $e - E$ mixing, including an $SU(4)$ sextet will lead to $d - D$ mixing and including $SU(4)$ decouplets will lead to mixing of both types which differs only by group theoretic factors.

more complicated multiplets could allow for a viable mass spectrum for the neutral and charged leptons without the need for the singlet S_L . In this situation we parametrise the general mass mixing matrix for the charged leptons as

$$\mathcal{L}_{eE} = \left(\overline{e_L} \quad \overline{E_L} \right) \underbrace{\begin{pmatrix} m_{ee} & m_{eE} \\ m_{Ee} & m_{EE} \end{pmatrix}}_{M_{eE}} \begin{pmatrix} e_R \\ E_R \end{pmatrix} + \text{H.c.}, \quad (5.1)$$

where the different elements of M_{eE} in terms of Lagrangian parameters are given in sections 4.1.1 and 4.1.2 for each possible case we have considered. Additionally we parametrise the diagonalisation matrices for M_{eE}

$$U_L^\dagger M_{eE} U_R = \text{diag}(\dots) = M_{eE}^{\text{diag}}, \quad (5.2)$$

by

$$U_{L/R} = \begin{pmatrix} V & W \\ X & Y \end{pmatrix}_{L/R} \quad (5.3)$$

where the unitarity condition on U implies $VV^\dagger + WW^\dagger = XX^\dagger + YY^\dagger = \mathbb{1}$. Therefore the relationship between the interaction and mass eigenstates for the charged leptons is given by

$$e_{L/R} = V_{L/R} e'_{L/R} + W_{L/R} E'_{L/R} \quad (5.4)$$

with $e'_{L/R}$ ($E'_{L/R}$) corresponding to the light (heavy) mass eigenstate. The fields $e_{L/R}$ correspond to the uncoloured components of $f_{L/R}$ charged under $SU(4)$ which couple to $d_{L/R}$ via X_μ .

Therefore the relevant physical mixing matrices between the light, SM-like states and down quarks relevant for meson decays is given similarly to the vanilla PS scenario by

$$K_L^{de} = (U_L^d)^\dagger V_L, \quad K_R^{de} = (U_R^d)^\dagger V_R \quad (5.5)$$

where now the matrices $V_{L/R}$ are no longer unitary. The condition required for a chiral suppression to occur in the relevant pseudoscalar meson decays is for one of $K_{L/R}^{de}$ to satisfy

$$\|K_{L/R}^{de}\| \ll 1 \quad (5.6)$$

such that the helicity-unsuppressed contribution to each decay is sufficiently reduced as discussed in section 3.2.

The limits on heavy charged-leptons are model-dependent but in all cases far exceed the masses of the SM charged leptons. For example for an $SU(2)_L$ triplet the limits are roughly 800 GeV [38] and reduce down to 300 GeV in the case of vector-like lepton doublets [39]. We will conservatively assume that the masses of the heavy charged-lepton states all exceed 1 TeV, this obviously requires at least one block appearing in M_{eE} to have all its singular values larger than 1 TeV.

Comparing the general form of M_{eE} in eq. (5.1) to those derived for the cases of either $SU(2)_{L/R}$ triplet or the bi-doublet given in eqs. (4.3), (4.6) and (4.12) respectively, we see that two possible mass terms can be significantly larger than the electroweak scale: either the Yukawa couplings $y_{\Psi_3}^R v_R$ or $y_{\Psi_{22}}^R v_R$ proportional to the scale of $SU(2)_R$ breaking (which is absent in the case of the $SU(2)_L$ triplet), or the bare mass terms μ_{Ψ_3} and $\mu_{\Psi_{22}}$ which are completely unconstrained. Therefore the correct phenomenological masses for the heavy charged leptons are possible in the scenarios where $\|y_{\Psi_3}^R v_R, y_{\Psi_{22}}^R v_R\| \geq 1$ TeV or $\|\mu_{\Psi_3}, \mu_{\Psi_{22}}\| \geq 1$ TeV. In all cases the mass term generated by v_R appears on the off-diagonal of M_{eE} , either in the top-right entry in the case of the bi-doublet extension and in the bottom-left entry for the case of an $SU(2)_R$ triplet. Although this term is absent in the case of the $SU(2)_L$ triplet, it may be generated in the bottom-left entry of M_{eE} by assuming a modified scalar sector, which we discuss further below, and therefore the discussion below remains relevant for this exotic fermion choice. The bare mass terms μ_{Ψ_3} and $\mu_{\Psi_{22}}$ appear in the bottom-right entry in all three cases. We suppress the labels Ψ_3 and Ψ_{22} below and write $y_{\Psi}^R v_R$ and μ_{Ψ} for simplicity.

Consider first the scenario where μ_{Ψ} is taken to be larger than all other mass terms, e.g. $\mu_{\Psi} = m_{EE} > m_{eE}, m_{Ee}, m_{ee}$. Following the results from appendix A.1 the resultant masses for the seesaw states are approximated by²¹

$$m_{\ell} \simeq \left| m_{ee} - \frac{m_{eE} m_{Ee}}{m_{EE}} \right| \quad \text{and} \quad m_{\hat{h}} \simeq m_{EE}. \quad (5.7)$$

Using eq. (A.4) the mass eigenstates relate to the interaction eigenstates by

$$e_L \simeq \underbrace{\left(1 - \frac{1}{2} \left(\frac{m_{eE}}{m_{EE}} \right)^2 \right)}_{V_L} e'_L + \underbrace{\left(\frac{m_{eE}}{m_{EE}} \right)}_{W_L} E'_L \quad (5.8)$$

²¹ $m_{\hat{h}}$ is the mass of the heavy fermion, not the Higgs boson.

for the left-handed states and

$$e_R \simeq \underbrace{\left(1 - \frac{1}{2} \left(\frac{m_{Ee}}{m_{EE}}\right)^2\right)}_{V_R} e'_R + \underbrace{\left(\frac{m_{Ee}}{m_{EE}}\right)}_{W_R} E'_R \quad (5.9)$$

for the right-handed states. One generation of fermions with real parameters has been assumed for simplicity in order to establish viability. Similar conclusions are reached for multi-generational scenarios where each entry of M_{eE} is promoted to a block matrix of appropriate dimension. The one-dimensional equivalents of $V_{L/R}$ and $W_{L/R}$ are indicated and, as can be seen in this scenario where the bare mass is the dominant term in the charged-lepton seesaw, both the left- and right-handed light charged lepton mass states are predominantly made up of the fields $e_{L/R}$ embedded in $f_{L/R}$. Therefore, while this would lead to a very mild suppression in the PS mass limits as $V_{L/R}$ are slightly suppressed compared to the scenario without charged-lepton mass mixing (where $V_{L/R} = 1$), the mass limits obtained for X_μ will be of similar size to those appearing in table 4 and therefore the limits will remain at around $\mathcal{O}(100 - 1000)$ TeV depending on the structure of $K_{L/R}^{de}$.

Alternatively, $y_\Psi^R v_R$ can be the dominant mass term within M_{eE} which corresponds to one of the off-diagonal terms in our parametrisation. Following a similar procedure we find

$$m_\ell \simeq \left| m_{Ee} - \frac{m_{ee} m_{EE}}{m_{eE}} \right| \quad (5.10)$$

and

$$\begin{aligned} e_L &\simeq - \underbrace{\frac{m_{EE}}{m_{eE}}}_{V_L} e'_L + \underbrace{\left(1 - \frac{1}{2} \left(\frac{m_{EE}}{m_{eE}}\right)^2\right)}_{W_L} E'_L \\ e_R &\simeq \underbrace{\left(1 - \frac{1}{2} \left(\frac{m_{ee}}{m_{eE}}\right)^2\right)}_{V_R} e'_R + \underbrace{\left(\frac{m_{ee}}{m_{eE}}\right)}_{W_R} E'_R \end{aligned} \quad (5.11)$$

for the scenario where m_{eE} is dominant and

$$m_\ell \simeq \left| m_{eE} - \frac{m_{ee} m_{EE}}{m_{Ee}} \right| \quad (5.12)$$

and

$$\begin{aligned}
e_L &\simeq \underbrace{\left(1 - \frac{1}{2} \left(\frac{m_{ee}}{m_{Ee}}\right)^2\right)}_{V_L} e'_L + \underbrace{\left(\frac{m_{ee}}{m_{Ee}}\right)}_{W_L} E'_L \\
e_R &\simeq - \underbrace{\frac{m_{EE}}{m_{Ee}}}_{V_R} e'_R + \underbrace{\left(1 - \frac{1}{2} \left(\frac{m_{EE}}{m_{Ee}}\right)^2\right)}_{W_R} E'_R
\end{aligned} \tag{5.13}$$

if m_{Ee} is dominant. In both cases, one of $e_{L/R}$ is predominantly made up of the light mass state $e'_{L/R}$ while the opposite chirality is predominantly made up from the heavy mass state $E'_{R/L}$. V_L or V_R are now significantly different in size from each other, where one will be suppressed compared to the other. If m_{eE} is the largest term then $V_L \ll V_R$ and the leptoquark X_μ will strongly couple e'_R and d'_R but not e'_L and d'_L and vice versa for m_{Ee} dominance. Therefore the desired helicity suppression in meson decays induced by X_μ will occur for the hierarchy $y_\Psi^R v_R > \mu_\Psi$ leading to decreased PS breaking limits, potentially as low as those appearing in table 7. Both an $SU(2)_R$ triplet or the $SU(2)_{L/R}$ bidoublet are therefore viable candidates as one off-diagonal term is proportional to v_R and therefore can be large in size. In the case of an $SU(2)_L$ triplet, assuming no modification to the scalar fields, the only mass term not tied to the electroweak scale is μ_Ψ and therefore helicity suppression in the relevant meson decays will not occur as μ_Ψ must be dominant phenomenologically.

For a multi-generational scenario all terms in M_{eE} are promoted to block matrices and using the results in appendix A.2 we find for $\|m_{Ee}\| > \|m_{ee}, m_{eE}, m_{EE}\|$

$$m_L \simeq m_{eE} - m_{ee} (m_{Ee}^{-1}) m_{EE} \tag{5.14}$$

and

$$\begin{aligned}
e'_L &\simeq \underbrace{\left(\mathbb{1} - \frac{1}{2} (m_{ee} m_{Ee}^{-1}) (m_{ee} m_{Ee}^{-1})^\dagger\right)}_{V_L} O_L e_L + \underbrace{m_{ee} m_{Ee}^{-1} O_L}_{W_L} E_L \\
e'_R &\simeq - \underbrace{m_{Ee}^{-1} m_{EE} O_R}_{V_R} e_R + \underbrace{\left(\mathbb{1} - \frac{1}{2} (m_{Ee}^{-1} m_{EE}) (m_{Ee}^{-1} m_{EE})^\dagger\right)}_{W_R} O_R E_R
\end{aligned} \tag{5.15}$$

where $O_{L/R}$ and $\mathcal{O}_{L/R}$ are the unitary matrices which diagonalise the light and heavy mass blocks which appear after block diagonalisation, e.g. $O_L^\dagger m_L O_R = \text{diag}(\dots)$. For obvious reasons these expressions are only valid when m_{Ee} is nonsingular. Similar expressions for m_{eE} dominance can be derived quite simply and the results only differ by the same permutations of parameters as between eqs. (5.10) and (5.11).

One last potential scenario which will lead to the heavy lepton masses exceeding 1 TeV occurs for the tuned case $y_\Psi v_R \simeq \mu_\Psi$. Consider for example when $m_{Ee} \simeq m_{EE}$ and are both dominant in M_{eE} . We find for one generation

$$m_\ell \simeq \left| \frac{m_{ee} - m_{eE}}{\sqrt{2}} \right| \quad (5.16)$$

and

$$\begin{aligned} e_L &\simeq - \underbrace{\left(1 - \frac{1}{4} \left(\frac{m_{eE} + m_{ee}}{m_{EE}} \right)^2 \right)}_{V_L} e'_L + \underbrace{\frac{1}{2} \left(\frac{m_{eE} + m_{ee}}{m_{EE}} \right)}_{W_L} E'_L \\ e_R &\simeq \underbrace{\frac{1}{\sqrt{2}} e'_R}_{V_R} + \underbrace{\frac{1}{\sqrt{2}} E'_R}_{W_R} \end{aligned} \quad (5.17)$$

with similar results if $m_{eE} \simeq m_{EE}$ except for the reassignments $L \leftrightarrow R$ on the fields above. Here the mass eigenstate e'_R is made up of a roughly equal amount of the fields e_R and E_R and therefore while the mixing parameter V_R is decreased, it remains an order one number. The overall strength of K_R^{de} will be lowered, however the helicity-unsuppressed contribution for each meson decay will remain dominant as it is several orders of magnitude larger than the helicity-unsuppressed contribution, as discussed in section 3.2. Therefore we find that in order for helicity suppression to allow for decreased experimental limits on the PS breaking scale, the hierarchy $y_\Psi^R v_R \gg \mu_\Psi$ is required.

We will therefore adopt the hierarchy $\|y_\Psi^R v_R\| > \|y_\Psi v_L, m_e, \mu_\Psi\|$ below in order to helicity suppress the mass limits of X_μ , further requiring the correct down-quark and charged-lepton masses with appropriate SM-like weak couplings as a secondary condition will further restrict the parameters in each mass mixing matrix.

Specifically for the case of an $SU(2)_R$ triplet, adopting the above hierarchy in M_{eE} leads to the light-mass block approximately given by

$$m_\ell \simeq -\frac{1}{v_R} m_d (Y_{\Psi_3})^{-1} \mu_{\Psi_3} \quad (5.18)$$

where we have introduced three generations of the triplet Ψ_3^R and Y_{Ψ_3} corresponds to a 3×3 matrix further assumed to be nonsingular. Unless stated otherwise y_Ψ and Y_Ψ will distinguish between when one or three generations of exotic fermions are introduced respectively. Within eq. (5.18) we have used the relation $m_e = m_d$ which is enforced by the PS symmetry and therefore the singular values of m_d are given by the down-quark masses run up to the PS breaking scale. Similarly the singular values of the light block m_ℓ must be given by the masses of the charged-leptons at the same scale. An unavoidable consequence of eq. (5.18) is that it necessarily predicts that all generations of charged leptons have masses strictly lighter than their corresponding generation of down-quark. We prove this

result in appendix A.3. While this is accurate for the first and third generations, this mass hierarchy is flipped in the second generation as shown in table 6 where the muon is heavier than the strange quark at least for energy scales below 1000 TeV which we are considering.

Therefore we find that eq. (5.18) is unable to reproduce the correct charged-lepton masses if $m_e = m_d$ is enforced by the PS symmetry to give the down-quark masses. The alternative seesaw scenario where $\|\mu_{\Psi_3}\| > \|Y_{\Psi_3} v_R\|$, although unable to lead to the desired chiral suppression in the PS breaking scale, is also unable to reproduce the correct muon and strange masses as it requires $m_\ell \simeq m_d$. Therefore a potential hybrid scenario where the hierarchy in the singular values between $Y_{\Psi_3}^R v_R$ and μ_{Ψ_3} flips for the second generation compared to the first and third would also not be viable. Similar arguments apply to the $SU(2)_L$ triplet, which was already unable to give sufficiently heavy masses to the charged-lepton partners. Therefore both triplet scenarios are unable to reproduce the correct charged-lepton masses in their minimal form. This is a direct consequence of the zero entry appearing in the mass matrix M_{eE} but applies to any similar scenario with quark-lepton mass unification and exotic mass mixing. Similar arguments apply to the scenario where both an $SU(2)_L$ and $SU(2)_R$ triplet are added as in eqs. (4.8) and (4.9) and therefore we find that $SU(2)_{L/R}$ triplets require a more exotic scalar sector such that all mass terms in the Yukawa Lagrangian can be generated.

5.1.1 Top-right dominance: Bi-doublet fermions

Turning to the case of the $SU(2)_{L/R}$ bi-doublet, now each entry of the charged-lepton mass matrix M_{eE} is non-zero. The choice $\|Y_{\Psi_{22}} v_R\| > \|\mu_{\Psi_{22}}\|$, such that the desired suppression in the PS limits occurs, implies that the top-right entry of M_{eE} is the dominant block, as can be seen in eq. (4.12). Therefore the light mass block is given by

$$m_\ell \simeq Y_{\Psi_{22}}^L v_L - \frac{1}{v_R} \mu_{\Psi_{22}} (Y_{\Psi_{22}}^R)^{-1} m_d \quad (5.19)$$

where again the PS symmetry enforces $m_e = m_d$. Now with the addition of the mass term $Y_{\Psi_{22}}^L v_L$ the correct charged-lepton masses can be generated. For example in the limit $\mu_{\Psi_{22}} \rightarrow 0_{3 \times 3}$ the charged lepton masses are simply given by

$$m_\ell \simeq Y_{\Psi_{22}}^L v_L \quad (5.20)$$

and therefore the effect of the seesaw in M_{eE} is to completely disassociate the mass origin of the SM-like charged leptons from the down quarks as now they arise from different Yukawa couplings and vevs and implies that $v_L \gtrsim m_\tau$.

Using appendix A.2, the mass states of the light leptons relate to the interaction states

by

$$\begin{aligned} e'_L &\simeq -(O_L^e)^\dagger \mathcal{X} e_L + (O_L^e)^\dagger \left(\mathbb{1} - \frac{1}{2} \mathcal{X} \mathcal{X}^\dagger \right) E_L \\ e'_R &\simeq (O_R^e)^\dagger \left(\mathbb{1} - \frac{1}{2} \mathcal{Z}^\dagger \mathcal{Z} \right) e_R - (O_R^e)^\dagger \mathcal{Z}^\dagger E_R \end{aligned} \quad (5.21)$$

where $O_{L/R}^e$ diagonalise the light mass block and

$$\begin{aligned} \mathcal{X} &\simeq \frac{1}{v_R} \mu_{\Psi_{22}} (Y_{\Psi_{22}}^R)^{-1} + \frac{v_L}{v_R^2} Y_{\Psi_{22}}^L m_d^\dagger [(Y_{\Psi_{22}}^R)^\dagger]^{-1} (Y_{\Psi_{22}}^R)^{-1}, \\ \mathcal{Z} &\simeq \frac{1}{v_R} (Y_{\Psi_{22}}^R)^{-1} m_d + \frac{v_L}{v_R^2} (Y_{\Psi_{22}}^R)^{-1} [(Y_{\Psi_{22}}^R)^\dagger]^{-1} \mu_{\Psi_{22}}^\dagger Y_{\Psi_{22}}^L \end{aligned} \quad (5.22)$$

and we have expanded up to second order in \mathcal{X} and \mathcal{Z} . In this seesaw regime, the light left-handed lepton states measured in experiments are predominately made up of E_L appearing in the bi-doublet whereas the right-handed light states are predominately made up of e_R appearing in f_R which interacts with X_μ .

For clarity, the relevant physical mixing matrices are given by

$$K_L^{de} \simeq -(U_L^d)^\dagger \mathcal{X}^\dagger O_L^e, \quad K_R^{de} \simeq (U_R^d)^\dagger \left(\mathbb{1} - \frac{1}{2} \mathcal{Z}^\dagger \mathcal{Z} \right) O_R^e \quad \text{and} \quad U_{\text{PMNS}} \simeq N_\nu^\dagger \left(\mathbb{1} - \frac{1}{2} \mathcal{X} \mathcal{X}^\dagger \right) O_L^e, \quad (5.23)$$

where N_ν corresponds to the relevant non-unitary submatrix of the neutral fermion diagonalising matrix for the active neutrinos. Therefore in this scenario the deviation from unitarity of the PMNS matrix arising from mixing in the charged lepton sector *and* the suppression of the matrix K_L^{de} is determined by the smallness of the matrix \mathcal{X} . In eq. (5.22) we have included the second order terms in the expansion as for sufficiently small values in the matrix $\mu_{\Psi_{22}}$ this deviation will be dominated by the second-order term. As $Y_{\Psi_{22}}^L v_L$ and m_d are fixed to give the correct SM charged-lepton and down-quark masses respectively, the second order term is therefore fixed for a given choice of $Y_{\Psi_{22}}^R v_R$ and therefore can place a lower bound on the scale v_R required to satisfy both PMNS unitarity constraints and lead to the desired chiral suppression in the rare meson decays which constrain PS.

The neutrino mass matrix with the addition of the fermion bi-doublets is given by the block matrix equivalent of eq. (4.13) which specifically for the hierarchy $\|Y_{\Psi_{22}}^R v_R\| > \|m_u, Y_{\Psi_{22}}^L v_L\| > \|\mu_{\Psi_{22}}\|$ leads to the following four mass blocks (after block diagonalisation):

$$\begin{aligned} m_{1,2} &\simeq v_R Y_{\Psi_{22}}^R & \nu_{1/2} &\simeq \frac{1/i}{\sqrt{2}} (\nu_L \pm N_R^c) \\ m_3 &\simeq \frac{v_L}{v_R} \left(Y_{\Psi_{22}}^L (Y_{\Psi_{22}}^R)^{-1} m_u + m_u^T [Y_{\Psi_{22}}^L (Y_{\Psi_{22}}^R)^{-1}]^T \right) & \nu_3 &\simeq \nu_R^c \\ m_4 &\simeq \frac{1}{v_L v_R} \mu_{\Psi_{22}} [(Y_{\Psi_{22}}^L)^T m_u^{-1} Y_{\Psi_{22}}^R + (Y_{\Psi_{22}}^R)^T (m_u^T)^{-1} Y_{\Psi_{22}}^L]^{-1} \mu_{\Psi_{22}}^T & \nu_4 &\simeq N_L. \end{aligned} \quad (5.24)$$

Here there is a heavy pseudo-Dirac pair with degenerate masses to the heavy charged leptons, a light neutrino block with mass arising from a linear seesaw mechanism whose

mass eigenstate is predominantly made up of ν_R . and an even-lighter neutrino mass block which is predominantly made up of N_L appearing in the bi-doublet. Therefore

$$m_{\nu_4} \ll m_{\nu_3} \ll m_{\nu_1}, m_{\nu_2} \quad (5.25)$$

where m_{ν_4} corresponds to the three light neutrinos observed through oscillation experiments. A more complete expression for the relationship between the neutrino mass and interaction eigenstates can be found at the end of appendix A.4. In appendix A.4 we argue that the above scenario where $\mu_{\Psi_{22}}$ is significantly smaller than all other mass parameters, which will lower the experimental limits on PS breaking, is the only scenario which allows for an experimentally valid spectrum of active neutrino masses unless a PS breaking scale larger than 10^{11} GeV is adopted. It is quite striking that the only hierarchy of parameters which allows for both low scale PS breaking and appropriately light active neutrino masses, when bi-doublet fermions are introduced, is the same hierarchy that will lead to a suppression in the experimental limits on the PS breaking scale. Additionally, in the limit $\mu_{\Psi_{22}} \rightarrow 0_{3 \times 3}$ where the lightest neutrinos are massless at tree-level, there is an additional global symmetry conserved in the Yukawa Lagrangian and therefore taking this mass matrix to be small is technically natural.

The correct charged-lepton masses for each generation and the active neutrino mass limits and differences can both be achieved with the addition of the bi-doublet without needing to introduce any additional states, such as the singlet S_L . Equations (5.19) and (5.24) can be solved simultaneously for the three unknown blocks $Y_{\Psi_{22}}^R$, $Y_{\Psi_{22}}^L$ and $\mu_{\Psi_{22}}$ with the assumed hierarchy between each block. In the one generational scenario, the masses of the two lightest neutrino states and the light charged lepton state are given by

$$m_{\nu_3} \simeq \frac{v_L}{v_R} \frac{2y_{\Psi_{22}}^L m_t}{y_{\Psi_{22}}^R} \quad (5.26)$$

$$m_{\nu_4} \simeq \frac{1}{v_L v_R} \frac{\mu_{\Psi}^2 m_t}{2y_{\Psi_{22}}^L y_{\Psi_{22}}^R} \quad (5.27)$$

$$m_\ell \simeq v_L y_{\Psi_{22}}^L - \frac{\mu_{\Psi} m_b}{v_R y_{\Psi_{22}}^R} \quad (5.28)$$

where we have fixed the masses of the quarks to the top- and bottom-quark respectively. Setting $m_\ell \simeq 1$ GeV in order to reproduce the correct tau mass and $m_b \simeq 4$ GeV and $m_t \simeq 173$ GeV leads to fig. 4 where we find the required size of $\mu_{\Psi_{22}}$ as a function of $y_{\Psi_{22}}^R v_R$ for different choices of the light neutrino mass. We find for sub-eV neutrino masses, setting v_R to be between 1 – 100 TeV requires $\mu_{\Psi_{22}}$ to be below the MeV scale. Due to the small size of $\mu_{\Psi_{22}}$ required from neutrino mass limits, the term $\mu_{\Psi_{22}} m_d / y_{\Psi_{22}}^R v_R$ entering the charged lepton masses is negligible compared to $y_{\Psi_{22}}^L v_L$ and therefore the correct charged-lepton masses are easily possible. As discussed, such small values of $\mu_{\Psi_{22}}$ required for neutrino mass quite conveniently also lead to a chiral suppression in the PS breaking scale. The mass of the intermediately heavy neutrino, ν_3 , will vary only with the size of $y_{\Psi_{22}}^R v_R$ as all other parameters are related to SM masses. The predicted mass of m_{ν_3} lies roughly

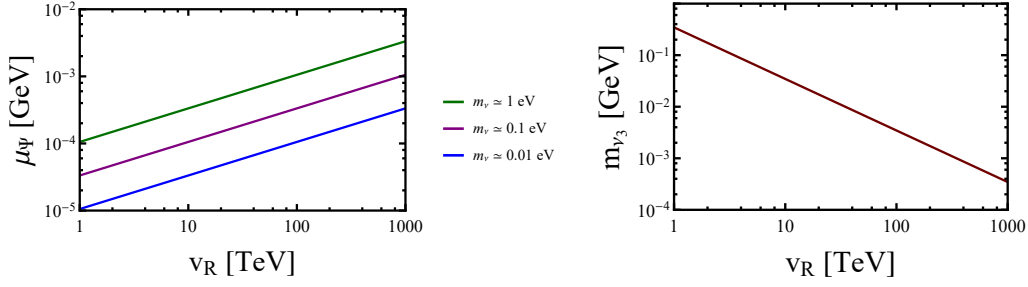


Figure 4. Plot of the required size of $\mu_{\Psi_{22}}$ in GeV as a function of v_R in TeV in the one generational scenario where $y_{\Psi_{22}}^R = 1$ has been assumed (**left**) and the masses of the intermediately heavy neutrino as a function of the same scale (**right**). Different lines correspond to different choices for the value of the neutrino masses and we have fixed $m_\ell \simeq 1$ GeV, $m_b \simeq 4$ GeV and $m_t \simeq 173$ GeV in order to reproduce the correct tau, bottom- and top-quark masses. Requiring sufficiently light neutrinos is only possible when $\mu_{\Psi_{22}}$ is sufficiently small which also happens to be the requirement in order to helicity-suppress the experimental limits on PS breaking.

between the MeV and GeV scales depending on the v_R breaking scale, with larger scales of $SU(2)_R$ breaking corresponding to lighter masses as demonstrated in the second plot of fig. 4. We note that for this proposed scenario, the quark masses arise from the vevs v_1 and v_2 from ϕ whereas the charged-lepton masses predominately arise from the vev v_L appearing in f_L .

The lightest neutrino mass eigenstate arises predominantly from the state N_L appearing in the bi-doublet fermion Ψ_{22} and therefore, as phenomenologically required, will have SM-like weak interactions. The left-handed charged-lepton mass eigenstates arise predominantly from the state E_L which appears in the same bi-doublet as N_L , as shown in eq. (4.11), additionally they form an $SU(2)_L$ doublet with each other after $SU(2)_R$ breaking. The (pseudo-unitary) PMNS matrix is identified from the coupling of W_L^\pm to N_L and E_L as

$$U_L = (\mathbb{1} - \eta') U_N^\dagger (\mathbb{1} - \eta') O_L^e \quad (5.29)$$

where

$$\eta' \simeq \frac{1}{2} \mathcal{X} \mathcal{X}^\dagger \quad (5.30)$$

measures the deviation from unitarity arising from mixing. We find the deviation to be the same in both sectors, at least at the lowest order, as explained in appendices A.2 and A.4. As usual U_N and O_L^e are the unitary matrices which diagonalise the light mass blocks in each sector of the block-diagonal mass matrices.

Writing

$$\begin{aligned}
U_L &= \left[(\mathbb{1} - \eta') U_N^\dagger (\mathbb{1} - \eta') O_L^e \right] \left[(O_L^e)^\dagger U_N U_N^\dagger O_L^e \right] \\
&= \left[(\mathbb{1} - \eta') U_N^\dagger (\mathbb{1} - \eta') U_N \right] U_N^\dagger O_L^e \\
&\simeq \left(\mathbb{1} - \eta' - U_N^\dagger \eta' U_N \right) U_N^\dagger O_L^e \\
&= (\mathbb{1} - \eta) U_{\text{PMNS}}
\end{aligned} \tag{5.31}$$

allows us to estimate the deviation from unitarity by $(\mathbb{1} - \eta)$, as is usually done, where

$$\eta \simeq \eta' + U_N^\dagger \eta' U_N \tag{5.32}$$

and we identify the combination $U_N^\dagger O_L^e$ with the unitary PMNS matrix as usual.

The left plot of fig. 5 shows the deviation from unitarity as a function of $\mathcal{X} \simeq \mu_{\Psi_{22}} (Y_{\Psi_{22}}^R)^{-1}$ where we have fixed $U_N = \mathbb{1}$ for simplicity. We further assumed that $Y_{\Psi_{22}}^R$ was diagonal with entries close to unity such that the vev of v_R can be as small as possible²². We then performed two scans over different values of v_R ranging from 1 TeV to 10^4 TeV. In the first scan (in blue) we randomly scanned over the entries of $\mu_{\Psi_{22}}$ and therefore do not generate the correct neutrino mass spectrum but establishes the relationship between η and $\mu_{\Psi_{22}}$. The second scan (in red) had $\mu_{\Psi_{22}}$ fixed for a given $v_R Y_{\Psi_{22}}^R$ through a Casas-Ibarra parametrisation in order to generate the correct charged lepton and neutrino masses. The resultant PMNS matrix was compared to the experimental limits on the deviation from unitarity, η^{exp} which we take from [40], and we find that the region which leads to a viable mass spectrum for the SM leptons predicts a deviation of unitarity many orders of magnitude below the current limit. This is due to the deviation being proportional to the small matrix $\mu_{\Psi_{22}}$. For alternative models where, for example, the size of $\mu_{\Psi_{22}}$ and therefore $\|\mathcal{X}\|_F$ is not fixed to be small by requiring small neutrino masses (through the introduction of additional neutral lepton mass mixing), deviation from unitarity limits constrain

$$\|\mathcal{X}\|_F \lesssim 10^{-1}. \tag{5.33}$$

Figure 6 plots the experimental limits on the mass of X_μ as a function of \mathcal{X} where again points in blue have the entries of $\mu_{\Psi_{22}}$ randomly scanned over and points in red correspond to where $\mu_{\Psi_{22}}$ has been fixed by through a Casas-Ibarra parameterisation. We find that the only region of parameter space which allows for a low-scale seesaw in the charged lepton and neutrino masses also happens to be the region where the limits on the mass of X_μ have been completely helicity suppressed to their lowest values. The plot on the left and right represent two different choices of $K_{L/R}^{de}$ where we find the same behaviour regardless of the form of $K_{L/R}^{de}$. For some more complicated scenario where the entries of

²²For a non-degenerate spectrum of singular values in $Y_{\Psi_{22}}$, requiring all the masses of the heavy charged leptons to be larger than 1 TeV requires larger v_R breaking scales, e.g. if $\sigma_1(Y_{\Psi_{22}}) = 1/100$ then this requires $v_R \geq 100$ TeV.

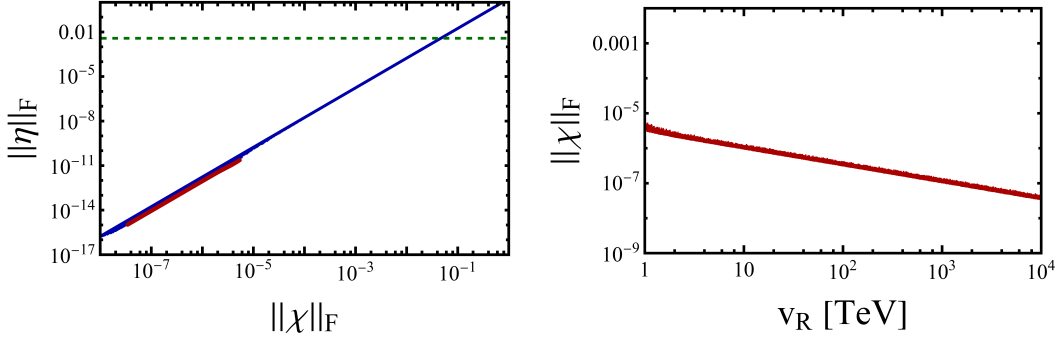


Figure 5. Plot of the deviation of unitarity (**left**) as a function of \mathcal{X} where points in blue correspond to a random scan on the entries of $\mu_{\Psi_{22}}$ and $Y_{\Psi_{22}}^R$ whereas points in red correspond to the region which gives the correct charged-lepton and neutrino masses through a Casas-Ibarra parameterisation. We find that there are no limits on the scale v_R from unitarity violation and furthermore the region with a viable neutrino mass spectrum predicts a deviation of unitarity many orders of magnitude less than the experimental precision. The (**right**) plot shows the generated \mathcal{X} through the Casas-Ibarra parameterisation as a function of v_R which leads to a viable charged-lepton and neutrino mass spectrum. As the deviation of unitarity is given by $\eta \simeq \mathcal{X}^2$, the deviation at all scales is significantly smaller than the current experimental limits. $\|\cdot\|_F$ corresponds to the Frobenius norm of the given matrix which we use to present the data and the limits on the deviation indicated by the dashed green line is taken from [40].

\mathcal{X} are not related to the smallness of neutrino mass, deviation from unitarity limits require $\|\mathcal{X}\|_F \lesssim 10^{-1}$ and therefore would at a minimum lead to the limits decreasing by about a factor of a half compared to the limits obtained without any charged-lepton mixing. For values where $\|\mathcal{X}\|_F \lesssim 10^{-2}$ the limits on the mass of X_μ are decreased by about an order of magnitude and for $\|\mathcal{X}\|_F \lesssim 10^{-3}$ the limits are completely helicity suppressed to their lowest values.

Therefore we find that with the addition of fermionic $SU(2)_{L/R}$ bi-doublets to the usual PS fermions the singlet S_L is no longer necessary for the generation of neutrino masses. The down-quark, charged-lepton and neutrino masses can all be successfully generated for low scales of PS breaking only in the region where $\|\mu_{\Psi_{22}}\|$ is smaller than all other mass parameters, and this region also leads to an order of magnitude reduction in the limits on m_X through helicity suppression. The smallness of the entries of $\mu_{\Psi_{22}}$ can be justified through technical naturalness, since a new global symmetry is recovered (which can be identified with a type of lepton number) when they are taken to zero. In this limit the active neutrino become massless, however other massive Majorana neutrinos are present.

A number of predictions for the exotic fermions can be made in the scenario where only $f_{L/R}$ and Ψ_{22} are present. Firstly heavy charged-lepton partners and pseudo-Dirac pairs of heavy neutrinos are predicted to have the same masses as each other at the scale of $SU(2)_R$ breaking and additional, intermediately heavy neutrinos are predicted to exist with masses between MeV to GeV which are sufficiently heavy to not violate any cosmological bounds.

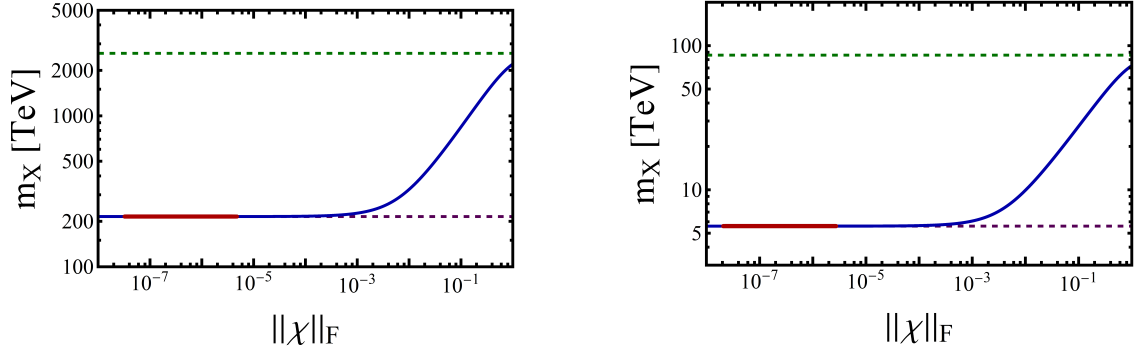


Figure 6. Plot of the experimental limits on m_X as a function of \mathcal{X} where we have assumed $K_{L/R}^{de} = \mathbb{1}$ (**left**) and mixing angles given by the fifth row of tables 5 and 9 (**right**). Points in blue correspond to a random scan over $\mu_{\Psi_{22}}$ in order to establish its variation whereas points in red correspond to where the entries of $\mu_{\Psi_{22}}$ are fixed through a Casas-Ibarra parameterisation to give a valid neutrino mass spectrum. We find that all regions which lead to a viable neutrino mass spectrum also imply that the limits on the mass of X_μ are completely helicity suppressed. This remains true for any choices of the physical mixing matrices $K_{L/R}^{de}$. The horizontal dashed green lines corresponds to the limits obtained without helicity suppression, as in tables 3 to 5, and the horizontal dashed purple lines corresponds to the limits calculated with exact helicity suppression as in tables 7 to 9. For large values of $\|\mathcal{X}\|_F$ the limits on the mass of X_μ approach their usual values whereas for values where $\|\mathcal{X}\|_F \lesssim 10^{-3}$ the limits on m_X are almost identical to the limits obtained with exact helicity suppression.

For more complicated scenarios with additional fermions (but the same charged-lepton mass mixing matrix), where the size of \mathcal{X} is not tied to the smallness of neutrino mass, we find that unitarity deviation constraints begin to constrain the overall size of \mathcal{X} and imply that the limits on m_X must be reduced by at least a factor of a half.

5.1.2 Bottom-left dominance: $SU(2)_{L/R}$ Triplet fermions

The analysis of the alternative scenario where the mass matrix $Y_\Psi^R v_R$ appears in the bottom-left entry of M_{eE} (such as when an $SU(2)_R$ triplet is added) follows very similarly to the above, with only a few key differences. As mentioned previously, the scalar content we have chosen is unable to generate a viable charged lepton mass spectrum in the case of the triplets due to the lack of an $e_L E_R$ or $E_L e_R$ mass term in the Yukawa sector, as per eqs. (4.3) and (4.6). However, these missing mass terms can be generated through a modified scalar sector. For example, if $\chi_L \sim (\mathbf{4}, \mathbf{2}, \mathbf{1})$ is replaced with $\chi' \sim (\mathbf{4}, \mathbf{2}, \mathbf{3})$ then, as was first noted in [15], the missing mass term in the top-right entry of M_{eE} in eq. (4.3), proportional to v_L , is generated for the case of an $SU(2)_R$ triplet. Similarly, if $\chi_R \sim (\mathbf{4}, \mathbf{1}, \mathbf{2})$ is replaced with $\chi'' \sim (\mathbf{4}, \mathbf{3}, \mathbf{2})$ then the missing mass term in the bottom-left entry of M_{eE} , proportional to v_R , is generated for the case of an $SU(2)_L$ triplet. We therefore assume that all mass terms are generated in what follows, with a $Y_{\Psi_3}^R v_R$ mass matrix appearing in the bottom-left entry of M_{eE} in eq. (4.6), but remain agnostic about

the scalar sector which generates it.

We shall also not undertake a detailed study of the requirements for neutrino masses in these modified scenarios, but make the following brief observations: A crucial difference between the triplet and bi-doublet scenarios is that the neutral lepton mass mixing matrix in the case of triplets is given by an inverse/linear seesaw similar to eq. (2.17), with the exception that the terms are also related to the charged-lepton mass mixing matrix. In appendix A.5 we argue that, unlike the bi-doublet case, the mass mixing matrices in this scenario are such that low-scale seesaws for the neutrinos and charged leptons are unable to correctly reproduce the SM lepton masses. A viable setup therefore requires additional physics to further decouple the charged- and neutral-lepton mass mixing matrices, for example with the addition of singlet fermions S_L [15] which also appear in the usual low-scale PS particle spectrum. Introducing $SU(2)_L$ or $SU(2)_R$ triplets therefore requires both a modification of the scalar content of the theory (to generate a viable charged-lepton mass spectrum), as well as *additional* fermionic states to generate sufficiently light neutrinos for low scales of PS breaking.

We therefore assume some additional physics is included in the neutrino sector to allow for a viable mass spectrum and simply comment on the implications of a charged-lepton mass matrix of the form

$$\mathcal{L}_{eE} = \begin{pmatrix} \overline{e_L} & \overline{E_L} \end{pmatrix} \begin{pmatrix} m_d & Y_{\Psi_3}^L v_L \\ \sqrt{2} Y_{\Psi_3}^R v_R^* & \mu_\Psi \end{pmatrix} \begin{pmatrix} e_R \\ E_R \end{pmatrix}, \quad (5.34)$$

where the dominant seesaw term in the bottom-left entry has on the limits on PS breaking through m_X .

Adopting the hierarchy $\|Y_{\Psi_3}^R\| > \|m_d, \mu_{\Psi_3}, Y_{\Psi_3}^L v_L\|$, necessary for a chiral suppression to occur, leads to

$$m_\ell \simeq v_L Y_{\Psi_3}^L - \frac{1}{v_R} m_d (Y_{\Psi_3}^R)^{-1} \mu_\Psi \quad (5.35)$$

for the light states after diagonalisation. The relationship between the interaction and mass eigenstates is now given by

$$\begin{aligned} e'_L &\simeq (O_L^e)^\dagger \left(\mathbb{1} - \frac{1}{2} \mathcal{X} \mathcal{X}^\dagger \right) e_L - (O_L^e)^\dagger \mathcal{X} E_L \\ e'_R &\simeq -(O_R^e)^\dagger \mathcal{Z}^\dagger e_R + (O_R^e)^\dagger \left(\mathbb{1} - \frac{1}{2} \mathcal{Z}^\dagger \mathcal{Z} \right) E_R \end{aligned} \quad (5.36)$$

where $O_{L/R}^e$ diagonalises the light mass block,

$$\begin{aligned} \mathcal{X} &\simeq \frac{1}{v_R} m_d (Y_{\Psi_3}^R)^{-1} + \frac{v_L}{v_R^2} Y_{\Psi_3}^L \mu_{\Psi_3}^\dagger [(Y_{\Psi_3}^R)^\dagger]^{-1} (Y_{\Psi_3}^R)^{-1} \\ \mathcal{Z} &\simeq \frac{1}{v_R} (Y_{\Psi_3}^R)^{-1} \mu_{\Psi_3} + \frac{v_L}{v_R^2} (Y_{\Psi_3}^R)^{-1} [(Y_{\Psi_3}^R)^\dagger]^{-1} m_d^\dagger Y_{\Psi_3}^L \end{aligned} \quad (5.37)$$

and we have expanded up to second order. The physical mixing matrices are now given by

$$K_L^{de} \simeq -(U_L^d)^\dagger \left(\mathbb{1} - \frac{1}{2} \mathcal{X} \mathcal{X}^\dagger \right) O_L^e, \quad K_R^{de} \simeq -(U_R^d)^\dagger \mathcal{Z} O_R^e \quad \text{and} \quad U_{\text{PMNS}} \simeq N_\nu^\dagger \left(\mathbb{1} - \frac{1}{2} \mathcal{X} \mathcal{X}^\dagger \right) O_L^e. \quad (5.38)$$

The notable differences to the results in the previous section where the top-right entry of M_{eE} is dominant are: (i) the leptoquark X_μ now effectively only couples to the left-handed states (compared with right-handed previously), and (ii) the parameter controlling the deviation from unitarity for the PMNS and the parameter determining the degree of helicity suppression in meson decays are different. Unitarity deviation is determined by \mathcal{X} , which is given at lowest order by $\mathcal{X} \simeq m_d (Y_{\Psi_3}^R v_R)^{-1}$, while the degree of helicity suppression in the X_μ couplings is given by $\mathcal{Z} \simeq (Y_{\Psi_3}^R v_R)^{-1} \mu_{\Psi_3}$. In the previous scenario of top-right entry dominance, both are controlled by \mathcal{X} which in that case was given by $\mathcal{X} \simeq (Y_{\Psi_3}^R v_R)^{-1} \mu_{\Psi_3}$. Unlike before where μ_{Ψ_3} could be lowered, the only way to decrease the deviation from unitarity is by increasing the scale v_R as m_d is fixed by the SM down-quark masses. This leads to larger masses for the leptoquark X_μ , and thus experimental limits on the deviation will more strongly constrain the allowed scales of $SU(2)_R$ breaking. As before, the degree of helicity suppression is controlled by $\mathcal{Z} \sim (Y_{\Psi_3}^R v_R)^{-1} \mu_{\Psi_3}$ but now there are no constraints on \mathcal{Z} from unitarity deviation.

The two plots of fig. 7 show the size of \mathcal{X} as a function of v_R where as before we consider the singular values in $Y_{\Psi_3}^R$ to vary between 0.1 and 1. Points in blue correspond to \mathcal{X} at first order where

$$\mathcal{X}^{(1)} \simeq m_d (Y_{\Psi_3}^R v_R)^{-1} \quad (5.39)$$

and points in light purple correspond to where \mathcal{X} has been calculated up to second order where

$$\mathcal{X}^{(2)} \simeq \mathcal{X}^{(1)} + \frac{v_L}{v_R^2} Y_{\Psi_3}^L \mu_{\Psi_3}^\dagger [(Y_{\Psi_3}^R)^\dagger]^{-1} (Y_{\Psi_3}^R)^{-1}. \quad (5.40)$$

As μ_{Ψ_3} is a free parameter – it is not fixed from the requirement of a viable neutrino mass spectrum – for regions where $\|\mu_{\Psi_3}\| \gg \|m_d\|$ the second order term in \mathcal{Z} can dominate leading to larger levels of unitarity deviation. Of course for larger values of μ_{Ψ_3} the degree of helicity suppression in the limits on m_X also decreases leading to larger limits on the PS breaking scale. The right plot of fig. 7 shows the level of unitarity deviation in the most experimentally constrained entry of η and it shows that for all values of v_R the deviation is below the current experimental limit. Unlike the previous scenario, as μ_{Ψ_3} enters \mathcal{X} at second order, large values of μ_{Ψ_3} are not constrained by requiring $|\eta_{ij}| < |\eta_{ij}^{\text{exp}}|$. For $v_R \sim 1$ TeV and large values in the entries of μ_{Ψ_3} , the deviation from unitarity in the most constrained entry of η is roughly one order of magnitude below the current experimental limits. For small values of μ_{Ψ_3} (which correspond to the region which helicity suppresses the limits on m_X) the predicted deviation in unitarity is roughly an order of magnitude smaller. Unlike the previous scenario, however, fig. 7 demonstrates that as the constraints on η^{exp} get stronger, they will lead to constraints on the allowed magnitude of v_R . This will require limits several orders of magnitude stronger than the current ones.

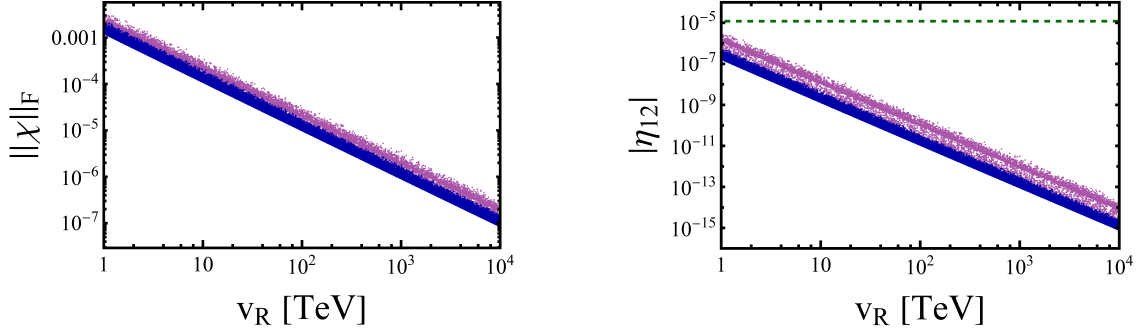


Figure 7. Plots of the variation of \mathcal{X} (left) and the variation of the most experimentally constrained entry of η (right) as a function of v_R . Points in blue correspond to where $\|\mu_{\Psi_3}\| < \|m_d\|$ and therefore $\mathcal{X} \simeq \mathcal{X}^{(1)}$ and points in purple correspond to the opposite regime where $\mathcal{X} \simeq \mathcal{X}^{(2)}$ where we have scanned over the entries of μ_{Ψ_3} only requiring $\|\mu_{\Psi_3}\| < \|Y_{\Psi_3}^R v_R\|$ such that the seesaw assumption is satisfied. Here there are no current experimental constraints on \mathcal{X} from unitarity deviation however future constraints on η will begin to constrain v_R .

Similarly to the scenario with top-right dominance, the level of chiral suppression in the couplings of X_μ is controlled by $\mathcal{Z} \simeq \mu_{\Psi_3} (Y_\Psi^R)^{-1}$. The left plot of fig. 8 demonstrates that the variation in the limits on m_X vary in the exact same way as fig. 6 and requiring complete helicity suppression in the limits on m_X requires $\|\mathcal{Z}\|_F \lesssim 10^{-3}$ as before.

Whereas in the bi-doublet scenario the smallness of $\mu_{\Psi_{22}}$ could be directly connected to the light neutrino masses, here we find additional physics is required for a phenomenologically-viable neutrino mass spectrum. Therefore the relationship between the bare mass term μ_{Ψ_3} and the light neutrino masses cannot be established without properly considering the possible hierarchies of parameters in the full neutrino mass matrix, which is itself model dependent. While we do not thoroughly analyse the neutrino mass matrix of a more complete model, we note that [15] found that if an $SU(2)_R$ triplet, Ψ_3 , was extended with additional fermionic singlets (such that the full Yukawa Lagrangian was given by a combination of eqs. (2.15) and (4.1)) a viable neutrino mass spectrum was recovered for $\|\mu_{\Psi_3}\| \lesssim 1$ GeV which would suggest that $\mathcal{Z} \ll 10^{-3}$ and therefore the limits on m_X will be helicity suppressed to their lowest values. However we note that the limit $\mu_{\Psi_3} \rightarrow 0$ does not recover a global symmetry of the Lagrangian as it does in the bi-doublet case and therefore it is unlikely that the smallness of μ_{Ψ_3} can be related to the smallness of neutrino mass. It may be possible that there are multiple regions in which viably light neutrino masses are recovered, some of which require the entries of μ_{Ψ_3} to be large, which would not lead to a reduction in the limits on m_X . While the smallness of μ_{Ψ_3} cannot be guaranteed by the smallness of the active neutrino masses, as in the bi-doublet scenario, the work in [15] at least indicates that there is a region of parameter space which recovers all SM fermion masses with μ_{Ψ_3} small enough to reduce fully the limits on m_X .

Therefore exotic PS fermion multiplets which introduce additional states which mix

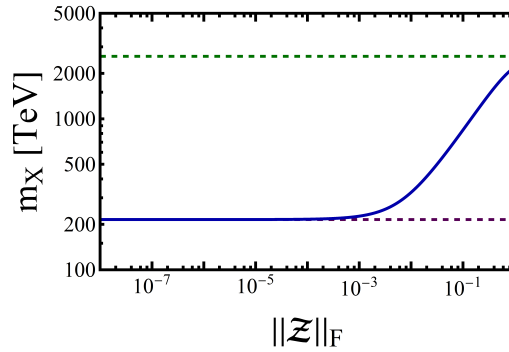


Figure 8. Plot of the limits on m_X as a function of $\|\mathcal{Z}\|_F$ assuming that $K_L^{de} = \mathbb{1}$. As the extent of chiral suppression in the couplings of X_μ to e'_R and d'_R is controlled by \mathcal{Z} , requiring full helicity suppression in the limits on m_X requires $\|\mathcal{Z}\|_F \lesssim 10^{-3}$ as in the previous section. Unlike the previous section \mathcal{Z} is not constrained by limits on unitarity deviation.

with the SM charged and neutral leptons are an attractive method for reducing the limits on PS breaking. As both multiplets considered contain both charged and neutral states, the mixings within both sectors are now coupled. Requiring a valid neutrino-mass spectrum leads to a chiral suppression in the limits on m_X . In the case of additional $SU(2)_{L/R}$ bi-doublets, a chiral suppression can be motivated through technical naturalness arguments. In the case of additional $SU(2)_{L/R}$ triplets, the usual PS scalar content is ruled out phenomenologically. However, if the scalar and fermion sectors are modified appropriately the desired masses and chiral suppression can be achieved. Although not linked to any technical naturalness arguments, previous studies with the triplets and more exotic scalar content suggest that a viable neutrino mass spectrum will still lead to a complete chiral suppression in the limits on m_X . Due to the fact that the mass hierarchy between the down quarks and charged leptons differs between the different generations, the correct masses are most naturally generated for the two fermion types by having their masses arise from different Yukawa couplings and vevs. In the two scenarios considered above, viable charged-lepton and down-quark masses implied that the masses of all quarks arise from couplings of $f_{L/R}$ to ϕ with vevs v_1 and v_2 , whereas the lepton masses are related to couplings of the relevant fermions to χ_L with vev v_L , suggesting the hierarchy $v_{1,2} \gg v_L \gtrsim 1$ GeV.

5.2 $d - D$ mixing: Sextet fermions

Mixing between the down quarks and heavy exotic partners is similar to the scenarios above involving lepton mixing. Only two possible fermion extensions lead to $d - D$ mixing of the fermion multiplets considered, $SU(4)$ sextets or decouplets, and as can be seen in eqs. (4.21) and (4.27) in both cases $y_{\Psi_6}^R v_R$ appears in the bottom-left entry of M_{dD} . The results for down-quark mixing will follow very similarly to section 5.1.2. In the case of the $SU(4)$ decouplets there is mixing both in the down-quark and charged-lepton sector; we will more thoroughly discuss this case further below. Here we will focus on the feasibility

of $d - D$ mixing alone in generating both a viable SM mass spectrum and a suppression of the mass limits on m_X which occurs through the addition of the aforementioned $SU(4)$ sextets but may also occur with higher dimensional PS multiplets.

Writing the down-quark mass mixing matrix similarly to the case of the charged leptons

$$\mathcal{L}_{dD} = \underbrace{\begin{pmatrix} \overline{d}_L & \overline{D}_L \end{pmatrix} \begin{pmatrix} m_{dd} & m_{dD} \\ m_{Dd} & m_{DD} \end{pmatrix} \begin{pmatrix} d_R \\ D_R \end{pmatrix}}_{M_{dD}} + \text{H.c} \quad (5.41)$$

and noting that the entries of eq. (4.21) appear similarly to the case of M_{eE} above allows us to draw the same conclusions which we will summarise. Limits on exotic quark states exceed 1 TeV [41] and therefore for phenomenological reasons a seesaw in M_{dD} is required. As before the only two entries of M_{dD} not tied to the electroweak scale are $y_{\Psi_6} v_R$ and μ_{Ψ_6} and, as discussed, a significant chiral suppression in limits on the PS breaking scale will only occur for the scenario where $\|y_{\Psi_6}^R v_R\| > \|m_d, y_{\Psi_6}^L v_L, \mu_{\Psi_6}\|$.

This hierarchy implies the down-quark masses are given upon diagonalisation by

$$m_d \simeq y_{\Psi_6}^L v_L^* - m_e (y_{\Psi_6}^R v_R)^{-1} \mu_{\Psi_6} \quad (5.42)$$

where the PS symmetry enforces that the singular values of m_e give the correct charged-lepton masses at the appropriate scale in the case where there are no additional multiplets that induce $e - E$ mixing. For the same reasons as with the $SU(2)_{L/R}$ triplets, the correct down-quark masses cannot be recovered in the limit $y_{\Psi_6}^L v_L \rightarrow 0$ as this would imply

$$m_d \simeq -m_e (y_{\Psi_6}^R v_R)^{-1} \mu_{\Psi_6} \quad (5.43)$$

suggesting all three generations of down-quarks are lighter than the corresponding generation of charged-lepton, as discussed in appendix A.3. In section 4.1.4 the constraint from baryon number violation suggested that imposing baryon number conservation required suppressing the Yukawa interactions of χ_L to the fermions (for example by removing the scalar). However as phenomenologically the mass term $y_{\Psi_6}^L v_L$ is required in order to generate a viable charged-lepton and down-quark mass spectrum, this suggests that models involving just $d - D$ mixing through the introduction of $SU(4)$ sextets are likely ruled out by proton lifetime measurements. An analysis of all possible proton and neutrino decay diagrams in the region where the correct down-quark and charged-lepton masses arise is beyond the scope of this work. If the dominant decay channels are two-body decays which proceed via $d = 6$ effective four-fermi interactions similar to fig. 3, estimates from [42] suggest that for TeV scale new physics the product of Yukawa couplings within the relevant loop diagram must satisfy $Y \lesssim 10^{-6}$. As $y_{\Psi_6}^L v_L$ is related to the down-quark masses in this case and for low scales of v_R , $y_{\Psi_6}^R$ is required to be close to unity such that the heavy D states are sufficiently heavy naïvely suggests difficulty in suppressing the decays.

If a viable model involving the $SU(4)$ sextets exists which can suppress the dangerous proton decay diagrams whilst generating the appropriate charged-lepton and down-quark masses in the regime where the mass term $|y_{\Psi_6}^R|$ is dominant, the requirements for a chiral suppression in the limits on m_X would follow almost identically to the $e - E$ mixing case above. For small values of μ_{Ψ_6} the couplings of X_μ to d'_R and e'_R will be suppressed and decreasing the experimental limits to their lowest value would roughly require

$$\|\mathcal{Z}\|_F \simeq (Y_{\Psi_6}^R)^{-1} \mu_{\Psi_6} \lesssim 10^{-3}. \quad (5.44)$$

The only difference between $d - D$ and $e - E$ mixing will be in the deviation of unitarity, where $e - E$ mixing is constrained by deviation of unitarity in the PMNS whereas $d - D$ mixing is constrained by deviation within the measured CKM matrix,

$$V_{\text{CKM}} \simeq (U_L^u)^\dagger \left(\mathbb{1} - \frac{1}{2} \mathcal{X} \mathcal{X}^\dagger \right) O_L^d \quad (5.45)$$

where

$$\begin{aligned} d'_L &\simeq (O_L^d)^\dagger \left(\mathbb{1} - \frac{1}{2} \mathcal{X} \mathcal{X}^\dagger \right) d_L - (O_L^d)^\dagger \mathcal{X} D_L \\ d'_R &\simeq -(O_R^d)^\dagger \mathcal{Z}^\dagger d_R + (O_R^d)^\dagger \left(\mathbb{1} - \frac{1}{2} \mathcal{Z}^\dagger \mathcal{Z} \right) D_R \end{aligned} \quad (5.46)$$

and

$$\begin{aligned} \mathcal{X} &\simeq \frac{1}{v_R} m_X (Y_\Psi^R)^{-1} + \frac{v_L}{v_R^2} Y_\Psi^L \mu_\Psi^\dagger [(Y_\Psi^R)^\dagger]^{-1} (Y_\Psi^R)^{-1} \\ \mathcal{Z} &\simeq \frac{1}{v_R} (Y_\Psi^R)^{-1} \mu_\Psi + \frac{v_L}{v_R^2} (Y_\Psi^R)^{-1} [(Y_\Psi^R)^\dagger]^{-1} m_d^\dagger Y_\Psi^L. \end{aligned} \quad (5.47)$$

In section 5.3 which involves coupled $e - E$ and $d - D$ mixing we find that limits from CKM unitarity deviation lead to very similar constraints on the level of mixing within the theory and therefore we find that $d - D$ mixing would be equally viable to the $e - E$ mixing above in the absence of proton decay issues.

5.3 Coupled $e - E$ and $d - D$ mixing: Decuplet fermions

Coupled mass mixing within the down-quark and charged-lepton sector will occur with the addition of $SU(4)$ decuplets. There are a few notable differences to this scenario compared to the others considered: (i) the singular values of the mass matrix for $\overline{d}_L d_R$ and $\overline{e}_L e_R$ (which the PS symmetry enforces to be equal) will no longer be given by the down-quark or charged-lepton masses, (ii) this is the only scenario in which exotic charged-leptons are introduced without additional neutral fields and therefore the neutrino mixing matrix is decoupled, and (iii) this is the only multiplet which predicts a non SM-like exotic particle. Specifically this model predicts the existence of a Dirac colour-sextet fermion with electric charge $1/3$. Its mass is given by

$$m_\psi = \mu_{\Psi_{10}} \quad (5.48)$$

and therefore requiring that the sextet is sufficiently heavy leads to constraints on the singular values of $\mu_{\Psi_{10}}$. The mass limits for a colour sextet fermion vary from roughly 100 GeV if stable on collider length scales [34] up to a TeV [43] for large couplings and possibly in the multi-TeV range [44].

As the mass mixing matrices $M_{eE/dD}$ in eqs. (4.26) and (4.27) differ only by group theoretic factors, assuming that $Y_{\Psi_{10}}^R v_R$ is the dominant block of M_{eE} and M_{dD} such that the desired chiral suppression will occur leads to

$$\begin{aligned} m_\ell &\simeq \sqrt{2} v_L Y_{\Psi_{10}}^L - \frac{1}{\sqrt{2} v_R} m_F (Y_{\Psi_{10}}^R)^{-1} \mu_{\Psi_{10}} \\ m_d &\simeq v_L Y_{\Psi_{10}}^L - \frac{1}{v_R} m_F (Y_{\Psi_{10}}^R)^{-1} \mu_{\Psi_{10}} \end{aligned} \quad (5.49)$$

for the light charged-lepton and down-quark mass matrices. As these equations only differ by factors of $\sqrt{2}$, it is easy to see that neither term in eq. (5.49) can be zero (or negligible compared to the other). The limit $Y_{\Psi_{10}}^L \rightarrow 0_{3 \times 3}$ has

$$\sigma_i(m_\ell) = \frac{1}{\sqrt{2}} \sigma_i(m_d) \quad (5.50)$$

at the PS breaking scale and

$$\sigma_i(m_\ell) = \sqrt{2} \sigma_i(m_d) \quad (5.51)$$

if the second terms in eq. (5.49) were removed (e.g. if $m_X \rightarrow 0_{3 \times 3}$). Here, as before, $\sigma_i(\dots)$ corresponds to the i -th singular value of the matrix and therefore the relevant particle's mass. As the hierarchy between the down-quark and charged-lepton masses flips between each generation, and the experimentally measured mass ratios are much larger than factors of $\sqrt{2}$, this implies that a viable spectrum for both particle types requires both terms in eq. (5.49) to be non-negligible. Interestingly, all scenarios considered have required the existence of the scalar χ_L (or some other potential scalar that can generate the relevant mass term) in order to generate a viable mass spectrum for the down-isospin fermions.

Requiring sufficiently heavy partner masses for D and E requires $\|Y_{\Psi_{10}}^R v_R\| \gtrsim 1$ TeV as usual, but additionally $\mu_{\Psi_{10}}$ must also be fixed in a similar way to satisfy mass bounds on the colour-sextet fermion. Since the hierarchy

$$\|Y_{\Psi_{10}}^R v_R\| > \|\mu_{\Psi_{10}}\| \quad (5.52)$$

is required for a chiral suppression of the mass limits on m_X to occur, the colour-sextet masses are predicted to be significantly smaller than the E and D states. In section 5.1 a small bare mass term, $\mu_{\Psi_{22}}$, was conveniently required in order to generate a viable neutrino mass spectrum. Now the entries of $\mu_{\Psi_{10}}$ are required to be relatively large, at least compared to the electroweak scale, and therefore the singular values of $Y_{\Psi_{10}}^R v_R$ must be even larger in order to satisfy eq. (5.52). Therefore requiring a sufficient level of chiral suppression in order to reduce the limits on m_X places limits on the minimum size of v_R . If the scale of v_R required for a significant chiral suppression in the mass limits exceeds

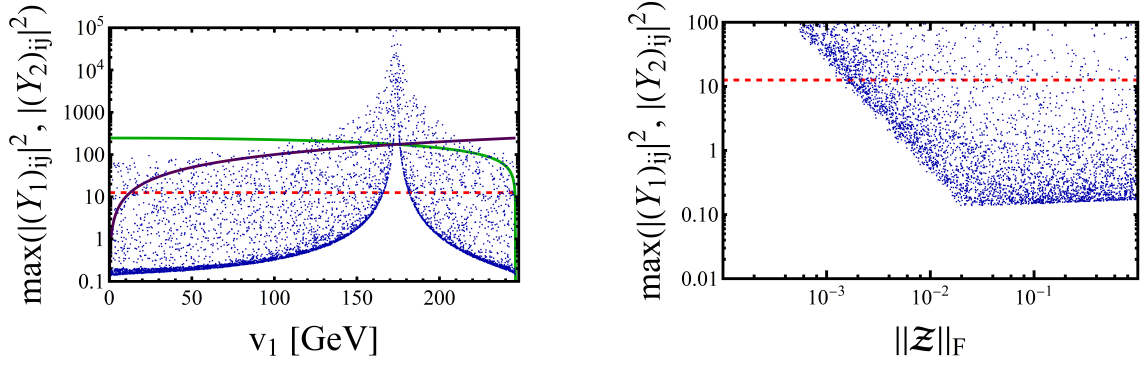


Figure 9. Plot of $\max(|(Y_{1/2})_{ij}|^2)$ as a function of v_1 (**left**) and $\|\mathcal{Z}\|_F$ (**right**). The red dashed line corresponds to our conservative perturbativity limit where $|y_{ij}|^2 < 4\pi$. The solid green line corresponds to the value of v_2 required for a given v_1 (where v_L is fixed by eq. (5.55) and the solid purple line corresponds to $y = v_1$. When $v_2 \simeq v_1$, then solving for m_X and m_U requires a large cancellation for the entries of Y_1 and Y_2 . The right plot indicates that for $\|\mathcal{Z}\|_F \lesssim 10^{-3}$ the required couplings of Y_1 and Y_2 are non perturbative regardless of the values of $v_{1/2}$.

the limits themselves, e.g. $v_R \gtrsim (100 - 1000)$ TeV, this will essentially negate the desired effect of lowering the experimental limit on PS breaking as $m_X \propto v_R$.

For a given choice of the matrices $Y_{\Psi_{10}}^R v_R$ and $\mu_{\Psi_{10}}$, eq. (5.49) can be solved for the remaining blocks of $M_{eE/dD}$:

$$\begin{aligned} Y_{\Psi_{10}}^L v_L &\simeq \sqrt{2} m_\ell - m_d \\ m_F &\simeq \left(\sqrt{2} m_\ell - 2 m_d \right) (\mu_{\Psi_{10}})^{-1} Y_{\Psi_{10}}^R v_R \\ &\simeq \left(\sqrt{2} m_\ell - 2 m_d \right) (\mathcal{Z}^{(1)})^{-1}. \end{aligned} \quad (5.53)$$

The PS symmetry fixes

$$m_U = v_1 Y_1 + v_2^* Y_2 \quad \text{and} \quad m_F = v_2 Y_1 + v_1^* Y_2 \quad (5.54)$$

from eq. (2.16) where $v_{1/2}$ and $Y_{1/2}$ correspond to the vevs and Yukawa couplings of ϕ to $f_{L/R}$. As the seesaw assumption enforces $\|\mathcal{Z}^{(1)}\| < 1$, eq. (5.53) implies that for sufficiently small values of the entries of \mathcal{Z} the couplings within Y_1 and Y_2 will become non-perturbative as the vevs v_1 and v_2 cannot be made arbitrarily large.

The plots in fig. 9 illustrate this point where we have scanned over different choices of \mathcal{Z} and then solved eqs. (5.53) and (5.54) in order to find the required matrices Y_1 and Y_2 . For simplicity we fixed the vev v_L by assuming

$$v_L = \max \left[\left| (Y_{\Psi_{10}}^L v_L)_{ij} \right| \right] \quad (5.55)$$

and therefore at least one entry of $Y_{\Psi_{10}}^L$ will be equal to one. We find that for $1 \lesssim v_R \lesssim 10^4$ TeV that the required v_L varies

$$(0.1 \lesssim v_L \lesssim 0.8) \text{ GeV}, \quad (5.56)$$

therefore in all scenarios the vev of χ_L is required to be roughly around the GeV scale, suggesting the hierarchy $v_L < v_{1,2}$. The vev v_1 was randomly scanned over and v_2 was fixed by $v_2 = \sqrt{v_{\text{EW}}^2 - v_1^2 - v_L^2}$ and for simplicity v_1 was taken to be real. The right plot of eq. (2.16) shows that as the entries of \mathcal{Z} decrease, the required entries of Y_1 or Y_2 must increase in order to generate the correct SM masses. The dashed line corresponds to the conservative perturbativity limit $|Y_{ij}|^2 < 4\pi$. For $\|\mathcal{Z}\|_F \lesssim 10^{-3}$, the required Yukawa couplings are always non-perturbative and therefore this places a lower bound on the size of \mathcal{Z} . Interestingly, the left plot of fig. 9 demonstrates that when $v_1 \simeq v_2$, the required Yukawa couplings are non-perturbative regardless of the entries of \mathcal{Z} . As the vevs are assumed real for simplicity, $v_1 = v_2$ corresponds to when $m_F = m_U$ via a *real* scalar ϕ and mass equality occurs for all isospin partners at the PS breaking scale (first noted in [35]).

Therefore if $m_F \neq m_u$ but $v_1 \simeq v_2$ (but not exactly equal) a large cancellation between the entries of Y_1 and Y_2 is required in order to solve for the entries of m_F and m_U . Fixing $m_F = m_U$ by hand and rearranging eq. (5.53) leads to

$$\mu_{\Psi_{10}} \simeq v_R Y_{\Psi_{10}}^R m_U^{-1} \left(\sqrt{2} m_\ell - 2 m_D \right) \quad (5.57)$$

but this implies

$$\sigma_3(\mu_{\Psi_{10}}) > \sigma_3(v_R Y_{\Psi_{10}}^R) \quad (5.58)$$

using simple properties of the singular values of the product of matrices. Therefore the seesaw assumption will be violated. Choosing ϕ to be real and then breaking the mass equality between all fermions using a seesaw for the e and d states *assuming* that $Y_{\Psi_{10}}^R v_R$ is the dominant block is not viable, though a real scalar bi-doublet may work in the scenario where $\mu_{\Psi_{10}}$ is dominant. As $\|\mathcal{Z}\|_F \lesssim 10^{-3}$ is required from fig. 9, this therefore implies that the mass of the colour-sextet fermions can maximally be three orders of magnitude smaller than the heavy E and D states.

The interaction and mass eigenstates are related by a combination of eqs. (5.36) and (5.46) and the relevant physical mixing matrices are now

$$\begin{aligned} K_L^{de} &\simeq (O_L^d)^\dagger \left(\mathbb{1} - \frac{1}{2} \mathcal{X} \mathcal{X}^\dagger \right)^2 O_L^e, & K_R^{de} &\simeq (O_R^d)^\dagger (\mathcal{Z}^\dagger \mathcal{Z}) O_R^e, \\ V_{\text{CKM}} &\simeq (U_L^u)^\dagger \left(\mathbb{1} - \frac{1}{2} \mathcal{X} \mathcal{X}^\dagger \right) O_L^d & \text{and} & \quad U_{\text{PMNS}} \simeq N_\nu^\dagger \left(\mathbb{1} - \frac{1}{2} \mathcal{X} \mathcal{X}^\dagger \right) O_L^e, \end{aligned} \quad (5.59)$$

where similarly to sections 5.1.2 and 5.2,

$$\begin{aligned} \mathcal{X} &\simeq \frac{1}{v_R} m_F (Y_{\Psi_{10}}^R)^{-1} + \frac{v_L}{v_R^2} Y_{\Psi_{10}}^L \mu_{\Psi_{10}}^\dagger [(Y_{\Psi_{10}}^R)^\dagger]^{-1} (Y_{\Psi_{10}}^R)^{-1} \\ \mathcal{Z} &\simeq \frac{1}{v_R} (Y_{\Psi_{10}}^R)^{-1} \mu_{\Psi_{10}} + \frac{v_L}{v_R^2} (Y_{\Psi_{10}}^R)^{-1} [(Y_{\Psi_{10}}^R)^\dagger]^{-1} m_F^\dagger Y_{\Psi_{10}}^L. \end{aligned} \quad (5.60)$$

A significant difference between the above mixing matrices and those derived in sections 5.1 and 5.2 is that K_R^{de} will experience a *double* suppression from the mixing in both the

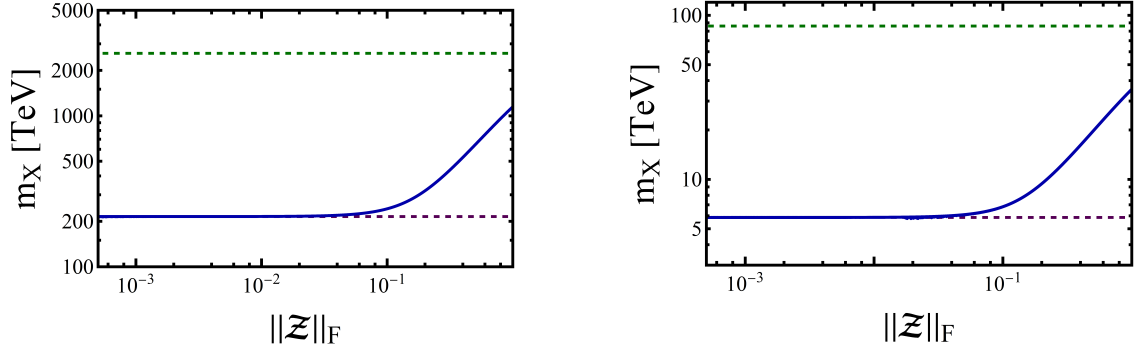


Figure 10. Plot of the experimental limits on m_X as a function of \mathcal{Z} where we have assumed $K_{L/R}^{de} = \mathbb{1}$ (**left**) and mixing angles given by the fifth row of table 9 (**right**). The horizontal dashed green lines corresponds to the limits obtained without helicity suppression, as in tables 3 to 5, and the horizontal dashed purple lines corresponds to the limits calculated with exact helicity suppression as in tables 7 to 9. Due to the double suppression appearing in K_R^{de} , only $\|\mathcal{Z}\|_F \lesssim 10^{-1}$ is required to reduce the limits to their lowest values compared to $\|\mathcal{Z}\|_F \lesssim 10^{-3}$ to the previous scenarios.

charged-lepton and down-quark sectors. Therefore a larger chiral suppression will occur in the limits of m_X in this scenario compared to scenarios with $e - E$ or $d - D$ mixing alone, for a given \mathcal{Z} .

Figure 10 plots the variation in the limits of m_X as a function of $\|\mathcal{Z}\|_F$ for $K_{L/R}^{de} = \mathbb{1}$ in the left plot (which leads to the largest limits on m_X) and where $K_{L/R}^{de}$ is given by the fifth row of tables 5 and 9 (which leads to some of the smallest limits). The same behaviour to the previous scenarios is observed where decreasing values in the entries of \mathcal{Z} leads to a reduction in the limits on m_X . Due to the double suppression in K_R^{de} , the mass limits on m_X are reduced to their lowest value for much larger values in \mathcal{Z} . We find that $\|\mathcal{Z}\|_F \lesssim 10^{-1}$ is sufficient in reducing the limits to their lowest value whereas previously $\|\mathcal{Z}\|_F \lesssim 10^{-3}$ was required.

Figure 11 plots the variation in the mixing matrices \mathcal{X} and \mathcal{Z} as a function of v_R for different values of the colour-sextet mass, which fixes the singular values of $\mu_{\Psi_{10}}$. As the limits on m_ψ increase, a larger v_R breaking scale (and therefore larger E and D masses) is required for a given value of $\|\mathcal{Z}\|_F$. For example, fixing the sextet masses to 5 TeV requires $SU(2)_R$ breaking scales around 50 – 80 TeV, if $\|\mathcal{Z}\|_F \simeq 10^{-1}$ is desired, which places a larger bound on m_X then obtained through limits from rare meson decay for many choices of K_R^{de} .

As \mathcal{Z}^{-1} fixes the size of m_F in our scans through eq. (5.53), larger values in the entries of \mathcal{Z} are required for smaller values in the entries of \mathcal{X} . As \mathcal{X} measures the deviation of unitarity in *both* the PMNS and CKM matrix through eq. (5.59), with the same deviation occurring in both matrices, this therefore leads to limits on the size of \mathcal{X} . Figure 12 plots

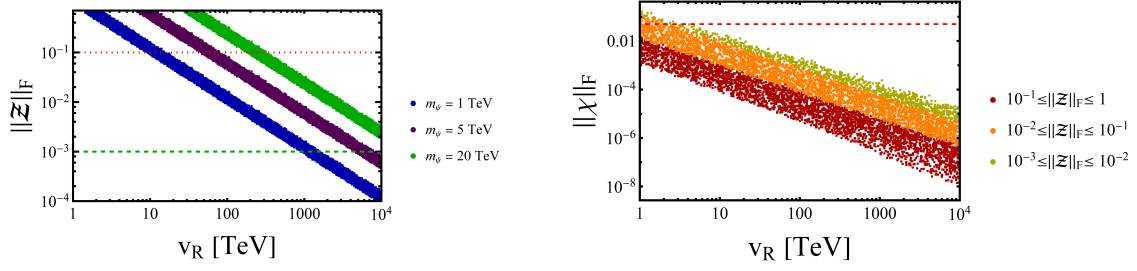


Figure 11. Plot of the variation in $\|\mathcal{Z}\|_F$ for fixed values of m_ψ (**left**) and $\|\mathcal{X}\|_F$ for random values of m_ψ (**right**) as a function of v_R . As the sextet masses increase the required size of v_R increases for a given \mathcal{Z} . If $\|\mathcal{Z}\|_F \lesssim 10^{-1}$ is required for a chiral suppression in the limits on m_X , indicated by the red-dashed line in the left plot, this implies that $v_R \gtrsim 10$ TeV for 1 TeV sextet masses and $v_R \gtrsim (50 - 80)$ TeV for 5 TeV sextet masses. The perturbativity requirement $\|\mathcal{Z}\|_F \gtrsim 10^{-3}$, which is indicated by the green dashed line, leads to upper bounds on the size of v_R in this model for a given sextet mass. Larger values of \mathcal{Z} lead to smaller levels of unitarity deviation in the CKM and PMNS matrices by reducing the size of the entries in m_F through eq. (5.53). The red dashed line on the right plot indicates the upper bound on $\|\mathcal{X}\|_F$ roughly derived from fig. 12.

the deviation in both the PMNS and CKM matrices as a function of $\|\mathcal{X}\|_F$. The left plot, related to the deviation in the PMNS matrix, is identical to the ones in section 5.1 which requires $\|\mathcal{X}\|_F \lesssim 5 \times 10^{-2}$ in order to satisfy the current experimental limits. The right plot measures the level of deviation within the CKM matrix which we measure by defining the parameters

$$\eta_j^r = 1 - \sum_i |(V_{\text{CKM}})_{ji}|^2 \quad \text{and} \quad \eta_k^c = 1 - \sum_i |(V_{\text{CKM}})_{ik}|^2. \quad (5.61)$$

The strongest experimental limits on $\eta^{r/c}$ come from the sum of the squares of the first row or column of the CKM matrix. However, due to the much larger masses of the third generation of quarks, we find that deviations in the sum of the third row and column of the CKM matrix lead to stronger constraints on \mathcal{X} . We find that η_3^r and η_3^c place almost identical limits on the magnitude of $\|\mathcal{X}\|_F$ and therefore only plot one for brevity. Using [34] places the limit

$$-0.01 \lesssim \eta_3^{r/c} \lesssim 0.09 \quad (5.62)$$

and therefore we conservatively set the limit $|\eta_3^{r/c}| < 10^{-2}$ at the PS breaking scale. The right plot of Figure 12 therefore sets a rough limit of $\|\mathcal{X}\|_F \lesssim 10^{-1}$ in order to prevent significant deviation occurring for the CKM matrix, a slightly weaker limit compared to that of PMNS deviation.

The combination of figs. 9 to 12 lead to constraints on the PS breaking scale which are much more complicated compared to those obtained in section 5.1. Requiring $\|\mathcal{Z}\|_F \gtrsim 10^{-3}$ for perturbativity of the couplings in Y_1 and Y_2 from fig. 9 places a maximum upper bound on v_R for a given mass of the colour-sextet fermions as shown in the left plot of fig. 11. For 1 TeV sextet masses, $v_R \lesssim 10^3$ TeV is roughly required and 5 TeV masses leads to $v_R \lesssim 5 \times 10^4$ TeV. The constraint on v_R comes from the left plot of fig. 11 which fixes v_R

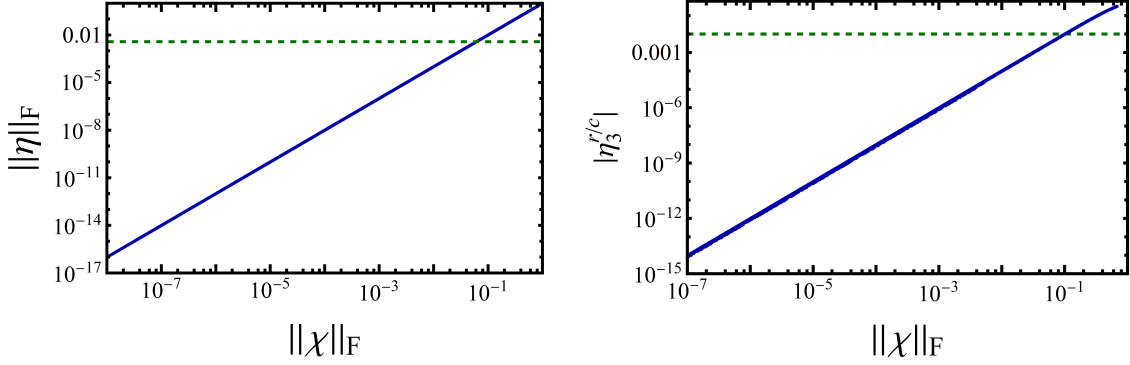


Figure 12. Plots of the deviation of unitarity in the PMNS (**left**) and the CKM (**right**) matrices as a function of $\|\mathcal{X}\|_F$ where the dashed green line in each plot roughly indicates the current experimental limit. In the case of the CKM matrix the deviation is measured as the difference in the sum of the squares of each row and column. Even though it is currently the least constrained, the sum of the squares of the third row and column provide the strongest bounds on the deviation due to the large masses of the third generation of quarks compared to the first and second generation. The right plot requires $\|\mathcal{X}\|_F \lesssim 10^{-1}$ with a slightly stronger limit set by the deviation of the PMNS matrix in the left plot of $\|\mathcal{X}\|_F \lesssim 5 \times 10^{-2}$. The limits in the case of the PMNS deviation is taken from [40] whereas the limits in the case of the CKM are taken from [34].

depending on the masses of the sextet fermions. For 5 TeV sextet masses, $v_R \gtrsim 50$ TeV is required in order to fully reduce the experimental limits on m_X which is a larger limit on m_X than the experimental constraints for many choices of K_R^{de} . For example the choices of mixing angles in $K_{L/R}^{de}$ which lead to experimental constraints as low as 5 TeV in the chiral limit, as shown in tables 8 and 9, are now much more significantly constrained by the experimental limits on the sextet masses compared to those of rare meson decay. For the scenarios where the experimental limits still exceed 100 TeV, such as $K_{L/R}^{de} = 1$, this can still have the full desired effect of lowering the scale of PS braking to be as low as possible, but will be affected as the sextet mass limits grow. Figure 13 demonstrates this behaviour by plotting the resultant limit on m_X as a function of m_ψ for different choices of v_R and therefore \mathcal{Z} . Here we set

$$m_X = \max\left(\frac{1}{\sqrt{2}}g_4 v_R, m_X^{\text{exp}}\right) \quad (5.63)$$

where m_X^{exp} corresponds to the would-be limit from rare meson decay, for the same two choices of K_R^{de} as in fig. 10. The right plot, which corresponds to $m_X^{\text{exp}} \simeq 5$ TeV in the full chiral limit, has m_X fixed by the requirements set on v_R from m_ψ and for $m_\psi > 5$ TeV requires v_R scales much larger than this chiral limit. The minimum PS breaking scale of 100 TeV can still be reduced compared to without mixing effects up until about $m_\psi \simeq 20$ TeV at which point the required limits on m_X exceed the meson decay limits completely. If $m_X < 50$ TeV is desired, this requires roughly $m_\psi < 20$ TeV. The left plot where $K_L^{de} = 1$, where the chirally suppressed decay limits on m_X are much larger, allows for the limits on m_X to be reduced to their lowest value for much larger values of m_ψ , but of course require $m_X \simeq 200$ TeV at a minimum.

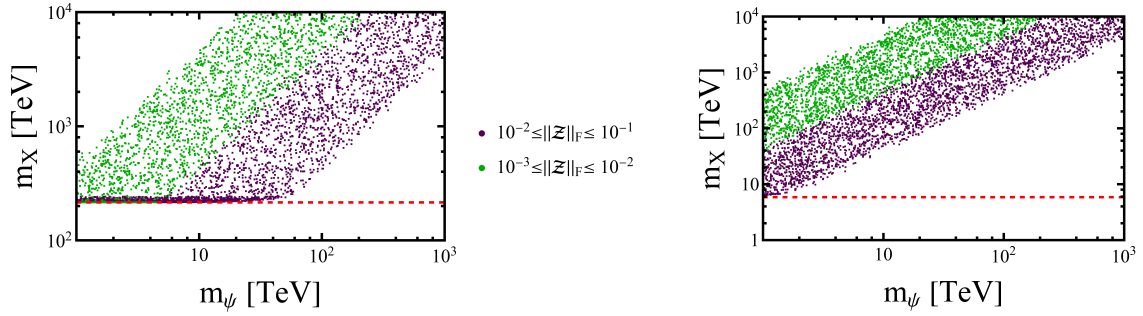


Figure 13. Combined limits on m_X as a function of m_ψ where we have assumed $K_{L/R}^{de} = \mathbb{1}$ (**left**) and mixing angles given by the fifth row of table 9 (**right**) for different values of v_R and therefore Z . For a given size of m_ψ requiring a sufficiently small value in the entries of Z , such that a suppression in the experimental limits on m_X can occur, requires a large enough size of v_R where we have randomly scanned of $Y_{\Psi_{10}}^R$ with entries close to unity. Choices of $K_{L/R}^{de}$ which allow for incredibly low limits on m_X such as the right plot, have the effects of the chiral suppression somewhat negated due to the required relationship between m_ψ and v_R . For sextet masses above 20 – 30 TeV, the required size of v_R leads to limits on m_X much larger than those obtained from rare meson decay experiments. For choices of $K_{L/R}^{de}$ which maximise the limits on m_X from meson measurements, the full chirally suppressed limits can be obtained for a large range of m_ψ , up to 50 TeV.

Therefore we find that the scenario of coupled $e - E$ and $d - D$ mixing which results from the addition of $SU(4)$ decuplets can also be effective at lowering the PS mass limits albeit with more constraints. The examples of $e - E$ mixing alone from section 5.1 allow for the mass limits to be lowered regardless of the choice of $K_{L/R}^{de}$ whereas here we find that the additional exotic states predicted lead to much more severe constraints for choices of $K_{L/R}^{de}$ which minimise the limits from rare meson decay. Additionally in the case of $e - E$ mixing, as the charged lepton mass mixing matrix was coupled to the neutrino mass mixing matrix, we found that a chiral-like coupling of X_μ to either the left- or right-handed e and d was well motivated by requiring small neutrino masses. In the case of the decuplets, the hierarchy $\|Y_{\Psi_{10}}^R v_R\| > \|\mu_{\Psi_{10}}\|$ is not motivated from any other physical arguments. If the opposite hierarchy occurred where $\|\mu_{\Psi_{10}}\| > \|Y_{\Psi_{10}}^R v_R\|$ a phenomenologically viable spectrum of fermion masses is possible even though there will be no reduction in the limits of m_X from meson decays. More exact limits on m_X require a more thorough evaluation of the current experimental limits on m_ψ , if the colour sextets could be made collider stable in these models, the allowed parameter space could drastically increase leading to much smaller v_R and therefore reducing the limits on m_X to their lowest possible.

5.4 Connection to $SO(10)$

While we are motivated by the experimentally attractive prospect of lowering the scale of PS breaking as low as possible, here we briefly consider how the exotic fermionic multiplets proposed could fit into an $SO(10)$ GUT and mention any obvious problems. We note

the smallest dimensional multiplets of $SO(10)$ which contain each exotic multiplet as well as additional states this would predict. It is well known that two standard PS fermion multiplets fit into the spinorial

$$\mathbf{16} \rightarrow (\mathbf{4}, \mathbf{1}, \mathbf{2}) \oplus (\mathbf{4}, \mathbf{2}, \mathbf{1}) = f_L \oplus f_R \quad (5.64)$$

of $SO(10)$. The fundamental representation of $SO(10)$,

$$\mathbf{10} \rightarrow (\mathbf{1}, \mathbf{2}, \mathbf{2}) \oplus (\mathbf{6}, \mathbf{1}, \mathbf{1}) = \Psi_{22} \oplus \Psi_6, \quad (5.65)$$

contains both the bi-doublet and sextet fermion states. While we find that the bi-doublet fermion is the most attractive candidate in lowering the PS breaking scale, the sextet fermion leads to undesirable proton decay diagrams. Some mechanism would therefore be desirable in order to significantly increase the masses of the D states from the sextet, and not the E and N states from the bi-doublet, in order to prevent large proton decay widths. This cannot be through different bare mass terms, e.g. $\mu_{\Psi_{22}} \ll \mu_{\Psi_6} \simeq 10^{16}$ GeV, as the $SO(10)$ symmetry now enforces the two terms to be equal.

The adjoint representation

$$\mathbf{45} \rightarrow (\mathbf{1}, \mathbf{3}, \mathbf{1}) \oplus (\mathbf{1}, \mathbf{1}, \mathbf{3}) \oplus (\mathbf{15}, \mathbf{1}, \mathbf{1}) \oplus (\mathbf{6}, \mathbf{2}, \mathbf{2}) \supset \Psi_{3_L} \oplus \Psi_{3_R} \quad (5.66)$$

contains both the $SU(2)_L$ and $SU(2)_R$ triplet fermions. Interestingly, the additional $(\mathbf{15}, \mathbf{1}, \mathbf{1})$ fermion contains a neutral state and therefore will contribute to the full neutrino mass matrix. As we found that the triplets alone are unable to generate a viable neutrino mass spectrum, due to the various mass equalities predicted, it is convenient that the minimal $SO(10)$ multiplet which contains these states also contains additional neutrino states which could possibly generate a viable spectrum of masses. The $(\mathbf{6}, \mathbf{2}, \mathbf{2})$ fermion will likely require a similar mechanism to the $(\mathbf{6}, \mathbf{1}, \mathbf{1})$ fermion in order to significantly increase its mass compared to the triplets within the theory. Finally the $SU(4)$ decuplets first appear in the $\mathbf{120}$ representation of $SO(10)$. This representation also contains the bi-doublet fermion which will itself allow for the generation of chiral-like couplings of X_μ as well as generate neutrino masses, which the decuplet fermions do not. An interesting possible direction of future work is to analyse the feasibility of embedding such low-scale variants of PS into an $SO(10)$ GUT in such a way that the required fermion states do not develop GUT scale masses whereas any fermion in a given embedding which may mediate proton decay, or similar undesirable processes, have masses developed at the $SO(10)$ breaking scale.

6 Conclusion

We have studied the implications of introducing additional fermionic states to the usual Pati-Salam fermion multiplets. In particular we have focused on multiplets of relatively low

dimensionality which contain partner states to the charged-leptons and/or down-quarks. The implications of mixing effects induced by these states were extensively studied, particularly with a focus on the feasibility of lowering the scale of PS breaking. We identified four multiplets that allow for the possibility of a suppression in the PS limits. Of the four, the inclusion of an $SU(2)_{L/R}$ bi-doublet alone can lead to a valid mass spectrum for all SM particles and a significant reduction in the PS limits. The decuplet, while viable, requires the addition of extra singlet states (at a minimum) for neutrino mass and is more significantly constrained due to the existence of a colour-sextet fermion and will generally lead to larger PS limits. The remaining two multiplets, the $SU(2)_L$ and $SU(2)_R$ triplets, require both a modification of the scalar sector for a viable charged-lepton mass spectrum as well as additional fermionic states for a viable neutrino mass spectrum. A common feature of all scenarios was the existence of scalars χ_L and χ_R in order to generate a viable down-quark and charged-lepton mass spectrum. Therefore three $SU(2)_L$ Higgs doublets are predicted.

The most attractive models, the $SU(2)_{L/R}$ bidoublet or triplets, contain only additional leptonic states, inducing both $e - E$ mixing as well as mixing within the neutrino sector. While both these models have already appeared in the literature, we have extended these analyses by rigorously studying the requirements for viable mass spectra of the down-quarks, charged-leptons and neutrinos as well as the implications for the PS breaking scale limits. We identify an attractive connection between the smallness of neutrino mass and the helicity suppression of the limits on m_X which, particularly in the case of the bi-doublet, necessarily has a chiral-like coupling of X_μ to the SM fermions.

The sextet option leads to mixing in the down-quark sector alone but we find that this likely leads to large proton decay widths in the only region which can generate a viable mass spectrum. Finally an interesting scenario with fermion decouplets, which lead to both $d - D$ and $e - E$ mixing, was considered. It also includes additional exotic states potentially discoverable at current and future colliders. The regime of interest, where the limits on PS breaking can be lowered, predicts a very specific hierarchy amongst the exotic states in this case and is very sensitive to future experimental limits on colour-sextet fermion masses.

We find that a chiral suppression in the PS breaking limits can reduce the usual limits of $81 - 2467$ TeV, depending on the structure of $K_{L/R}^{de}$, down to as low as $5.6 - 194$ TeV. An attractive property of models which lead to a chiral suppression is that only one of $K_{L/R}^{de}$ is required to have a specific structure. Without a chiral suppression, the lowest PS limits obtained required both of $K_{L/R}^{de}$ to have a specific structure which might suggest a parity symmetry in conflict with the assumed low-scale setup.

A number of extensions to our analysis are possible. The addition of $SU(2)$ triplets has already been explored in the context of the current B-anomalies [14, 15]. As we have identified $SU(4)$ decouplets as an alternative possibility for low scale PS, it may be interesting to explore the feasibility of this model to explain the anomalies. In particular requiring

the mass of X_μ to be in a specific region as a candidate for some of the B-anomalies will lead to predictions on the required colour-sextet masses, which can be probed. This however requires a detailed analysis on the predicted lifetime/stability of the colour sextet in this model. A more in-depth examination of baryon number violation implications in the case with $SU(4)$ sextets is required before it can be ruled out as a low-scale candidate. Additionally, due to the mass mixing induced, collider constraints for other particles predicted (such as the W' and Z') could lead to significantly smaller mass limits than what is usually expected. Exploring the reach of the LHC and future colliders for these extended PS scenarios with chiral-like gauge couplings may be required.

Acknowledgments

This work was supported in part by the Australian Research Council. TPD thanks John Gargalionis for helpful discussion and advice during the early parts of this work and Graham White for email correspondence.

A Various Seesaw Properties

A.1 Singular Values in One Generation

Consider the matrix $M \in M_2(\mathbb{C})$ given by

$$M = \begin{pmatrix} a & b \\ c & d \end{pmatrix}. \quad (\text{A.1})$$

This matrix can be diagonalised via its singular value decomposition:

$$U_L^\dagger M U_R = M_d = \begin{pmatrix} m_\ell & 0 \\ 0 & m_h \end{pmatrix}. \quad (\text{A.2})$$

There exist exact analytic expressions for U_L , U_R , m_ℓ and m_h for this 2×2 matrix, however in the seesaw limit where the absolute value of one entry of eq. (A.1) is significantly larger than the others, these expressions can be significantly simplified by writing them as perturbation series. For example, in the limit where $|d| \gg |a|, |b|, |c|$ we find for the

unitary-diagonalisation matrices

$$\begin{aligned}
U_L &= \underbrace{\begin{pmatrix} 1 - \frac{1}{2} \left| \frac{ac^* + bd^*}{|d|^2} \right|^2 & \frac{ac^* + bd^*}{|d|^2} \\ - \left(\frac{ac^* + bd^*}{|d|^2} \right)^* & 1 - \frac{1}{2} \left| \frac{ac^* + bd^*}{|d|^2} \right|^2 \end{pmatrix}}_{Q_L} \underbrace{\begin{pmatrix} \sqrt{\frac{m_\ell}{|m_\ell|}} & 0 \\ 0 & \sqrt{\frac{m_{\tilde{h}}}{|m_{\tilde{h}}|}} \end{pmatrix}}_{K_L} + \mathcal{O}(\epsilon^3) \\
U_R &= \underbrace{\begin{pmatrix} 1 - \frac{1}{2} \left| \frac{ab^* + cd^*}{|d|^2} \right|^2 & \left(\frac{ab^* + cd^*}{|d|^2} \right)^* \\ - \frac{ab^* + cd^*}{|d|^2} & 1 - \frac{1}{2} \left| \frac{ab^* + cd^*}{|d|^2} \right|^2 \end{pmatrix}}_{Q_R} \underbrace{\begin{pmatrix} \sqrt{\frac{m_\ell^*}{|m_\ell|}} & 0 \\ 0 & \sqrt{\frac{m_{\tilde{h}}^*}{|m_{\tilde{h}}|}} \end{pmatrix}}_{K_R} + \mathcal{O}(\epsilon^3) \quad (\text{A.3})
\end{aligned}$$

where $Q_{L/R}$ removes the off-diagonal entries of M , $K_{L/R}$ is required to ensure the remaining diagonal entries are real and positive and $\epsilon \sim \frac{1}{|d|}$. The singular values of M written up to sub-subleading order are

$$\begin{aligned}
m_\ell &= \left| a - \frac{bc}{d} - \frac{a}{2} \left(\frac{|b|^2 + |c|^2}{|d|^2} \right) \right| + \mathcal{O}(\epsilon^3) \\
m_{\tilde{h}} &= \left| d + \frac{1}{2} \left(\frac{|b|^2 + |c|^2}{d^*} \right) + \frac{a^* bc}{|d|^2} \right| + \mathcal{O}(\epsilon^3). \quad (\text{A.4})
\end{aligned}$$

Note that in the type-I seesaw scenario ($a = 0$, $b = c = m_D$, $d = m_R$), eq. (A.3) implies $U_L^\dagger = U_R^T$ and therefore the (now symmetric) matrix M can be diagonalised either by $U_R^T M U_R$ or $U_L^\dagger M U_L^*$ with the singular values of eq. (A.4) simplifying to

$$\begin{aligned}
m_\ell &= \left| \frac{m_D^2}{m_R} \right| + \mathcal{O}(\epsilon^2) \\
m_{\tilde{h}} &= \left| m_R + \frac{|m_D|^2}{m_R} \right| + \mathcal{O}(\epsilon^2) \quad (\text{A.5})
\end{aligned}$$

as expected.

The results above can be applied to find similar expressions for U_L , U_R , m_ℓ and $m_{\tilde{h}}$ in scenarios where different entries of M are the largest in the seesaw through appropriate permutations. For example consider when $|c| \gg |a|, |b|, |d|$, as before there exist U_L and U_R which diagonalise M , however we note that eq. (A.2) can be rewritten,

$$U_L^\dagger \begin{pmatrix} a & b \\ c & d \end{pmatrix} U_R = U_L^\dagger \begin{pmatrix} b & a \\ d & c \end{pmatrix} \tau_1 U_R = (U_L')^\dagger \begin{pmatrix} b & a \\ d & c \end{pmatrix} U_R' = \text{diag}(m_\ell, m_{\tilde{h}}) \quad (\text{A.6})$$

where τ_1 corresponds to the first Pauli matrix.

The results in eqs. (A.3) and (A.4) can now be applied to eq. (A.6) as c is assumed to be the largest entry of M . Therefore m_ℓ and $m_{\tilde{h}}$ are given by the expressions in eq. (A.4) with the permutations $a \leftrightarrow b$ and $c \leftrightarrow d$, and the unitary diagonalisation matrices are given by $U_L' = U_L$ and $U_R' = \tau_1 U_R$ taken from eq. (A.3) with similar permutations. Applying a similar procedure for $|b| \gg |a|, |c|, |d|$ we find that $U_L' = \tau_1 U_L$ and $U_R' = U_R$ and the

results from eqs. (A.3) and (A.4) are valid with permutations $a \leftrightarrow c$ and $b \leftrightarrow d$. Finally when $|a| \gg |b|, |c|, |d|$ we find $U'_L = \tau_1 U_L$ and $U'_R = \tau_1 U_R$ with the permutations $a \leftrightarrow d$ and $b \leftrightarrow c$ applied to eqs. (A.3) and (A.4).

A.2 Singular Values for Multiple Generations

Consider now a general matrix $M_B \in \mathbb{C}^{m \times n}$ which can be partitioned into a 2×2 block matrix of the form

$$M_B = \begin{pmatrix} A_{m_1 \times n_1} & B_{m_1 \times l_1} \\ C_{l_1 \times n_1} & D_{l_1 \times l_1} \end{pmatrix} \quad (\text{A.7})$$

where the subscripts on the matrix blocks correspond to their dimensions, $m_1 + l_1 = m$, $n_1 + l_1 = n$ and D is restricted to be nonsingular. This matrix can be *block* diagonalised by

$$Q_L^\dagger M_B Q_R = M_{\mathcal{D}} = \text{diag}(m_L, m_H) = \begin{pmatrix} m_L & 0_{m_1 \times l_1} \\ 0_{l_1 \times n_1} & m_H \end{pmatrix} \quad (\text{A.8})$$

where m_L and m_H now correspond to $m_1 \times n_1$ and $l_1 \times l_1$ block matrices respectively and $0_{n_1 \times l_1}$ corresponds to a matrix of zeroes with dimension $n_1 \times l_1$. Unlike in the 2×2 case, exact analytical expressions for the block matrices m_L and m_H or the diagonalisation matrices Q_L and Q_R do not exist. However in the seesaw limit, where the lightest singular value of the square block D is assumed to be significantly larger than the largest singular value of all other blocks, a similar perturbative expansion can be derived. This is done by assuming, as an ansatz, that the block matrices U_L and U_R have a similar form to the matrices appearing in eq. (A.3)²³ in combination with the conditions $U_L^\dagger (M_B M_B^\dagger) U_L = \text{diag}(m_L m_L^\dagger, m_H m_H^\dagger)$ and $U_R^\dagger (M_B^\dagger M_B) U_R = \text{diag}(m_L^\dagger m_L, m_H^\dagger m_H)$ which allows $U_{L/R}$ to be solved separately from each other.

In this limit, $\|D\| \gg \|A, B, C\|$, we find M_B can be *fully* diagonalised at sub-subleading order by

$$\begin{aligned} U_L &\simeq \underbrace{\begin{pmatrix} \mathbb{1}_{n \times n} - \frac{1}{2} X X^\dagger & X \\ -X^\dagger & \mathbb{1}_{n \times n} - \frac{1}{2} X^\dagger X \end{pmatrix}}_{Q_L} \underbrace{\begin{pmatrix} V_L & 0 \\ 0 & W_L \end{pmatrix}}_{K_L} \\ U_R &\simeq \underbrace{\begin{pmatrix} \mathbb{1}_{n \times n} - \frac{1}{2} Z^\dagger Z & Z^\dagger \\ -Z & \mathbb{1}_{n \times n} - \frac{1}{2} Z Z^\dagger \end{pmatrix}}_{Q_R} \underbrace{\begin{pmatrix} V_R & 0 \\ 0 & W_R \end{pmatrix}}_{K_R} \end{aligned} \quad (\text{A.9})$$

where

$$\begin{aligned} X &= (AC^\dagger + BD^\dagger)(DD^\dagger)^{-1} \simeq BD^{-1} \\ Z &= (D^\dagger D)^{-1}(B^\dagger A + D^\dagger C) \simeq D^{-1}C. \end{aligned} \quad (\text{A.10})$$

²³In other words that U_L and U_R can be written perturbatively in terms of an expansion parameter ϵ related to the seesaw in M .

Dominant Block	Permutations	(U'_L, U'_R)
A	$A \leftrightarrow D \ \& \ B \leftrightarrow C$	$(\mathbb{I}(l_1, m_1) U_L, \mathbb{I}(n_1, l_1) U_R)$
B	$A \leftrightarrow C \ \& \ B \leftrightarrow D$	$(\mathbb{I}(l_1, m_1) U_L, U_R)$
C	$A \leftrightarrow B \ \& \ C \leftrightarrow D$	$(U_L, \mathbb{I}(n_1, l_1) U_R)$
D	—	(U_L, U_R)

Table 12. Required rotations on U_L and U_R and permutations of block elements for the formulas in eqs. (A.9) to (A.11) to be valid for different block elements assumed to be the nonsingular-square dominant block of M_B in seesaw scenarios. $\mathbb{I}(l_1, m_1)$ is defined in eq. (A.13) and here l_1 is taken to be the dimension of the dominant square matrix block and (m_1, n_1) correspond to the dimensions of the matrix block diagonally opposite.

Similar to the 2×2 case, $Q_{L/R}$ remove the off-diagonal entries of M_B , $K_{L/R}$ diagonalise the blocks $m_{L/H}$ via $(V/W)_L^\dagger m_{L/H} (V/W)_R = m_{L/H}^d = \text{diag}(\dots)$ and the expression for $V_{L/R}$ and $W_{L/R}$ depends on the structure of the submatrices m_L and m_H .

Applying eqs. (A.9) and (A.10) to eq. (A.8) gives the light and heavy submatrices at sub-subleading order as per

$$\begin{aligned}
m_L &\simeq \left(A - BD^{-1}C - \frac{1}{2} \left(BD^{-1}(D^\dagger)^{-1}B^\dagger A + AC^\dagger(D^\dagger)^{-1}D^{-1}C \right) \right) \\
m_H &\simeq D + \frac{1}{2} \left(CC^\dagger(D^\dagger)^{-1} + (D^\dagger)^{-1}B^\dagger B \right) \\
&\quad + \frac{1}{2} \left((D^\dagger)^{-1}D^{-1}CA^\dagger B + CA^\dagger BD^{-1}(D^\dagger)^{-1} \right). \tag{A.11}
\end{aligned}$$

Note that eq. (A.11) agrees with eq. (A.4) in the special case where $M_B \in \mathbb{C}^{2 \times 2}$, i.e. all the blocks of M_B are just complex numbers, $A \rightarrow a \dots D \rightarrow d$.

In the special case of eq. (A.7) where $B = C^T = m_D$ (implying $n_1 = m_1$), $A = \emptyset_{n_1 \times n_1}$ and $D = M_R$ is a symmetric matrix, which occurs in the n-dimensional type-I seesaw model of neutrino mass, $U_L^\dagger = U_R^T$ and m_L and m_H simplify to at sub-subleading order

$$\begin{aligned}
m_L &\simeq -m_D M_R^{-1} m_D^T \\
m_H &\simeq M_R + \frac{1}{2} \left(m_D^T m_D^* (M_R^*)^{-1} + (M_R^*)^{-1} m_D^\dagger m_D \right) \tag{A.12}
\end{aligned}$$

where $M_R = M_R^T$ has been used. Therefore the usual results are recovered in this case and we find them to be in full agreement²⁴ with [45] which derived an algorithm to find the light and heavy mass matrices in neutrino seesaw models at arbitrary order.

In a similar way to the case with $M \in \mathbb{C}^{2 \times 2}$, the results above can be extended to find m_L , m_H , U_L and U_R in situations where the norm of different blocks in eq. (A.7) are

²⁴We also find agreement in the case where $A = A^T \neq 0_{n \times n}$ which for example is relevant in hybrid type-I+II models.

dominant²⁵. Once again consider a scenario where $\|C\| \gg \|A, B, D\|$ (and C is square) and note that

$$M_B = \begin{pmatrix} A_{m_1 \times l_1} & B_{m_1 \times n_1} \\ C_{l_1 \times l_1} & D_{l_1 \times n_1} \end{pmatrix} = \begin{pmatrix} B_{m_1 \times n_1} & A_{m_1 \times l_1} \\ D_{l_1 \times n_1} & C_{l_1 \times l_1} \end{pmatrix} \underbrace{\begin{pmatrix} 0_{n_1 \times l_1} & \mathbb{1}_{n_1 \times n_1} \\ \mathbb{1}_{l_1 \times l_1} & 0_{l_1 \times n_1} \end{pmatrix}}_{\mathbb{I}(n_1, l_1)}. \quad (\text{A.13})$$

Therefore eqs. (A.9) to (A.11) are valid if $U'_L = U_L$, $U'_R = \mathbb{I}(n_1, l_1) U_R$ and the permutations $A \leftrightarrow B$ and $C \leftrightarrow D$ are performed, where $(U'_L)^\dagger M_B U'_R = \text{diag}(m_L, m_H)$. This can be performed for any of the four blocks of M_B being dominant and the results for this are summarised in table 12.

A.3 Gap properties between the charged leptons and down quarks

Below we briefly prove the claim that, in the triplet scenario, the charged-lepton mass matrices defined in eq. (4.3) imply that the SM-like charged lepton masses must be lighter than the down-quark masses for all generations. This arises due to the zero block appearing in their mass matrices diagonally opposite the dominant block in the seesaw. Unlike the previous section which relied on an approximate block diagonalisation technique with neglected higher-order terms, the results below are exact statements that do not rely on any perturbative arguments. We closely follow the work presented in [46] which proved a similar gap property specifically for the type-I seesaw symmetric mass matrix, which we will generalise to an arbitrary complex matrix relevant to our charged-lepton seesaw.

We state without proof three matrix properties related to the Courant-Fischer-Weyl min-max theorem:

- For two hermitian $n \times n$ matrices A and B , if $C = A + B$ then

$$a_k + b_1 \leq c_k \leq a_k + b_n \quad (\text{A.14})$$

where x_i corresponds to the i -th largest eigenvalue of the matrix X and $k \leq n$. For $k = 1$ this reduces to the special case

$$\min(A) + \min(B) \leq \min(A + B) \quad (\text{A.15})$$

where $\min(X) = x_1$.

- For all $A \geq 0$ and $B \in M_n(\mathbb{C})$, if $C = B^\dagger A B$ then

$$a_k \min(B^\dagger B) \leq c_k. \quad (\text{A.16})$$

²⁵This is with the caveat that M_B can be partitioned such that the dominant block has a well defined inverse.

- If Q is an $n \times n$ submatrix of the $N \times N$ matrix M then

$$m_k \leq q_k \leq m_{N-n+k} \quad (\text{A.17})$$

for every $k \leq n$, this is known as the Cauchy interlacing theorem.

Additional details including proofs for some of these properties can be found in [46].

We take the mass mixing matrix M_{eE} to have the same structure as the case of an $SU(2)_R$ triplet defined in eq. (4.3):

$$M_{eE} = \begin{pmatrix} m_{ee} & 0_{3 \times 3} \\ m_{Ee} & m_{EE} \end{pmatrix}, \quad (\text{A.18})$$

where we are assuming three generations of the exotic triplet fermion and therefore each block is 3×3 and we further assume m_{Ee} is nonsingular. As discussed in section 5.1, in order to achieve the desired helicity-suppression in the PS limits we require the hierarchy $\|m_{Ee}\| > \|m_{ee}, m_{EE}\|$ to be satisfied which implies

$$\sigma_n(m_{ee}), \sigma_n(m_{EE}) < \sigma_1(m_{Ee}) \quad (\text{A.19})$$

where $\sigma_i(X)$ corresponds to the i -th largest singular value of the matrix X and $n = 3$. This defines a seesaw in M_{eE} with m_{Ee} as the dominant block.

The bottom-right sub-matrix of

$$\left(M_{eE} M_{eE}^\dagger\right)^{-1} = \begin{pmatrix} \cdot & \cdot \\ \cdot & m_{EE}^{-1} m_{Ee} m_{ee}^{-1} (m_{ee}^\dagger)^{-1} m_{Ee}^\dagger (m_{EE}^\dagger)^{-1} + m_{EE}^{-1} (m_{EE}^\dagger)^{-1} \end{pmatrix} \quad (\text{A.20})$$

which we will label as X satisfies the property defined in eq. (A.17), where the dots correspond to sub-matrices which are not relevant. As the sub-matrix X has dimensions $n \times n$ and the full matrix has dimensions $2n \times 2n$ the interlacing theorem implies

$$x_{n-k} \leq m_{2n-k} \quad (\text{A.21})$$

where we have chosen $k = n - k$ in eq. (A.17). As $M_{eE} (M_{eE}^\dagger)^{-1}$ is Hermitian, its eigenvalues correspond to the squared singular values of M_{eE} . Furthermore, from simple properties of eigenvalues, the i -th *largest* eigenvalue of an $n \times n$ matrix M^{-1} corresponds to the $(n-i)$ -th *smallest* eigenvalue of M . Therefore eq. (A.21) implies

$$x_{n-k} \leq \frac{1}{\sigma_k(M_{eE})^2}. \quad (\text{A.22})$$

Applying eq. (A.15) to x_{n-k} leads to the inequality

$$\left[m_{EE}^{-1} m_{Ee} m_{ee}^{-1} (m_{ee}^\dagger)^{-1} m_{Ee}^\dagger (m_{EE}^\dagger)^{-1} \right]_{n-k} + \min(m_{EE}^{-1} (m_{EE}^\dagger)^{-1}) \leq x_{n-k} \quad (\text{A.23})$$

and now with repeated applications of eq. (A.16) to the first term of eq. (A.23) leads to

$$\left(\left[m_{ee}^{-1} (m_{ee}^\dagger)^{-1} \right]_{n-k} \min \left(m_{Ee} m_{Ee}^\dagger \right) + \mathbb{1} \right) \min(m_{EE}^{-1} (m_{EE}^\dagger)^{-1}) \leq x_{n-k} \quad (\text{A.24})$$

which implies

$$\frac{1}{\sigma_n(m_{EE})^2} \left(\frac{\sigma_1(m_{Ee})^2}{\sigma_k(m_{ee})^2} \right) \leq \frac{1}{(\sigma_k(M_{eE}))^2} \quad (\text{A.25})$$

and therefore

$$\sigma_k(M_{eE}) \leq \sigma_k(m_{ee}) \frac{\sigma_n(m_{EE})}{\sqrt{\sigma_1(m_{Ee})^2 + \sigma_k(m_{ee})^2}} < \sigma_k(m_{ee}) \frac{\sigma_n(m_{EE})}{\sigma_1(m_{Ee})} \quad (\text{A.26})$$

where we have used the seesaw assumption that $\sigma_n(m_{ee}, m_{EE}) < \sigma_1(m_{Ee})$.

The exact same procedure can be applied to the matrix $(M_{eE}^\dagger)^{-1} M_{eE}$ which instead leads to the inequality

$$\sigma_k(M_{eE}) \leq \sigma_k(m_{EE}) \frac{\sigma_n(m_{ee})}{\sqrt{\sigma_1(m_{Ee})^2 + \sigma_k(m_{EE})^2}} < \sigma_k(m_{EE}) \frac{\sigma_n(m_{ee})}{\sigma_1(m_{Ee})}. \quad (\text{A.27})$$

Combining eqs. (A.26) and (A.27) leads to an upper-bound on the k-th largest *light* singular value of M_{eE}

$$\sigma_k(M_{eE}) < \frac{\min[\sigma_k(m_{ee})\sigma_n(m_{EE}), \sigma_k(m_{EE})\sigma_n(m_{ee})]}{\sigma_1(m_{Ee})} \leq \frac{\sigma_n(m_{ee})\sigma_n(m_{EE})}{\sigma_1(m_{Ee})}. \quad (\text{A.28})$$

Comparing eq. (A.28) to the charged-lepton mass matrix in the case of the $SU(2)_R$ triplet in eq. (4.3) leads to the strict inequality

$$\sigma_k(m_\ell) < \sigma_k(m_d) \left(\frac{\sigma_3(\mu_\Psi)}{v_R \sigma_1(Y_\Psi)} \right) \quad (\text{A.29})$$

and as the singular values of each matrix correspond to the physical masses, each light lepton mass of a given generation must be strictly lighter than the corresponding down-quark mass of the same generation. This is due to the seesaw assumption which enforces the fraction in brackets to be strictly smaller than one. As shown in table 6 the charged-lepton and down-quark mass hierarchies change between generations at low scales, therefore due to the PS symmetry, a matrix of the form in eq. (A.18) is phenomenologically ruled out.

Although not relevant in our analysis, a similar procedure can be applied to the Hermitian matrices $(M_{eE}^\dagger)M_{eE}$ and $M_{eE}(M_{eE}^\dagger)$ to derive inequalities on the masses of the n heavy states of M_{eE} and for example leads to

$$\sigma_{n+1}(M_{eE}) \geq \max \left(\sqrt{\sigma_1(m_{Ee})^2 + \sigma_1(m_{ee})^2}, \sqrt{\sigma_1(m_{Ee})^2 + \sigma_1(m_{EE})^2} \right) > \sigma_1(m_{Ee}) \quad (\text{A.30})$$

Therefore the strict hierarchy implied by these inequalities leads to the ‘gap property’

$$\sigma_1(M_{eE}) \leq \dots \leq \sigma_n(M_{eE}) \leq \frac{\sigma_n(m_{ee})\sigma_n(m_{EE})}{\sigma_1(m_{Ee})} \ll \sigma_1(m_{Ee}) < \sigma_{n+1}(M_{eE}) \leq \dots \leq \sigma_{2n}(M_{eE}) \quad (\text{A.31})$$

which does not rely on any perturbative arguments and we emphasise that these results are only valid for ‘type-I like’ scenarios where the entry diagonally opposite the dominant block is zero. Our results agree with the gap properties derived in [46] in the type-I limit which assumes $m_{ee} = (m_{EE})^T = m_D$ and $m_{Ee} = m_R$ and recovers the usual type-I hierarchy.

A.4 Lepton masses with additional bi-doublets

The neutrino mass matrix which arises with the addition of an $SU(2)_{L/R}$ bi-doublet to the usual PS fermions $f_{L/R}$ is given by

$$\mathcal{L}_{\nu N} = \frac{1}{2} \begin{pmatrix} \overline{\nu_L} & \overline{\nu_R^c} & \overline{N_L} & \overline{N_R^c} \end{pmatrix} \begin{pmatrix} 0 & m_u & 0 & y_{\Psi_{22}}^R v_R \\ m_u & 0 & 0 & y_{\Psi_{22}}^L v_L^* \\ 0 & 0 & 0 & \mu_{\Psi_{22}} \\ y_{\Psi_{22}}^R v_R & y_{\Psi_{22}}^L v_L^* & \mu_{\Psi_{22}} & 0 \end{pmatrix} \begin{pmatrix} \nu_L^c \\ \nu_R \\ N_L^c \\ N_R \end{pmatrix} \quad (\text{A.32})$$

where we have labelled the fields as in eq. (4.11). A phenomenologically-viable mass spectrum for the heavy charged lepton states requires either $y_{\Psi}^R v_R$ or μ_{Ψ} to have masses at a TeV or above as discussed in section 5.1 for the charged-lepton mass mixing matrix

$$\mathcal{L}_{eE} = \begin{pmatrix} \overline{e_L} & \overline{E_L} \end{pmatrix} \begin{pmatrix} m_d & y_{\Psi_{22}}^R v_R \\ y_{\Psi_{22}}^L v_L^* & \mu_{\Psi_{22}} \end{pmatrix} \begin{pmatrix} e_R \\ E_R \end{pmatrix}. \quad (\text{A.33})$$

The parameter m_u is fixed by the up-quark masses due to the PS symmetry, m_d is fixed by the down-quark masses, $y_{\Psi_{22}}^L v_L$ is tied to the electroweak scale, $y_{\Psi_{22}}^R v_R$ can at most be the size of $SU(2)_R$ /PS breaking and $\mu_{\Psi_{22}}$ is unconstrained.

Different hierarchies between the parameters appearing in eq. (A.32) lead to different neutrino mass phenomenology and here we show that only one possibility allows for a viable mass spectrum for the charged leptons as well as sufficiently light neutrino masses assuming a low scale PS breaking. We will use a one-generational example for illustrative purposes as the same statements hold true for the more complicated multi-generational scenario. As discussed in section 5.1 at least one of $y_{\Psi_{22}}^R v_R$ or $\mu_{\Psi_{22}}$ must have masses at least an order of magnitude larger than the electroweak scale such that the charged lepton partners are sufficiently heavy phenomenologically.

Firstly in the scenario where $|\mu_{\Psi}| \gg |y_{\Psi_{22}}^R v_R, y_{\Psi_{22}}^L v_L, m_u|$ the light, charged-lepton masses are given by

$$m_{\ell} \simeq m_d - v_L v_R y_{\Psi_{22}}^L (\mu_{\Psi_{22}})^{-1} y_{\Psi_{22}}^R \quad (\text{A.34})$$

and diagonalising eq. (A.32) leads to two different pairs of pseudo-Dirac neutrinos with masses given at first order by

$$\begin{aligned} m_{1,2} &\simeq \mu_{\Psi_{22}} & \nu_{1,2} &\simeq \frac{1}{\sqrt{2}} N_L \pm \frac{1}{\sqrt{2}} N_R^c \\ m_{3,4} &\simeq m_u & \nu_{3,4} &\simeq \frac{1}{\sqrt{2}} \nu_L \pm \frac{1}{\sqrt{2}} \nu_R^c. \end{aligned} \quad (\text{A.35})$$

Therefore the lightest neutrino masses would be predicted to have masses and splittings similar to the up-quark sector. The above equation is true irrespective of the hierarchy between the non-dominant parameters $y_{\Psi_{22}}^R v_R$, $y_{\Psi_{22}}^L v_L$ and m_u . Therefore we find that this hierarchy of couplings does not lead to the desired seesaw required to explain the lightness of the active neutrino masses for any scale of PS breaking.

Turning to the alternate possibility where $|y_{\Psi_{22}}^R v_R| \gg |\mu_{\Psi_{22}}, y_{\Psi_{22}}^L v_L, m_u|$ the charged lepton masses are now given by

$$m_\ell \simeq y_{\Psi_{22}}^L v_L - \frac{m_d \mu_{\Psi_{22}}}{y_{\Psi_{22}}^R v_R}. \quad (\text{A.36})$$

Here we find two different neutrino mass regimes depending on the hierarchy between the non-dominant parameters $|\mu_{\Psi_{22}}|$ and $|y_{\Psi_{22}}^L v_L|$.

For the hierarchy $|y_{\Psi_{22}}^R v_R| \gg |\mu_{\Psi_{22}}| > 2|y_{\Psi_{22}}^L v_L|$ the physical neutrino states have masses given at first order by

$$\begin{aligned} m_{1,2} &\simeq y_{\Psi_{22}}^R v_R & \nu_{1,2} &\simeq \frac{1}{\sqrt{2}} \nu_L \pm \frac{1}{\sqrt{2}} N_R^c \\ m_{3,4} &\simeq \frac{m_u}{y_{\Psi_{22}}^R v_R} (\mu_{\Psi_{22}} \pm y_{\Psi_{22}}^L v_L) & \nu_{3,4} &\simeq \frac{1}{\sqrt{2}} N_L \pm \frac{1}{\sqrt{2}} \nu_R^c \end{aligned} \quad (\text{A.37})$$

where the above results are insensitive to the relative size of $|m_u|$ to $|y_{\Psi_{22}}^L v_L|$ and $|\mu_{\Psi_{22}}|$. Sufficiently light neutrinos now implies the ratio

$$\frac{m_\nu}{m_u} \simeq \frac{\mu_{\Psi_{22}}}{y_{\Psi_{22}}^R v_R} \simeq 10^{-11} \quad (\text{A.38})$$

where we have estimated $m_\nu \lesssim 10^{-9}$ GeV from known neutrino upper mass limits and $m_u \simeq 170$ GeV in the case of the top quark. This consequently implies that

$$m_\ell \simeq y_{\Psi_{22}}^L v_L \quad (\text{A.39})$$

for the charged-lepton masses as the second term in eq. (A.36) will be highly suppressed. Therefore in order to recover the correct charged-lepton masses we require $y_{\Psi_{22}}^L v_L \simeq 1$ GeV for the tau lepton and as we have assumed $|\mu_{\Psi_{22}}| > |y_{\Psi_{22}}^L v_L|$ this necessarily implies

$$|\mu_{\Psi_{22}}| > 1 \text{ GeV} \quad (\text{A.40})$$

and therefore

$$|y_{\Psi_{22}}^R v_R| > 10^{11} \text{ GeV} \quad (\text{A.41})$$

using eq. (A.38). Therefore for $|\mu_{\Psi_{22}}| > |y_{\Psi_{22}}^L v_L|$, sufficiently light neutrino masses are only possible for very large $SU(2)_R$ /PS breaking scales.

Alternatively the hierarchy $|y_{\Psi_{22}}^R v_R| \gg |y_{\Psi_{22}}^L v_L| > \frac{1}{2} |\mu_{\Psi_{22}}|$ leads to

$$\begin{aligned}
m_{1,2} &\simeq v_R y_{\Psi_{22}}^R & \nu_{1,2} &\simeq \frac{1}{\sqrt{2}} \nu_L \pm \frac{1}{\sqrt{2}} N_R^c \\
m_3 &\simeq \frac{v_L}{v_R} \frac{2 y_{\Psi_{22}}^L m_u}{y_{\Psi_{22}}^R} & \nu_3 &\simeq \nu_R^c \\
m_4 &\simeq \frac{1}{v_L v_R} \frac{\mu_{\Psi_{22}}^2 m_u}{2 y_{\Psi_{22}}^L y_{\Psi_{22}}^R} & \nu_4 &\simeq N_L
\end{aligned} \tag{A.42}$$

where again the results are insensitive to the overall size of m_u as long as it is smaller than $y_{\Psi_{22}}^R v_R$. This scenario therefore leads to the neutrino mass hierarchy

$$m_{\nu_4} \ll m_{\nu_3} \ll m_{\nu_{1,2}} \tag{A.43}$$

Sufficiently light neutrinos implies

$$\frac{m_\nu}{m_u} y_{\Psi_{22}}^L v_L \simeq 10^{-11} \text{ GeV} \simeq \frac{1}{2} \frac{\mu_{\Psi_{22}}^2}{y_{\Psi_{22}}^R v_R} \tag{A.44}$$

for the same estimates. Once again this implies that the second term in eq. (A.36) will be subdominant and therefore the charged lepton masses are given by $m_\ell \simeq y_{\Psi_{22}}^L v_L$. Now light neutrinos are possible for low PS breaking scales for similar reasons to the usual inverse seesaw mechanism, for example for $y_{\Psi_{22}}^R v_R \simeq 10 \text{ TeV}$ we can estimate

$$\mu_{\Psi_{22}} \simeq 4.4 \times 10^{-3} \text{ GeV}. \tag{A.45}$$

Therefore we find for a mass matrix of the form in eq. (A.32), only one hierarchy of parameters leads to a viable neutrino mass spectrum for low scales of PS breaking. As this requires the term $\mu_{\Psi_{22}}$ to be very small, this also conveniently leads to a helicity-suppression in the PS mediated rare meson decays, and therefore allows the limits for PS breaking to be significantly lowered as discussed in section 5.1.

In the multi-generational scenario we find the block diagonalisation of eq. (A.32), assuming the hierarchy $\|Y_{\Psi_{22}}^R v_R\| \gg \|Y_{\Psi_{22}}^L v_L\| > \|\mu_{\Psi_{22}}\|$ ²⁶, is given at first order by

$$\begin{aligned}
m_{1,2} &\simeq v_R Y_{\Psi_{22}}^R \\
m_3 &\simeq \frac{v_L}{v_R} \left(Y_{\Psi_{22}}^L (Y_{\Psi_{22}}^R)^{-1} m_u + m_u^T [Y_{\Psi_{22}}^L (Y_{\Psi_{22}}^R)^{-1}]^T \right) \\
m_4 &\simeq \frac{1}{v_L v_R} \mu_{\Psi_{22}} \left[(Y_{\Psi_{22}}^R)^T (m_u^T)^{-1} Y_{\Psi_{22}}^L + (Y_{\Psi_{22}}^L)^T m_u^{-1} Y_{\Psi_{22}}^R \right]^{-1} \mu_{\Psi_{22}}^T
\end{aligned} \tag{A.46}$$

for each mass block where $Y_{\Psi_{22}}^{L/R}$, m_u and $\mu_{\Psi_{22}}$ are now matrices of appropriate dimension.

²⁶More accurately, the hierarchy between each matrix required for a low scale spectrum is given by $\|\mu_{\Psi_{22}} (y_{\Psi_{22}}^R v_R)^{-1} m_u\| < \|v_L v_R (Y_{\Psi_{22}}^L (y_{\Psi_{22}}^R v_R)^{-1} m_u + [Y_{\Psi_{22}}^L (y_{\Psi_{22}}^R v_R)^{-1} m_u]^T)\|$ for non-commuting matrices. This should in general imply the hierarchy $\|\mu_{\Psi_{22}}\| < \|Y_{\Psi_{22}}^L v_L\|$ however.

We estimate the relationship between the mass and interaction eigenstates for the relevant light neutrinos states to be

$$\begin{aligned}
\nu_4 &\simeq U_N^\dagger [\mu_{\Psi_{22}}(y_{\Psi_{22}}^R)^{-1}]^\dagger \nu_L^c - \frac{1}{2} U_N^\dagger \left[Y_{\Psi_{22}}^L (y_{\Psi_{22}}^R)^{-1} ([y_{\Psi_{22}}^R]^\dagger)^{-1} \mu_{\Psi_{22}}^\dagger \right]^\dagger \nu_R \\
&\quad + U_N^\dagger \left[\mathbb{1} - \frac{1}{2} \mu_{\Psi_{22}} (Y_{\Psi_{22}}^R)^{-1} ([Y_{\Psi_{22}}^R]^\dagger)^{-1} \mu_{\Psi_{22}}^\dagger \right]^\dagger N_L^c \\
\nu_3 &\simeq O_3^\dagger [Y_{\Psi_{22}}^L (Y_{\Psi_{22}}^R)^{-1}]^\dagger \nu_L^c - \frac{1}{2} O_3^\dagger \left[Y_{\Psi_{22}}^L (Y_{\Psi_{22}}^R)^{-1} ([Y_{\Psi_{22}}^R]^\dagger)^{-1} \mu_{\Psi_{22}}^\dagger \right]^\dagger N_L^c + O_3^\dagger [m_u^T (Y_{\Psi_{22}}^R)^{T-1}]^\dagger N_R \\
&\quad + O_3^\dagger \left[\mathbb{1} - \frac{1}{2} \left(Y_{\Psi_{22}}^L (Y_{\Psi_{22}}^R)^{-1} ([Y_{\Psi_{22}}^R]^\dagger)^{-1} (Y_{\Psi_{22}}^L)^\dagger + m_u^T (Y_{\Psi_{22}}^R)^{T-1} ([Y_{\Psi_{22}}^R]^*)^{-1} m_u^* \right) \right]^\dagger \nu_R
\end{aligned} \tag{A.47}$$

using a perturbative seesaw expansion where U_N^\dagger and O_3 diagonalise the lightest and next-to-lightest mass blocks of the neutrino mass matrix after block diagonalisation. Therefore for the lightest neutrino states, ν_4 , the deviation from unitarity between its couplings to the SM charged leptons, which are predominantly made up of E_L which weakly couples to N_L , is given at lowest order by the matrix

$$\eta \simeq \frac{1}{2} \mu_{\Psi_{22}} (Y_{\Psi_{22}}^R)^{-1} (\mu_{\Psi_{22}} (Y_{\Psi_{22}}^R)^{-1})^\dagger. \tag{A.48}$$

This determines the degree of non-unitarity in the physical PMNS matrix which stems from mixing effects within the neutral sector. As the fermion bi-doublet also introduced additional exotic charged-lepton states, there will additionally be mixing effects within the charged sector which leads to additional non-unitarity effects for the PMNS. Interestingly, as shown in section 5.1.1 we find the deviation of non-unitarity within the charged lepton sector to be the same as in the neutral sector above implying

$$U_{\text{PMNS}} \simeq (\mathbb{1} - \eta) U_N^\dagger (\mathbb{1} - \eta) O_L^c. \tag{A.49}$$

Figure 14 plots the norm of the required matrix $\mu_{\Psi_{22}}$ for a given choice of v_R and $Y_{\Psi_{22}}^R$ which leads to a viable mass spectrum for the active neutrinos where we have fixed the lightest neutrino mass to

$$m_{\nu_1} = 10^{-10} \text{ GeV} \tag{A.50}$$

and assumed a normal ordering for the remaining masses. The matrix $Y_{\Psi_{22}}^R$ was randomly scanned over for a degenerate spectrum such that the singular values of the matrix were within an order of magnitude to each other. The $SU(2)_R$ breaking scale v_R was scanned between $1 - 10^4$ TeV and $\mu_{\Psi_{22}}$ was fixed by

$$\mu_{\Psi_{22}} = U_\nu^* m_\nu^{1/2} A [Y_L m_u^{-1} Y_{\Psi_{22}}^R + (Y_{\Psi_{22}}^R)^T (m_u^T)^{-1} Y_L]^{1/2} \tag{A.51}$$

through a Casas-Ibarra parametrisation [47]. Here U_ν corresponds to the unitary matrix which diagonalises the lightest neutrino mass block, m_ν is a diagonal matrix composed of the assumed neutrino masses and A is a random orthogonal matrix. The left plot of fig. 14

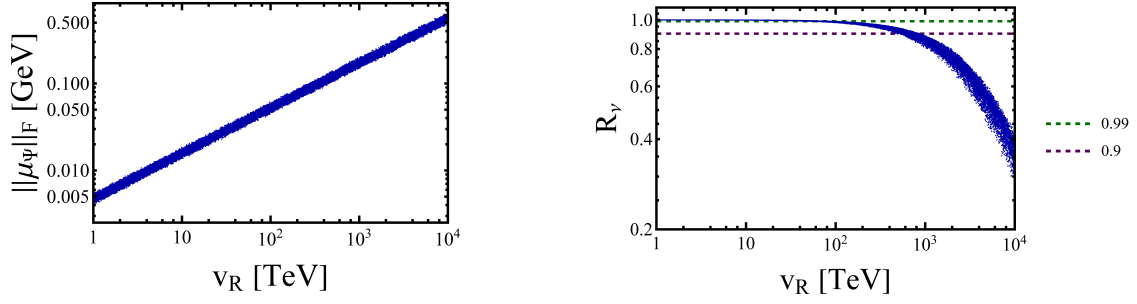


Figure 14. The Frobenius norm of the matrix $\mu_{\Psi_{22}}$ generated through a Casas-Ibarra parametrisation as a function of v_R (**left**) and R_ν as a function of the same scale (**right**), where R_ν is defined in eq. (A.52). Here we have randomly scanned over a degenerate spectrum for $Y_{\Psi_{22}}^R$ such that the heavy charged lepton partners have masses at around the scale v_R . For larger values of v_R the generated $\mu_{\Psi_{22}}$ develops singular values larger than the required hierarchy $\|Y_{\Psi_{22}}^L\| > \|\mu_{\Psi_{22}}\|$ where $Y_{\Psi_{22}}^L v_L$ is fixed to give the correct SM charged-lepton masses and the resultant neutrino masses begin to disagree with experimental values.

shows that as v_R increases, the singular values of $\mu_{\Psi_{22}}$ must increase for a fixed neutrino mass scale. As a result at around 10^3 TeV, the singular values of $\mu_{\Psi_{22}}$ become larger than $Y_{\Psi_{22}}^L$ spoiling the required hierarchy of scales for light neutrinos at low scales. The right plot of fig. 14 plots the same scale as a function of R_ν where

$$R_\nu = \prod_i \frac{m_i}{m_i^{\text{input}}} \quad (\text{A.52})$$

where m_i corresponds to the mass of the i -th generation of the three active neutrinos numerically calculated after diagonalising the mass matrix and m_i^{input} to the masses inputted via the Casas-Ibarra parameterisation. Clearly larger scales for v_R are unable to reproduce the correct neutrino masses. For all points considered the light states from the charged-lepton mass matrix reproduce the charged-lepton masses with $m_e \simeq Y_{\Psi_{22}}^L$ to a high degree of accuracy. Therefore the neutral- and charged-lepton mass matrices generated in the scenario with additional fermionic bi-doublets are viable candidates for a low-scale PS setup provided that

$$y_{\Psi_{22}}^R v_R \lesssim 10^3 \text{ TeV}. \quad (\text{A.53})$$

A.5 Lepton masses with additional triplets

The neutrino mass matrix which arises with the addition of $SU(2)_{L/R}$ triplets is given by the usual linear/inverse seesaw:

$$\mathcal{L}_{\nu N} = \frac{1}{2} \begin{pmatrix} \overline{\nu_L} & \overline{\nu_R^c} & \overline{N_R^c} \end{pmatrix} \begin{pmatrix} 0 & m_u & y_{\Psi_3}^L v_L \\ m_u & 0 & y_{\Psi_3}^R v_R^* \\ y_{\Psi_3}^L v_L & y_{\Psi_3}^R v_R^* & \mu_\Psi \end{pmatrix} \begin{pmatrix} \nu_L^c \\ \nu_R \\ N_R \end{pmatrix} \quad (\text{A.54})$$

where we have labelled the fields as in eq. (4.2) and the PS symmetry enforces that the singular values of m_u are given by the up-quark masses. As discussed in sections 4.1.1 and 5.1, both $y_{\Psi_3}^L v_L$ and $y_{\Psi_3}^L v_R$ are required in order to generate a phenomenologically valid charged lepton mass spectrum. Both terms will not be present if the usual scalars $\chi_{L/R}$ are assumed and therefore require a more exotic choice of scalars. For example if $\chi_L \sim (\mathbf{4}, \mathbf{2}, \mathbf{1})$ is replaced with $\chi' \sim (\mathbf{4}, \mathbf{2}, \mathbf{3})$ in the case of the $SU(2)_R$ triplet as was done in [15], the missing mass term in the Yukawa Lagrangian will now be generated. We will therefore assume in what follows that the scalar spectrum is such that all the terms appearing in eq. (A.54) are present. Consequently the charged lepton mass matrix will be given by

$$\mathcal{L}_{eE} = \begin{pmatrix} \bar{e}_L & \bar{E}_L \end{pmatrix} \begin{pmatrix} m_d & \sqrt{2} y_{\Psi_3}^L v_L \\ \sqrt{2} y_{\Psi_3}^R v_R^* & \mu_{\Psi_3} \end{pmatrix} \begin{pmatrix} e_R \\ E_R \end{pmatrix} \quad (\text{A.55})$$

where now the top-right entry is non-zero and therefore a valid spectrum of charged-lepton masses is possible, unlike before.

Unlike the usual low-scale PS setup, as described in section 2.2, the neutral lepton mass mixing matrix is related to a charged lepton mass mixing matrix and a viable neutrino mass spectrum may not be possible whilst simultaneously generating a viable charged-lepton mass spectrum. As in appendix A.4 we analyse all possible hierarchies of parameters in the two mass matrices in order to establish whether a viable charged-lepton and neutrino mass spectrum can be simultaneously generated for the SM-like states for low scales of PS breaking.

In the scenario where μ_{Ψ_3} is the dominant block in each mass matrix, there are multiple different possible neutrino mass regimes depending on the hierarchy between the non-dominant parameters.

Firstly if $|\mu_{\Psi_3}| > |m_u| > \left| \frac{(y_{\Psi_3}^L v_L)^2}{\mu_{\Psi_3}}, \frac{(y_{\Psi_3}^R v_R)^2}{\mu_{\Psi_3}} \right|$ is satisfied the mass states are given at first order by

$$\begin{aligned} m_1 &\simeq \mu_{\Psi} & \nu_{1,2} &\simeq N_R^c \\ m_{2,3} &\simeq m_u & \nu_{3,4} &\simeq \frac{1}{\sqrt{2}} \nu_L \pm \frac{1}{\sqrt{2}} \nu_R^c \end{aligned} \quad (\text{A.56})$$

and therefore this hierarchy is ruled out as the light neutrinos would be pseudo-Dirac with masses comparable to the up-quark sector.

If instead $|\mu_{\Psi_3}| > \left| \frac{(y_{\Psi_3}^R v_R)^2}{\mu_{\Psi_3}} \right| > |m_u|$ is satisfied the mass spectrum is now given by

$$\begin{aligned}
m_1 &\simeq \mu_{\Psi_3} & \nu_{1,2} &\simeq N_R^c \\
m_2 &\simeq \frac{(y_{\Psi_3}^R)^2 v_R^2}{\mu_{\Psi_3}} & \nu_2 &\simeq \nu_R^c \\
m_3 &\simeq \left| \frac{1}{v_R^2} \left(\frac{m_u}{y_{\Psi_3}^R} \right)^2 \mu_{\Psi_3} - \frac{2v_L}{v_R} \frac{y_{\Psi_3}^L m_u}{y_{\Psi_3}^R} \right| & \nu_3 &\simeq \nu_L
\end{aligned} \tag{A.57}$$

which is rather interesting as the lightest mass state contains a term linearly (rather than inversely) proportional to the dominant term in the seesaw but is still small due to the hierarchy in the non-dominant parameters. The SM charged lepton has a mass given by

$$m_\ell \simeq m_d - v_L v_R \frac{y_{\Psi}^L y_{\Psi}^R}{\mu_{\Psi}} \tag{A.58}$$

by diagonalising eq. (A.55). These equations can be solved for $y_{\Psi_3}^L v_L$ and $y_{\Psi_3}^R v_R$ as a function of μ_{Ψ_3} for the required lepton masses. In the case of the third generation where $m_d \simeq 4.2$ GeV, $m_u \simeq 173$ GeV, $m_\ell \simeq 1.7$ GeV and setting $m_\nu \simeq 10^{-10}$ GeV leads to

$$\frac{(y_{\Psi_3}^L v_L)^2}{\mu_{\Psi_3}} \simeq 10^{-14} \text{ GeV} \quad \text{and} \quad \frac{(y_{\Psi_3}^R v_R)^2}{\mu_{\Psi_3}} \simeq 10^{14} \text{ GeV} \tag{A.59}$$

which implies that $\mu_{\Psi} > 10^{14}$ GeV by the initial seesaw assumption, therefore requiring both a viable charged-lepton and neutrino mass spectrum with μ_{Ψ} dominant is only possible for high scale PS breaking scenarios. The final possible hierarchy where $|\mu_{\Psi_3}| > \left| \frac{(y_{\Psi_3}^L v_L)^2}{\mu_{\Psi_3}} \right| > |m_u|$ is also unviable for similar arguments.

The alternative scenario where $|y_{\Psi_3}^R v_R|$ is the dominant term in the mass matrix recovers the usual inverse/linear seesaw

$$\begin{aligned}
m_{1,2} &\simeq y_{\Psi_3}^R v_R & \nu_{1,2} &\simeq \frac{1}{\sqrt{2}} N_R^c \pm \frac{1}{\sqrt{2}} \nu_R^c \\
m_3 &\simeq \left| \frac{1}{v_R^2} \left(\frac{m_u}{y_{\Psi_3}^R} \right)^2 \mu_{\Psi_3} - \frac{2v_L}{v_R} \frac{y_{\Psi_3}^L m_u}{y_{\Psi_3}^R} \right| & \nu_3 &\simeq \nu_L.
\end{aligned} \tag{A.60}$$

and the lightest charged-lepton mass is given by

$$m_\ell \simeq v_L y_{\Psi}^L - \frac{1}{v_R} \frac{m_d \mu_{\Psi}}{y_{\Psi}^R}. \tag{A.61}$$

The lightest neutrino state is now suppressed by the scale $y_{\Psi_3}^R v_R$ as usual, it is quite interesting that the lightest neutrinos in eqs. (A.57) and (A.60) have identical masses for completely different hierarchies of parameters.

For three generations of each fermion multiplet the light mass blocks are given by

$$m_\nu \simeq \frac{1}{v_R^2} m_u [(Y_{\Psi_3}^R)^T]^{-1} \mu_{\Psi_3} (Y_{\Psi_3}^R)^{-1} m_u^T - \frac{v_L}{v_R} m_u [(Y_{\Psi_3}^R)^T]^{-1} (Y_{\Psi_3}^L)^T - \frac{v_L}{v_R} Y_{\Psi_3}^L (Y_{\Psi_3}^R)^{-1} m_u^T \quad (\text{A.62})$$

for the neutrinos and

$$m_\ell \simeq Y_{\Psi_3}^L v_L - \frac{1}{v_R} m_d (Y_{\Psi_3}^R)^{-1} \mu_{\Psi_3} \quad (\text{A.63})$$

for the charged leptons.

For a given choice of $v_R Y_{\Psi_3}^R$, the unknown matrices $v_L Y_{\Psi}^L$ and μ_{Ψ} are fixed by solving the above equations. Due to the complexity of solving the above matrix equations we solve eqs. (A.62) and (A.63) numerically where we assume a normal ordering for the light neutrino masses and fix the lightest neutrino mass to

$$m_{\nu_1} = 10^{-10} \text{ GeV}. \quad (\text{A.64})$$

The left plot in fig. 15 plots the Frobenius norm of the required matrix μ_{Ψ_3} (in blue) required in order to solve the two above equations for different choices of $v_R Y_{\Psi_3}^R$. The orange line corresponds to $\|\mu_{\Psi_3}\|_F = \|v_R Y_{\Psi_3}^R\|_F$ and for any choice of $v_R Y_{\Psi_3}^R$ the required size of μ_{Ψ_3} in order to solve the above equations is larger, destroying the hierarchy assumed in deriving eqs. (A.62) and (A.63). The right plot of fig. 15 plots

$$R_{\nu/e} = \prod_i \frac{m_i}{m_i^{\text{input}}} \quad (\text{A.65})$$

where m_i corresponds to the numerically computed mass for the i -th generation of lepton and m_i^{input} corresponds to the experimental values for the masses inputted (run up to the appropriate scale). The charged lepton masses which result are significantly departed from their SM values whilst the neutrino values are well predicted, this is a coincidence due to the light neutrino mass block having the same formula regardless of the hierarchy²⁷ between $\|\mu_{\Psi_3}\|$ and $\|Y_{\Psi_3}^R v_R\|$ as can be seen in eqs. (A.57) and (A.60).

The light, charged-lepton mass block however is different depending on the hierarchy and we therefore find that due to the SM parameters m_u and m_d entering eqs. (A.54) and (A.55) as well as requiring viable correct charged-lepton and neutrino masses upon diagonalisation is not possible for low seesaw scales (for the entries of $Y_{\Psi_3}^R v_R$ which we scanned over). Though unlikely, it may be possible that special textures within $Y_{\Psi_3}^R v_R$ could lead to valid charged-lepton and neutrino masses for the appropriate hierarchy of block matrices. Therefore the addition of triplets to the usual PS multiplets will in general require additional physics, in [15] for example an additional fermionic singlet S_L was introduced and a viable mass spectrum for the leptons was recovered. The addition of both an $SU(2)_L$ and $SU(2)_R$ triplet was found to lead to an unviable mass spectrum for the scalars χ_L and χ_R , if more exotic scalars were introduced such that all mass terms in the Yukawa sector

²⁷ $\|Y_{\Psi_3}^R v_R\| > \|m_u\|$ is always satisfied in our scan.

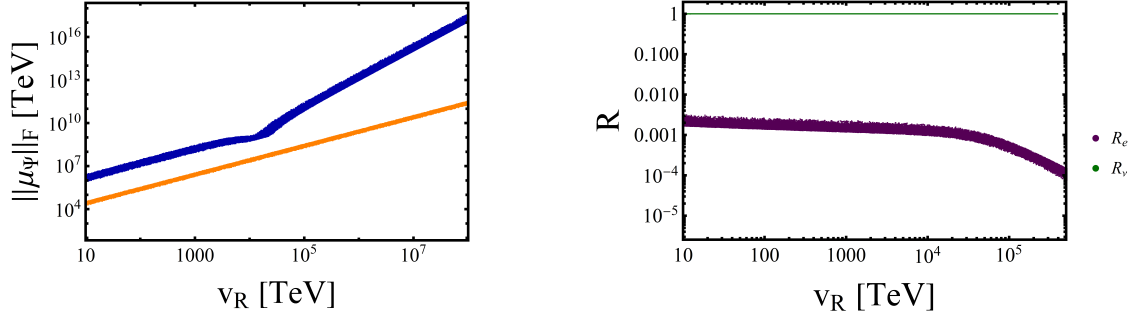


Figure 15. Plot of the Frobenius norm of μ_{Ψ_3} generated by solving eqs. (A.54) and (A.55) (left) as a function of the scale v_R with a random scan over $Y_{\Psi_3}^R$ with degenerate singular values and a plot of $R_{\nu/e}$ (right), defined in eq. (A.65), as a function of the same scale. The orange line in the left plot corresponds to $\|\mu_{\Psi_3}\|_F = \|Y_{\Psi_3}^R\|_F v_R$ and therefore at all scales considered the required size of μ_{Ψ_3} spoils the assumed hierarchy of parameters in order to achieve an inverse/linear seesaw. Though $R_\nu \simeq 1$, the resultant charged-lepton masses after diagonalisation are significantly different to their input values and therefore we find that additional triplets to the usual PS fermions alone are not sufficient to lead to a viable mass spectrum for all SM fermions (due to the quark-lepton symmetry assumed).

were generated, a viable mass spectrum would likely be generated for a specific hierarchy of parameters which may or may not lead to a chiral suppression of the X_μ mass limits as with the bi-doublet. In this case however the neutrino mass matrix would not be given by an inverse/linear seesaw and would be similar to eq. (4.9) with additional entries.

B Running of Gauge and Yukawa couplings

In order to estimate the running of the relevant SM parameters up to the potential scale of PS breaking we solve the simultaneous differential equation

$$\mu \frac{dx}{d\mu} = \frac{1}{(4\pi)^2} \beta_x^{(1)} + \dots \quad (\text{B.1})$$

where for simplicity we restrict ourselves to the one-loop renormalisation group equations. We make two reasonable assumptions on the running of each parameter: the exotic PS particle content does not significantly affect the running of the SM parameters below the scale of PS breaking we are interested in (due to their masses) and secondly as a simplifying assumption, we only include the contribution from the top-quark Yukawa coupling and gauge couplings in the evaluation of all relevant parameters due to its dominant role.

The beta functions $\beta_x^{(i)}$ have been extensively studied for the SM [48–51], at one-loop the beta functions which are non-zero when only the gauge and top-quark couplings are

included²⁸ are

$$\begin{aligned}
\beta_{g_i}^{(1)} &= b_i [g_i(\mu)]^3 \\
\beta_{y_{d,i}}^{(1)} &= y_{d,i}(\mu) \left(a_i [y_{u,3}(\mu)]^2 - \left\{ \frac{1}{4} [g_1(\mu)]^2 + \frac{9}{4} [g_2(\mu)]^2 + 8 [g_3(\mu)]^2 \right\} \right) \\
\beta_{y_{\ell,i}}^{(1)} &= y_{\ell,i}(\mu) \left(3 [y_{u,3}(\mu)]^2 - \frac{9}{4} \left\{ [g_1(\mu)]^2 + [g_2(\mu)]^2 \right\} \right) \\
\beta_{y_{u,i}}^{(1)} &= y_{u,i}(\mu) \left((3a_i - 2c_i) [y_{u,3}(\mu)]^2 - \left\{ \frac{17}{20} [g_1(\mu)]^2 + \frac{9}{4} [g_2(\mu)]^2 + 8 [g_3(\mu)]^2 \right\} \right) \\
\beta_{\theta_i}^{(1)} &= \theta_i(\mu) \left(c_i [y_{u,3}(\mu)]^2 \right). \tag{B.2}
\end{aligned}$$

Here $y_{d,i} = (y_d, y_s, y_b)$ and similarly for the charged-lepton and up-type Yukawa couplings, $\theta_i = (\theta_{13}, \theta_{23}, \theta_{12})$ are the CKM mixing angles and

$$a_i = \begin{cases} 3 & i = 1, 2 \\ \frac{3}{2} & i = 3 \end{cases}, \quad b_i = \begin{cases} \frac{41}{10} & i = 1 \\ -\frac{19}{6} & i = 2 \\ -7 & i = 3 \end{cases} \quad \text{and} \quad c_i = \begin{cases} 3 & i = 1, 2 \\ 0 & i = 3 \end{cases} \tag{B.3}$$

where the gauge coupling g_1 is given as it usually is in $SU(5)$ normalisation: $g_1^2 = 5/3g_Y^2$. The beta functions (at one-loop) for the CP-violating CKM parameter δ_{CKM} and all the parameters related to the neutrino sector are zero for our stated assumptions and therefore will not run. The parameters in eq. (B.2) are run up from $\mu = m_Z$ with initial values taken from [52] which utilised the Mathematica package RunDec to evolve the QCD parameters up to $m_Z \simeq 91.19$ GeV in the $\overline{\text{MS}}$ scheme and are summarised in table 13.

The results of eqs. (B.1) and (B.2) are shown in fig. 16 for the Yukawa couplings, gauge couplings and relevant CKM parameters run from $\mu = m_Z$ up to $\mu = 1000$ TeV. The points on the left plots correspond to the results obtained using RunDec at two-loops [52] at 1, 3 and 10 TeV in the SM. The plots on the right correspond to the ratio of the running parameter to its initial value at $\mu = m_Z$. The quark Yukawa couplings all significantly decrease as the energy scale increases whereas the charged-lepton Yukawa modestly increase. Due to the approximations we assume in eq. (B.2), the ratios $\beta_x^{(1)}/x$ are equal for the first and second generations of quark Yukawas, all three generations of charged-lepton Yukawas as well as between θ_{13} and θ_{23} .

As is often chosen, we work in a basis where the Yukawa coupling matrix for the up-type quarks and charged leptons is diagonal. Therefore the running of each relevant Yukawa coupling matrix, for the SM fermions, at a given energy scale is given by

$$\begin{aligned}
Y_u(\mu) &= \text{diag}[y_u(\mu), y_c(\mu), y_t(\mu)] \\
Y_d(\mu) &= V_{\text{CKM}}^\dagger [\theta_{12}^q(\mu), \theta_{23}^q(\mu), \theta_{13}^q(\mu), \delta_{\text{CKM}}(\mu)] \text{diag}[y_d(\mu), y_s(\mu), y_b(\mu)] \\
Y_\ell(\mu) &= \text{diag}[y_e(\mu), y_\mu(\mu), y_\tau(\mu)] \tag{B.4}
\end{aligned}$$

²⁸Additionally as in [49], terms smaller than $\mathcal{O}(10^{-3})$ in β_x/x were approximated to zero for simplicity.

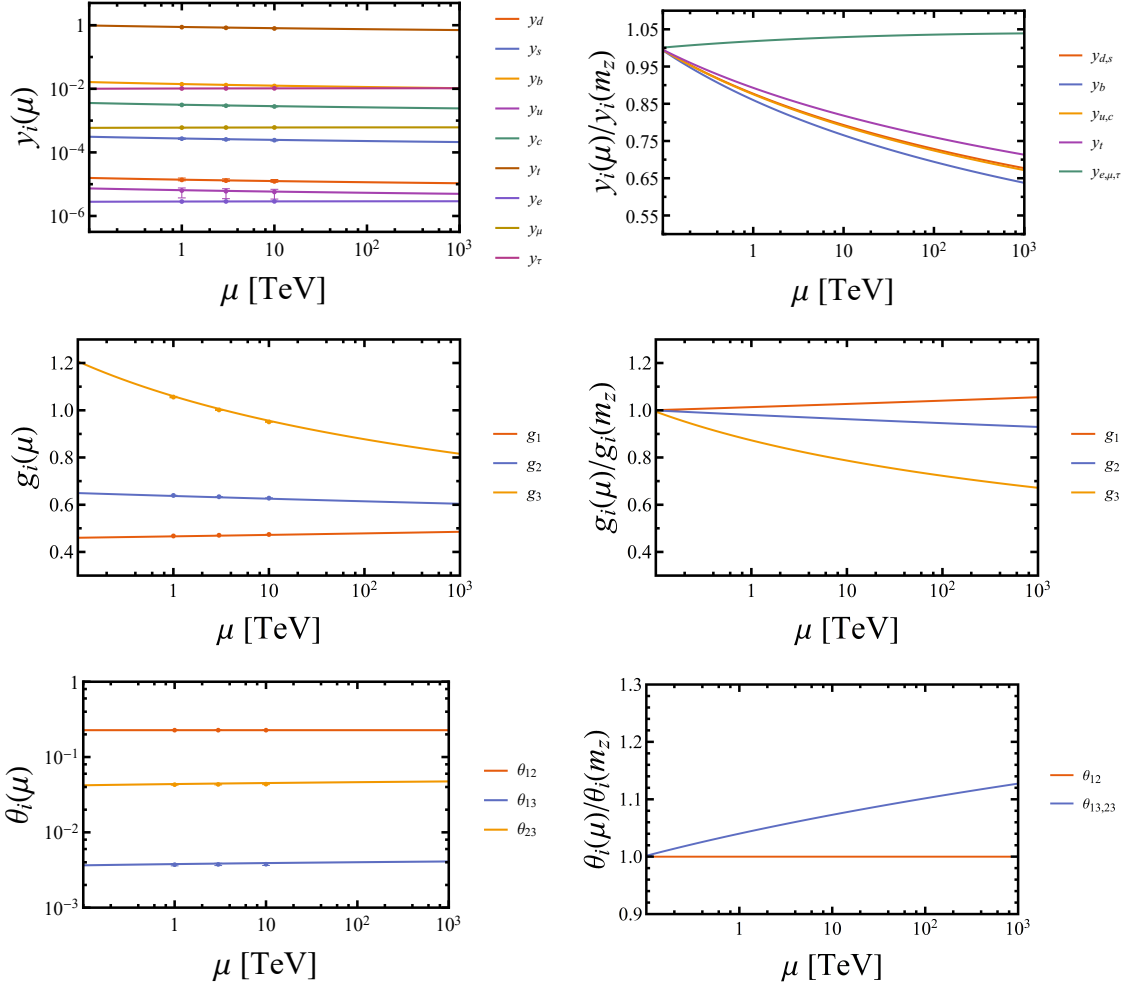


Figure 16. Plot of the numerical running of various SM parameters (**left**) (run up from $\mu = m_Z$) at one-loop as a function of the energy scale μ . The points correspond to values taken from [52] at $1, 3$ and 10 TeV with their respective 1σ uncertainties, where the running was performed to two-loops to demonstrate the accuracy of our one-loop approximations. Also shown are the ratios (**right**) of the run parameter against its initial value at $\mu = m_Z$.

where we use the numerical results from solving eqs. (B.1) and (B.2) using table 13 as the initial values.

$\mu = m_Z$		$\mu = m_Z$		$\mu = m_Z$	
g_1	$0.461425^{+0.000044}_{-0.000043}$	y_u	$7.4^{+1.5}_{-3.0} \times 10^{-6}$	y_e	$2.79^{+0.000015}_{-0.000016} \times 10^{-6}$
g_2	$0.65184^{+0.00018}_{-0.00017}$	y_c	$3.6^{+0.11}_{-0.11} \times 10^{-3}$	y_μ	$5.90^{+0.000019}_{-0.000018} \times 10^{-4}$
g_3	$1.2143^{+0.000044}_{-0.000043}$	y_t	$0.9861^{+0.0086}_{-0.0087}$	y_τ	$1.00^{+0.00090}_{-0.00091} \times 10^{-2}$
		y_d	$1.58^{+0.23}_{-0.10} \times 10^{-5}$	θ_{12}^ℓ	$0.59^{+0.0136}_{-0.0133}$
		y_s	$3.12^{+0.17}_{-0.16} \times 10^{-4}$	θ_{23}^ℓ	$0.84^{+0.0192}_{-0.0332}$
		y_b	$1.639^{+0.015}_{-0.015} \times 10^{-2}$	θ_{13}^ℓ	$0.15^{+0.0023}_{-0.0023}$
		θ_{12}^q	$0.22735^{+0.00072}_{-0.00071}$	δ_{PMNS}	$3.87^{+0.6632}_{-0.4887}$
		θ_{23}^q	$4.208^{+0.064}_{-0.064} \times 10^{-2}$	$\Delta m_{21}^2/\text{eV}^2$	$7.39^{+0.21}_{-0.20} \times 10^{-5}$
		θ_{13}^q	$3.64^{+0.13}_{-0.13} \times 10^{-3}$	$\Delta m_{31}^2/\text{eV}^2$	$2.523^{+0.032}_{-0.030} \times 10^{-3}$
		δ_{CKM}	$1.208^{+0.054}_{-0.054}$		

Table 13. Values used for the SM parameters at $\mu = m_Z$ in the $\overline{\text{MS}}$ scheme taken from table 1 of [52] for the gauge couplings, quark and charged-lepton parameters with their respective 1σ uncertainty. The neutrino parameters with their 1σ uncertainty are taken from [53], which are not measured at $\mu = m_Z$, however as the PMNS parameters do not significantly run at low energies [54] (in the SM) we take these values to be valid at this scale.

References

- [1] J. C. Pati and A. Salam, *Lepton Number as the Fourth Color*, *Phys. Rev.* **D10** (1974) 275–289.
- [2] J. C. Pati, A. Salam and U. Sarkar, *Delta B = - Delta L, neutron $\rightarrow e^- \pi^+$, $e^- K^+$, $\mu^- \pi^+$ and $\mu^- K^+$ DECAY modes in $SU(2)_L \times SU(2)_R \times SU(4)_C$ or $SO(10)$* , *Phys. Lett.* **133B** (1983) 330–336.
- [3] R. N. Mohapatra, *Unification and Supersymmetry. The Frontiers of Quark-Lepton Physics, Section 6.6 - $\sin^2\theta_W$ and the Scale of Partial Unification*. Springer, Berlin, 1986, 10.1007/978-1-4757-1928-4.
- [4] R. Foot, *An Alternative $SU(4) \times SU(2)_L \times SU(2)_R$ model*, *Phys. Lett.* **B420** (1998) 333–339, [hep-ph/9708205].
- [5] R. Foot and G. Filewood, *Implications of TeV scale $SU(4) \times SU(2)_L \times SU(2)_R$ quark lepton-lepton unification*, *Phys. Rev.* **D60** (1999) 115002, [hep-ph/9903374].
- [6] LHCb collaboration, R. Aaij et al., *Measurement of the ratio of branching fractions $\mathcal{B}(\bar{B}^0 \rightarrow D^{*+} \tau^- \bar{\nu}_\tau) / \mathcal{B}(\bar{B}^0 \rightarrow D^{*+} \mu^- \bar{\nu}_\mu)$* , *Phys. Rev. Lett.* **115** (2015) 111803, [1506.08614].
- [7] LHCb collaboration, R. Aaij et al., *Test of lepton universality with $B^0 \rightarrow K^{*0} \ell^+ \ell^-$ decays*, *JHEP* **08** (2017) 055, [1705.05802].
- [8] LHCb collaboration, R. Aaij et al., *Test of lepton universality using $B^+ \rightarrow K^+ \ell^+ \ell^-$ decays*, *Phys. Rev. Lett.* **113** (2014) 151601, [1406.6482].

- [9] LHCb collaboration, R. Aaij et al., *Search for lepton-universality violation in $B^+ \rightarrow K^+ \ell^+ \ell^-$ decays*, *Phys. Rev. Lett.* **122** (2019) 191801, [[1903.09252](#)].
- [10] J. Heeck and D. Teresi, *Pati-Salam explanations of the B-meson anomalies*, *JHEP* **12** (2018) 103, [[1808.07492](#)].
- [11] L. Di Luzio, A. Greljo and M. Nardecchia, *Gauge leptoquark as the origin of B-physics anomalies*, *Phys. Rev. D* **96** (2017) 115011, [[1708.08450](#)].
- [12] L. Calibbi, A. Crivellin and T. Li, *Model of vector leptoquarks in view of the B-physics anomalies*, *Phys. Rev. D* **98** (2018) 115002, [[1709.00692](#)].
- [13] M. Bordone, C. Cornella, J. Fuentes-Martin and G. Isidori, *A three-site gauge model for flavor hierarchies and flavor anomalies*, *Phys. Lett. B* **779** (2018) 317–323, [[1712.01368](#)].
- [14] S. Balaji, R. Foot and M. A. Schmidt, *Chiral $SU(4)$ explanation of the $b \rightarrow s$ anomalies*, *Phys. Rev. D* **99** (2019) 015029, [[1809.07562](#)].
- [15] S. Balaji and M. A. Schmidt, *Unified $SU(4)$ theory for the $R_{D^{(*)}}$ and $R_{K^{(*)}}$ anomalies*, *Phys. Rev. D* **101** (2020) 015026, [[1911.08873](#)].
- [16] G. Valencia and S. Willenbrock, *Quark - lepton unification and rare meson decays*, *Phys. Rev. D* **50** (1994) 6843–6848, [[hep-ph/9409201](#)].
- [17] D. Chang, R. N. Mohapatra, J. Gipson, R. E. Marshak and M. K. Parida, *Experimental Tests of New $SO(10)$ Grand Unification*, *Phys. Rev. D* **31** (1985) 1718.
- [18] R. N. Mohapatra and J. W. F. Valle, *Neutrino Mass and Baryon Number Nonconservation in Superstring Models*, *Phys. Rev. D* **34** (1986) 1642.
- [19] F. Deppisch and J. W. F. Valle, *Enhanced lepton flavor violation in the supersymmetric inverse seesaw model*, *Phys. Rev. D* **72** (2005) 036001, [[hep-ph/0406040](#)].
- [20] D. Wyler and L. Wolfenstein, *Massless Neutrinos in Left-Right Symmetric Models*, *Nucl. Phys. B* **218** (1983) 205–214.
- [21] E. Ma, *Lepton Number Nonconservation in $E(6)$ Superstring Models*, *Phys. Lett. B* **191** (1987) 287.
- [22] M. C. Gonzalez-Garcia and J. W. F. Valle, *Fast Decaying Neutrinos and Observable Flavor Violation in a New Class of Majoron Models*, *Phys. Lett. B* **216** (1989) 360–366.
- [23] M. C. Gonzalez-Garcia, A. Santamaria and J. W. F. Valle, *Isosinglet Neutral Heavy Lepton Production in Z Decays and Neutrino Mass*, *Nucl. Phys. B* **342** (1990) 108–126.
- [24] S. M. Barr, *A Different seesaw formula for neutrino masses*, *Phys. Rev. Lett.* **92** (2004) 101601, [[hep-ph/0309152](#)].
- [25] M. Malinsky, J. C. Romao and J. W. F. Valle, *Novel supersymmetric $SO(10)$ seesaw mechanism*, *Phys. Rev. Lett.* **95** (2005) 161801, [[hep-ph/0506296](#)].
- [26] E. K. Akhmedov, M. Lindner, E. Schnapka and J. W. F. Valle, *Dynamical left-right symmetry breaking*, *Phys. Rev. D* **53** (1996) 2752–2780, [[hep-ph/9509255](#)].
- [27] D. Croon, T. E. Gonzalo and G. White, *Gravitational Waves from a Pati-Salam Phase Transition*, *JHEP* **02** (2019) 083, [[1812.02747](#)].
- [28] A. D. Smirnov, *Contributions of gauge and scalar leptoquarks to $K0(L) \rightarrow l(i) + l(j)^-$ and $B0 \rightarrow l(i) + l(j)^-$ decay and constraints on leptoquark masses from the decays $K0(L) \rightarrow e^- + \mu^+ +$ and $B0 \rightarrow e^- + \tau^+ +$* , *Phys. Atom. Nucl.* **71** (2008) 1470–1480.

- [29] M. D. Goodsell, S. Liebler and F. Staub, *Generic calculation of two-body partial decay widths at the full one-loop level*, *Eur. Phys. J. C* **77** (2017) 758, [[1703.09237](#)].
- [30] A. V. Kuznetsov and N. V. Mikheev, *Vector leptoquarks could be rather light?*, *Phys. Lett. B* **329** (1994) 295–299, [[hep-ph/9406347](#)].
- [31] Y. Cai, J. Gargalionis, M. A. Schmidt and R. R. Volkas, *Reconsidering the One Leptoquark solution: flavor anomalies and neutrino mass*, *JHEP* **10** (2017) 047, [[1704.05849](#)].
- [32] A. D. Smirnov, *Mass limits for scalar and gauge leptoquarks from $K(L)0 \rightarrow e^- + \mu^\pm + \tau^\pm$ decays*, *Mod. Phys. Lett. A* **22** (2007) 2353–2363, [[0705.0308](#)].
- [33] A. D. Smirnov, *Vector leptoquark mass limits and branching ratios of $K_L^0, B^0, B_s \rightarrow l_i^+ l_j^-$ decays with account of fermion mixing in leptoquark currents*, *Mod. Phys. Lett. A* **33** (2018) 1850019, [[1801.02895](#)].
- [34] PARTICLE DATA GROUP collaboration, P. Zyla et al., *Review of Particle Physics*, *PTEP* **2020** (2020) 083C01.
- [35] R. R. Volkas, *Prospects for mass unification at low-energy scales*, *Phys. Rev. D* **53** (1996) 2681–2698, [[hep-ph/9507215](#)].
- [36] H. Georgi and C. Jarlskog, *A New Lepton - Quark Mass Relation in a Unified Theory*, *Phys. Lett.* **86B** (1979) 297–300.
- [37] J. Hisano, H. Murayama and T. Yanagida, *Nucleon decay in the minimal supersymmetric $SU(5)$ grand unification*, *Nucl. Phys. B* **402** (1993) 46–84, [[hep-ph/9207279](#)].
- [38] CMS collaboration, A. M. Sirunyan et al., *Search for Evidence of the Type-III Seesaw Mechanism in Multilepton Final States in Proton-Proton Collisions at $\sqrt{s} = 13$ TeV*, *Phys. Rev. Lett.* **119** (2017) 221802, [[1708.07962](#)].
- [39] N. Kumar and S. P. Martin, *Vectorlike Leptons at the Large Hadron Collider*, *Phys. Rev. D* **92** (2015) 115018, [[1510.03456](#)].
- [40] E. Fernandez-Martinez, J. Hernandez-Garcia and J. Lopez-Pavon, *Global constraints on heavy neutrino mixing*, *JHEP* **08** (2016) 033, [[1605.08774](#)].
- [41] ATLAS collaboration, G. Aad et al., *Search for the production of single vector-like and excited quarks in the Wt final state in pp collisions at $\sqrt{s} = 8$ TeV with the ATLAS detector*, *JHEP* **02** (2016) 110, [[1510.02664](#)].
- [42] J. C. Helo, M. Hirsch and T. Ota, *Proton decay at one loop*, *Phys. Rev. D* **99** (2019) 095021, [[1904.00036](#)].
- [43] T. Han, I. Lewis and Z. Liu, *Colored Resonant Signals at the LHC: Largest Rate and Simplest Topology*, *JHEP* **12** (2010) 085, [[1010.4309](#)].
- [44] CMS collaboration, A. M. Sirunyan et al., *Search for high mass dijet resonances with a new background prediction method in proton-proton collisions at $\sqrt{s} = 13$ TeV*, *JHEP* **05** (2020) 033, [[1911.03947](#)].
- [45] W. Grimus and L. Lavoura, *The Seesaw mechanism at arbitrary order: Disentangling the small scale from the large scale*, *JHEP* **11** (2000) 042, [[hep-ph/0008179](#)].
- [46] F. Besnard, *A remark on the mathematics of the seesaw mechanism*, *J. Phys. Comm.* **1** (2018) 015005, [[1611.08591](#)].
- [47] J. A. Casas and A. Ibarra, *Oscillating neutrinos and $\mu \rightarrow e, \gamma$* , *Nucl. Phys. B* **618** (2001) 171–204, [[hep-ph/0103065](#)].

- [48] M. E. Machacek and M. T. Vaughn, *Two Loop Renormalization Group Equations in a General Quantum Field Theory. 2. Yukawa Couplings*, *Nucl. Phys. B* **236** (1984) 221–232.
- [49] C. Balzereit, T. Mannel and B. Plumper, *The Renormalization group evolution of the CKM matrix*, *Eur. Phys. J. C* **9** (1999) 197–211, [[hep-ph/9810350](#)].
- [50] M.-x. Luo and Y. Xiao, *Two loop renormalization group equations in the standard model*, *Phys. Rev. Lett.* **90** (2003) 011601, [[hep-ph/0207271](#)].
- [51] S. R. Juarez Wysozka, S. Herrera H., P. Kielanowski and G. Mora, *Scale dependence of the quark masses and mixings: Leading order*, *Phys. Rev. D* **66** (2002) 116007, [[hep-ph/0206243](#)].
- [52] S. Antusch and V. Maurer, *Running quark and lepton parameters at various scales*, *JHEP* **11** (2013) 115, [[1306.6879](#)].
- [53] I. Esteban, M. Gonzalez-Garcia, A. Hernandez-Cabezudo, M. Maltoni and T. Schwetz, *Global analysis of three-flavour neutrino oscillations: synergies and tensions in the determination of θ_{23} , δ_{CP} , and the mass ordering*, *JHEP* **01** (2019) 106, [[1811.05487](#)].
- [54] S. Antusch, J. Kersten, M. Lindner, M. Ratz and M. A. Schmidt, *Running neutrino mass parameters in see-saw scenarios*, *JHEP* **03** (2005) 024, [[hep-ph/0501272](#)].